



# UFSAR Revision 30.0

 An AEP Company	<b>INDIANA MICHIGAN POWER</b> <b>D. C. COOK NUCLEAR PLANT</b> <b>UPDATED FINAL SAFETY ANALYSIS REPORT</b>	Revised: 29.0 Section:14.3.4.1 Page: i of i
---	---	---

<b>14.3 REACTOR COOLANT SYSTEM PIPE RUPTURE (LOSS OF COOLANT ACCIDENT) .....</b>	<b>1</b>
<b>14.3.4 Containment Integrity Analysis .....</b>	<b>1</b>
14.3.4.1 Containment Structure .....	1
14.3.4.1.1 Design Basis .....	1
14.3.4.1.2 Design Features .....	2
14.3.4.1.3 Design Evaluation .....	3
14.3.4.1.3.1 Loss of Coolant Accident .....	3
14.3.4.1.3.1.1 Compression Ratio Analysis .....	3
14.3.4.1.3.1.1.a Introduction .....	3
14.3.4.1.3.1.1.b Air Compression Process Description .....	4
14.3.4.1.3.1.1.c Sensitivity to Blowdown Energy .....	7
14.3.4.1.3.1.1.d Effect of Blowdown Rate .....	8
14.3.4.1.3.1.1.e Effect of Steam Bypass .....	8
14.3.4.1.3.1.1.f Effect of Dead-Ended Volumes .....	10
14.3.4.1.3.1.2 Long Term Containment Pressure Analysis .....	11
14.3.4.1.3.1.3 Peak Containment Pressure Transient .....	12
14.3.4.1.3.1.4 Structural Heat Removal .....	15
14.3.4.1.3.1.5 Relevant Acceptance Criteria .....	16
14.3.4.1.3.1.6 Conclusions .....	16
14.3.4.1.3.2 Steam Line Break .....	17
14.3.4.1.3.2.1 Peak Containment Temperature Transients .....	18
14.3.4.1.3.2.2 Results .....	19
14.3.4.1.3.2.3 Sensitivity of the Results .....	19

 An AEP Company	<p style="text-align: center;">INDIANA MICHIGAN POWER D. C. COOK NUCLEAR PLANT UPDATED FINAL SAFETY ANALYSIS REPORT</p>	<p>Revised: 29.0 Section: 14.3.4.1 Page: 1 of 21</p>
---	---	--

## **14.3 REACTOR COOLANT SYSTEM PIPE RUPTURE (LOSS OF COOLANT ACCIDENT)**

### **14.3.4 Containment Integrity Analysis**

#### **14.3.4.1 Containment Structure**

##### **14.3.4.1.1 Design Basis**

The steel-lined, reinforced concrete containment structure, including foundations, access hatches, and penetrations is designed and constructed to maintain full containment integrity when subjected to accident temperatures and pressures, and the postulated earthquake conditions. Details of the Containment System are described in Chapter 5.

The containment design internal pressure is 12 psig. The effects of pipe rupture in the primary coolant system, up to and including a double-ended rupture of the largest pipe as well as a rupture of the main steam line, are considered in determining the peak accident pressure.

The internal structures of the containment vessel are also designed for subcompartment differential accident pressures. The accident pressures considered are due to the same postulated pipe ruptures as described for the containment vessel.


The other simultaneous loads in combination with the accident pressures, and the applicable load factors, are presented in detail in Chapter 5.

The functional design of the containment is based upon the following accident input source term assumptions and conditions:

1. The design basis accident blowdown mass and energy is put into the containment.
2. The hot metal energy is considered.
3. A reactor core power of 3484 MWt (100.34% of 3470 MWt) is used for decay heat generation.
4. Minimum Engineering Safety Features performance is assumed based upon the limiting single failure criterion.

The ice condenser is designed to limit the containment pressure below the design pressure for all reactor coolant pipe break sizes up to and including a double-ended severance. Characterizing the performance of the ice condenser requires consideration of the rate of addition of mass and energy to the containment, as well as the total amounts of mass and energy added. Analyses

## UFSAR Revision 30.0

 An AEP Company	<b>INDIANA MICHIGAN POWER</b> <b>D. C. COOK NUCLEAR PLANT</b> <b>UPDATED FINAL SAFETY ANALYSIS REPORT</b>	Revised: 29.0 Section: 14.3.4.1 Page: 2 of 21
---	---	---

have shown that the accident which produces the highest blowdown rate into the ice condenser containment results in the maximum containment pressure rise. That accident is the double-ended severance of a reactor coolant pipe.

Post-blowdown energy releases can also be accommodated without exceeding the containment design pressure.

### **14.3.4.1.2 Design Features**

The reactor containment is a reinforced concrete structure consisting of a vertical cylinder, a hemispherical dome and a flat base. The interior is divided into three volumes, a lower volume which houses the reactor and Reactor Coolant System, an intermediate volume housing the energy absorbing ice bed in which steam is condensed and an upper volume which accommodates the air displaced from the other two volumes during a design basis pipe break accident.


The type of containment used for Donald C. Cook Unit 2 was selected for the following reasons:

1. The Ice Condenser Containment can accept large amounts of energy and mass inputs and maintain low internal pressures and leakage rates. A particular advantage of the ice condenser is its passive design not requiring an actuation signal.
2. The Ice Condenser Containment combines the required integrity, compact size, and carefully considered advanced design desirable for a nuclear station.

Consideration is given to subcompartment differential pressure resulting from a design basis accident. If an accident were to occur due to a pipe rupture in one of these relative small volumes, the pressure would build up at a faster rate than in the containment, thus imposing a differential pressure across the wall of the structure. Section 14.3.4.2, "Containment Subcompartments", presents the subcompartment differential pressure analyses.

The Ice Condenser Containment, incorporating forced circulation of the containment atmosphere together with the containment spray system, ensures the functional capability of containment for as long as necessary following an accident. The peak pressure occurring as the result of the complete blowdown of the reactor coolant through any rupture of the Reactor Coolant System up to and including the hypothetical double-ended severance does not exceed the design pressure of the containment. The design pressure is also not exceeded during subsequent long term pressure transients.

# UFSAR Revision 30.0

 <b>INDIANA MICHIGAN POWER</b> <small>An AEP Company</small>	<b>INDIANA MICHIGAN POWER D. C. COOK NUCLEAR PLANT UPDATED FINAL SAFETY ANALYSIS REPORT</b>	Revised: 29.0 Section: 14.3.4.1 Page: 3 of 21
--	---	---

## **14.3.4.1.3 Design Evaluation**

### **14.3.4.1.3.1 Loss of Coolant Accident**

The time history of conditions within an ice condenser containment during a postulated loss-of-coolant accident can be divided into two periods for calculational purposes:

1. The initial reactor coolant blowdown, which for the largest assumed pipe break occurs in approximately 30 seconds.
2. The post blowdown phase of the accident which begins following the blowdown and extends several hours after the start of the accident.

During the first few seconds of the blowdown period following a large rupture of the Reactor Coolant System, containment conditions are characterized by rapid pressure and temperature transients. To calculate these transients a detailed spatial and short time increment analysis is necessary. This analysis is performed with the TMD code with the calculation time of interest extending up to a few seconds following the accident initiation.

Physically, tests at the Waltz Mill ice condenser test facility have shown that the blowdown phase represents that period of time in which the lower compartment air, and a portion of the ice condenser air, are displaced and compressed into the upper compartment and the remainder of the ice condenser. The containment pressure at or near the end of blowdown is governed by this air compression process.

Containment pressure during the post blowdown phase of the accident is calculated with the LOTIC Code, which models the containment structural heat sinks and containment safeguards systems.


The paragraphs that follow describe key physical phenomena considered in the design pressure determination and the containment pressure response analysis. The methods of accounting for these phenomena in the analysis is also discussed.

#### **14.3.4.1.3.1.1 Compression Ratio Analysis**

##### **14.3.4.1.3.1.1.a Introduction**

Following the initial pressure peak from a double-ended cold leg break, blowdown continues and the pressure in the lower compartment again increases, reaching a peak at or before the end of blowdown. The pressure in the upper compartment continues to rise from beginning of blowdown and reaches a peak, which is approximately equal to the lower compartment pressure.

# UFSAR Revision 30.0

 An AEP Company	<p style="text-align: center;"><b>INDIANA MICHIGAN POWER</b> <b>D. C. COOK NUCLEAR PLANT</b> <b>UPDATED FINAL SAFETY ANALYSIS REPORT</b></p>	<p>Revised: 29.0 Section: 14.3.4.1 Page: 4 of 21</p>
---	--	--

After blowdown is complete, the steam in the lower compartment continues to flow through the doors into the ice bed compartment and is condensed.

The primary factor in producing this upper containment pressure peak, and, therefore, in determining design pressure, is the displacement of air from the lower compartment into the upper compartment. The ice condenser quite effectively performs its function of condensing virtually all the steam that enters the ice beds. Essentially, the only source of steam entering the upper containment is from leakage through the drain holes and other leakage around crack openings in hatches in the operating deck, which separate the lower and upper portions of the containment building.

A method of analysis of the compression peak pressure was developed based on the results of full scale section tests. This method consists of the calculation of the air mass compression ratio, the polytropic exponent for the compression process, and the effect of steam bypass through the operating deck on this compression.

In the following sections, a discussion of the major parameters affecting the compression peak will be discussed. Specifically they are: air compression, steam bypass, blowdown rate, and blowdown energy.


#### **14.3.4.1.3.1.1.b Air Compression Process Description**

The volumes of the various containment compartments determine directly the air volume compression ratio. This is basically the ratio of the total active containment air volume to the compressed air volume during blowdown. During blowdown, air is displaced from the lower compartment and compressed into the ice condenser beds and into the upper containment above the operating deck. It is this air compression process which primarily determines the peak in containment pressure following the initial blowdown release.

The actual Waltz Mill test compression ratios were found by performing air mass balances before the blowdown and at the time of the compression peak pressure, using the results of three full scale special section tests. These three tests were conducted with an energy input representative of the plant design.

In the calculation of the mass balance for the ice condenser, the compartment is divided into two subvolumes; one volume representing the flow channels and one volume representing the ice baskets. The flow channel volume is further divided into four subvolumes, and the partial air pressure and mass in each subvolume are found from thermocouple readings, assuming that the air is saturated with steam at the measured temperature. From these results, the average

## UFSAR Revision 30.0

 An AEP Company	<b>INDIANA MICHIGAN POWER</b> <b>D. C. COOK NUCLEAR PLANT</b> <b>UPDATED FINAL SAFETY ANALYSIS REPORT</b>	Revised: 29.0 Section: 14.3.4.1 Page: 5 of 21
---	---	---

temperature of the air in the ice condenser compartment is found, and the volume occupied by the air at the total condenser pressure is found from the equation of state as follows:

$$V_a = \frac{M_a R_a T_a}{P} \quad (1)$$

where:

- $V_a$  = Volume of ice condenser occupied by air (ft<sup>3</sup>).
- $M_a$  = Mass of air in ice condenser compartment (lb.).
- $T_a$  = Average temperature of air in ice condenser (°F).
- $P$  = Total ice condenser pressure (lb/ft<sup>2</sup>).

The partial pressure and mass of air in the lower compartment are found by averaging the temperatures indicated by the thermocouples during the test located in that compartment and assuming saturation conditions. For these three tests, it was found that the partial pressure, and hence the mass of air in the lower compartment, were zero at the time of the compression peak pressure.

The actual Waltz Mill test compression ratio is then found from the following:

$$C_r = \frac{V_1 + V_2 + V_3}{V_3 + V_a} \quad (2)$$

where:

- $V_1$  = Lower compartment volume (ft<sup>3</sup>).
- $V_2$  = Ice condenser compartment volume (ft<sup>3</sup>).
- $V_3$  = Upper compartment volume (ft<sup>3</sup>).


The polytropic exponent for these tests is then found from the measured compression pressure and the compression ratio calculated above. Also considered is the pressure increase that results from the leakage of steam through the deck into the upper compartment.

The compression peak pressure in the upper compartment for the tests for containment design is then given by:

$$P = P_o (C_r)^n + \Delta P_{\text{deck}} \quad (3)$$

where:

## UFSAR Revision 30.0

 An AEP Company	<b>INDIANA MICHIGAN POWER</b> <b>D. C. COOK NUCLEAR PLANT</b> <b>UPDATED FINAL SAFETY ANALYSIS REPORT</b>	Revised: 29.0 Section: 14.3.4.1 Page: 6 of 21
---	---	---

$P_o$	=	Initial pressure (psia).
$P$	=	Compression peak pressure (psia).
$C_r$	=	Volume compression ratio.
$n$	=	Polytropic exponent.
$\Delta P_{\text{deck}}$	=	Pressure increase caused by deck leakage (psi).

Using the method of calculation described above, the compression ratio was calculated for the three full scale section tests. From the results of the air mass balances, it was found that air occupied 0.645 of the ice condenser compartment volume at the time of peak compression, or

$$V_a = 0.645V_2 \quad (4)$$

The final compression volume includes the volume of the upper compartment as well as part of the volume of air in the ice condenser. The results of the full scale section tests (Figure 14.3.4-1) show a variation in steam partial pressure from 100% near the bottom of the ice condenser to essentially zero near the top. The thermocouples and pressure detectors confirm that at the time when the compression peak pressure is reached steam occupies less than half of the volume of the ice condenser. The analytical model used in defining the containment pressure peak uses the upper compartment volume 64.5 percent of the ice condenser air volume as the final volume. This 64.5 percent value was determined from appropriate test results.

The calculated volume compression ratios are shown in Figure 14.3.4-2, along with the compression peak pressures for these tests. The compression peak pressure is determined from the measured pressure, after accounting for the deck leakage contribution. From the results shown in Figure 14.3.4-2, the polytropic exponent for these tests is found to be 1.13.


For the long-term containment integrity analysis, the compression pressure is used to initialize the calculations.

The Donald C. Cook volume compression ratio, not accounting for the dead ended volume effect, is calculated using Equation 2 and using data from Table 14.3.4-1. The Table 14.3.4-1 containment compartment volume data have been adjusted, per the analysis methodology, to conservatively bias the analysis (References 35 & 36). Using the following volume information:

$V_1$	=	293,801 ft <sup>3</sup>
$V_2$	=	110,520 ft <sup>3</sup>
$V_3$	=	727,628 ft <sup>3</sup>

the compression ratio becomes:

## UFSAR Revision 30.0

 An AEP Company	<p style="text-align: center;"><b>INDIANA MICHIGAN POWER</b> <b>D. C. COOK NUCLEAR PLANT</b> <b>UPDATED FINAL SAFETY ANALYSIS REPORT</b></p>	<p>Revised: 29.0 Section: 14.3.4.1 Page: 7 of 21</p>
---	--	--

$$C_r = \frac{1,131,949}{727,628 + 0.645 * 110,520} = 1.42$$

The peak compression pressure, based on an initial containment pressure of 15.0 psia, is then given by Equation 3 as:

$$P_3 = 15.0 (1.42)^{1.13} + 0.4 = 22.64 \text{ psia or } 7.94 \text{ psig}$$

The peak compression pressure in the upper compartment for the D.C. Cook Unit 2 design is 7.94 psig. This peak compression pressure includes a pressure increase of 0.4 psi from steam bypass. The nitrogen partial pressure from the accumulators is not included, since it is not added to the containment atmosphere until after the compression peak has passed. Accumulator nitrogen is considered in the long-term performance analysis of the containment pressure decay following blowdown, using the LOTIC code.

#### **14.3.4.1.3.1.1.c Sensitivity to Blowdown Energy.**

The sensitivity of the upper compartment compression pressure peak versus the amount of energy released is shown in Figure 14.3.4-3. This figure shows the magnitude of the peak compression pressure versus the amount of energy released in terms of percentage of reactor coolant system energy release. These data are based on test results wherein each of the tests were run at 110% and 200% of the initial blowdown rate equivalent to the maximum coolant pipe break flow.

These test results indicate the very large capacity of the ice condenser for additional amounts of energy with only a small effect on compression peak pressure. For example, during testing, 100% energy release gave a pressure of about 6.8 psig, while an increase up to 220% energy release gave an increase in peak pressure of only about 2 psi. It is also important to note that maldistribution of steam into different sections of the ice condenser would not cause even the small increase in peak pressure that is shown in Figure 14.3.4-3. For every section of the ice condenser that may receive more energy than that of the average section, other sections of the ice condenser would receive less energy than the average section. Thus, the compression pressure in the upper compartment would be indicated by the test performance based on 100% energy release rather than either the maximum energy release section or the minimum energy release section.



## UFSAR Revision 30.0


 An AEP Company	<p style="text-align: center;"><b>INDIANA MICHIGAN POWER</b> <b>D. C. COOK NUCLEAR PLANT</b> <b>UPDATED FINAL SAFETY ANALYSIS REPORT</b></p>	<p>Revised: 29.0 Section: 14.3.4.1 Page: 8 of 21</p>
---	--	--

Figure 14.3.4-4 gives some insight as to the very large capacity for energy absorption of the ice condenser as obtained from test results. Figure 14.3.4-4 is a plot of the amount of ice melted versus the amount of energy released based on test results at different energies and blowdown rates. These test results indicate that a 200% energy release melts only about 60% of the ice while 100% energy release melts only 30% of the ice. Thus, even for energy release considerably in excess of 200% there would still be a substantial amount of ice remaining in the ice condenser.

### **14.3.4.1.3.1.1.d      Effect of Blowdown Rate**

Figure 14.3.4-5 shows the effect of blowdown rate upon the final compression pressure in the upper compartment. Figure 14.3.4-5 is based on the results of a series of tests, all with the plant design ice condenser configuration, but with the important difference that all of these tests were run with 185% of the Reactor Coolant System energy release quantity. There are two important effects to note from Figure 14.3.4-5. One, the magnitude of the compression peak pressure in the upper compartment is low (about 7.8 psig) for the reactor plant design blowdown rate; and two, even an increase in this rate up to 200% blowdown rate produces only a small increase in the magnitude of this peak pressure (about 1 psi).


### **14.3.4.1.3.1.1.e      Effect of Steam Bypass**

The method of analysis used to obtain the maximum allowable deck leakage capacity as a function of the primary system break size is presented next. Two analyses were used to demonstrate the margin between the original design leakage value of 5 ft<sup>2</sup> and the maximum allowable. Considering the current design basis value of 7 sq. ft. for the deck leakage, the following discussion remains valid.

During the blowdown transient, steam and air will flow through the ice condenser doors and also through the deck bypass area into the upper compartment. For the containment the bypass area is composed of two parts, a known leakage area of 2.2 ft<sup>2</sup> with a geometric loss coefficient of 1.5 through the deck drainage holes location at the bottom of the refueling cavity, and an undefined deck leakage area with a conservatively small loss coefficient of 2.5. Leakage through the backdraft damper of the air return fans was determined to be 0.18 sq. ft./damper and was considered in the known leakage area. For the CEQ Fan Ventwell and Stairwell drains, the identified divider barrier bypass area is increased by approximately 0.16 ft<sup>2</sup> as a result of the removal of the check valve internals.

A resistance network similar to that used in TMD is used to represent 6 lower compartment volumes, each with a representative portion of the deck leakage and the lower inlet door flow

## UFSAR Revision 30.0

 An AEP Company	<b>INDIANA MICHIGAN POWER</b> <b>D. C. COOK NUCLEAR PLANT</b> <b>UPDATED FINAL SAFETY ANALYSIS REPORT</b>	Revised: 29.0 Section: 14.3.4.1 Page: 9 of 21
---	---	---

resistance adjacent to the lower compartment element. The inlet door flow resistance and flow area are calculated for small breaks that would only partially open these doors.


The coolant blowdown rate as a function of time is used with this flow network to calculate the differential pressures on the lower inlet doors and across the operating deck. The resultant deck leakage rate and integrated steam leakage into the upper compartment are then calculated. The lower inlet doors are initially held shut by the cold head of air behind the doors (approximately 1/2 - 1 pound per square foot). The initial blowdown from a small break opens the doors and removes the cold head on the doors. With the door differential pressure removed the door position is slightly open. An additional pressure differential of one pound per square foot is then sufficient to fully open the doors. The nominal door opening characteristic are based on test results.

The first analysis conservatively assumed that flow through the postulated leakage paths is pure steam. During the actual blowdown transient, steam and air representative of the lower compartment mixture would leak through the holes; thus less steam would enter the upper compartment. If flow were considered to be a mixture of liquid and vapor, the total leakage mass would increase but the steam flow rate would decrease. The analysis also assumed that no condensing of the flow occurs due to structural heat sinks. The peak air compression in the upper compartment for the various break sizes is assumed with steam mass added to this value to obtain the total containment pressure. Air compression for the various break sizes is obtained from previous full scale section tests conducted at Waltz Mill.

The allowable leakage area for the following Reactor Coolant System break sizes was determined: DE, 0.6 DE, 3 ft<sup>2</sup>, 8 inch diameter, 6 inch diameter, 2.5 inch diameter, and 0.5 inch diameter. For break sizes 3 ft<sup>2</sup> and above a series of deck leakage sensitivity studies was made to establish the total steam leakage to the upper compartment over the blowdown transient. This steam was added to the air in the upper compartment to establish a peak pressure. Air and steam were assumed to be in thermal equilibrium, with the air partial pressure increased over the air compression value to account for heating effects. For these breaks, sprays were neglected. Reduction in compression ratio by return of air to the lower compartment was conservatively neglected. The results of this analysis are shown in Table 14.3.4-2. This analysis is confirmed by Waltz Mill tests conducted with various deck bypass leakages equivalent to over 50 ft<sup>2</sup> of deck leakage for the double ended blowdown rate.

For breaks 8 inches in diameter and smaller, the effect of containment sprays was included. The method used is as follows: For each time step of the blowdown the amount of steam leaking into

## UFSAR Revision 30.0

 An AEP Company	<p style="text-align: center;"><b>INDIANA MICHIGAN POWER</b> <b>D. C. COOK NUCLEAR PLANT</b> <b>UPDATED FINAL SAFETY ANALYSIS REPORT</b></p>	<p>Revised: 29.0 Section: 14.3.4.1 Page: 10 of 21</p>
---	--	---

the upper compartment was calculated to obtain the steam mass in the upper compartment. This steam was mixed with the air in the upper compartment, assuming thermal equilibrium with air. The air partial pressure was increased to account for air heating effects. After sprays were initiated, the pressure was calculated based on the rate of accumulation of steam in the upper compartment. Reduction in pressure due to operation of the air recirculation fans has been conservatively neglected.

This analysis was conducted for the 8 inch, 6 inch and 2-1/2 inch break sizes assuming two spray pumps were operating (4000 gpm at 80°F). As shown in Table 14.3.4-2, the 8 inch break is the limiting case for this range of break sizes although the 0.6 DE is the limiting case for the entire spectrum of break sizes. With one spray pump operating (2000 gpm at 80°F) the limiting case for the entire spectrum of break sizes is the 8 inch case and results in an allowable deck leakage area of approximately 35 ft<sup>2</sup>.


A second, more realistic, method was used to analyze this limiting case. This analysis assumed a 30 percent air, 70 percent steam mixture flowing through the deck leakage area. This is conservative considering the amount of air in the lower compartment during this portion of the transient. Operation of the deck fan would increase the air content of the lower compartment, thus increasing the allowable deck leakage area. Based on the LOTIC Code analysis a structural heat removal rate of over 8000 Btu/sec from the upper compartment is indicated. Therefore a steam condensation rate of 8 lbm/sec was used for the upper compartment. The results indicated that with one spray pump operating and a deck leakage area of 56 ft<sup>2</sup>, the peak containment pressure will be below design for the 8 inch case.

The 1/2 inch diameter break is not sufficient to open the ice condenser inlet doors. For this break, either the lower compartment or the upper compartment spray is sufficient to condense the break steam flow.

In conclusion, it is apparent that there is a substantial margin between the design deck leakage area and that, which can be tolerated without exceeding containment design pressure. This is true for both the original design deck leakage area of 5 sq. ft. and the current design deck leakage of 7 sq. ft.

### **14.3.4.1.3.1.1.f      Effect of Dead-Ended Volumes**

In the preceding analysis of the containment compression ratio, it is conservatively assumed that only steam flows into the dead-ended volumes during the reactor coolant system blowdown. There are several dead-ended compartments in the plant containment design which are connected to the lower compartment. The dead-ended volumes considered in the containment integrity

 An AEP Company	<p style="text-align: center;"><b>INDIANA MICHIGAN POWER</b> <b>D. C. COOK NUCLEAR PLANT</b> <b>UPDATED FINAL SAFETY ANALYSIS REPORT</b></p>	<p>Revised: 29.0 Section: 14.3.4.1 Page: 11 of 21</p>
---	--	---

analysis are the instrumentation room and the pipe trench. Additional study has shown that the fan accumulator rooms would also act as dead-ended volumes. The storage of air in the dead-ended volumes has the effect of reducing the mass of air stored in the downstream volumes at the time of the compression peak pressure. Since including the dead-ended volumes reduces the calculated peak compression pressure, the results presented for the preceding analysis are conservative. It should be noted that the inclusion of the dead-ended volumes does not affect the magnitude of the second pressure peak, which occurs after the ice condenser has been exhausted, and after the dynamic effects of the blowdown have equalized throughout the containment. The second peak is controlling for plant design, therefore this discussion does not affect the available design margin.

The effect of the including the dead-ended volume was shown to decrease the final peak compression pressure by 0.2 psi. The magnitude of this effect was substantiated by a series of tests at Waltz Mill which were run at a mass compression ratio closely representative of the Cook plant design. Tests were run with and without a dead-ended volume equivalent to 155,000 ft<sup>3</sup> for the containment design. In these tests, the effect of the dead-ended volume was measured to be 0.5 psig, which is equivalent to a 0.32 psi decrease in final peak pressure per 100,000 ft<sup>3</sup> of dead-ended volume. At D.C. Cook, the dead-ended volume has been conservatively calculated to be 61,309 ft<sup>3</sup>.


#### **14.3.4.1.3.1.2 Long Term Containment Pressure Analysis**

Early in the ice condenser development program it was recognized that there was a need for modeling of long term ice condenser containment performance. It was realized that the model would have to have capabilities comparable to those of the dry containment (COCO Code) model. These capabilities would permit the model to be used to solve problems of containment design and optimize the containment and safeguards systems. This has been accomplished in the development of the LOTIC Code. (Reference 1)

The model of the containment consists of five distinct control volumes, as follows: the upper compartment, the lower compartment, the portion of the ice bed from which the ice has melted, the portion of the ice bed containing unmelted ice, and the dead ended compartments. The ice condenser control volume with unmelted ice is further subdivided into six subcompartments to allow for maldistribution of break flow to the ice bed.

The conditions in these compartments are obtained as a function of time by the use of fundamental equations solved through numerical techniques. These equations are solved for three distinct phases in time. Each phase corresponds to a distinct physical characteristic of the

# UFSAR Revision 30.0

 An AEP Company	<p style="text-align: center;"><b>INDIANA MICHIGAN POWER</b> <b>D. C. COOK NUCLEAR PLANT</b> <b>UPDATED FINAL SAFETY ANALYSIS REPORT</b></p>	<p>Revised: 29.0 Section: 14.3.4.1 Page: 12 of 21</p>
---	--	---

problem. Each of these phases has a unique set of simplifying assumptions based on test results from the Waltz Mill ice condenser test facility. These phases are the blowdown period, the depressurization period, and the long term.

The most significant simplification of the problem is the assumption that the total pressure in the containment is uniform. This assumption is justified by the fact that after the initial blowdown of the Reactor Coolant System, the remaining mass and energy released from this system into the containment are small and very slowly changing. The resulting flow rates between the control volumes will also be relatively small. These small flow rates are unable to maintain significant pressure differences between the compartments.


In the control volumes, which are always assumed to be saturated, steam and air are assumed to be uniformly mixed and at the control volume temperature. The air is considered a perfect gas and the thermodynamic properties of steam are taken from the ASME steam tables.

### **14.3.4.1.3.1.3 Peak Containment Pressure Transient**

The following are the major input assumptions used in the LOTIC analysis for the limiting double ended cold leg pipe rupture case with the steam generators considered as an active heat source for the Donald C. Cook Unit 2 containment:


1. Minimum safeguards are employed in all calculations, e.g., one of two spray pumps and one of two spray heat exchangers; one of two residual heat removal pumps and one of two residual heat removal heat exchangers with cross-tie valves open providing flow to the core; one of two safety injection pumps and one of two centrifugal charging pumps; and one of two air return fans.
2.  $2.2 \times 10^6$  pounds of ice initially in the ice condenser which is at 27°F. This temperature assumption maximizes the peak calculated pressure and corresponds to the 27°F Technical Specification limit.
3. The mass and energy releases described in Section 14.3.4.3 were used.
4. Blowdown and post blowdown ice condenser drain temperatures of 190°F and 130°F are used. (These numbers are based on Reference 2.)
5. Nitrogen from the accumulators in the amount of 4802.7 pounds is included in the calculations.
6. Essential service water temperature of 88.9°F is used for the spray heat exchanger and the component cooling heat exchanger.

## UFSAR Revision 30.0

 <p><b>INDIANA MICHIGAN POWER</b> <small>An AEP Company</small></p>	<p><b>INDIANA MICHIGAN POWER D. C. COOK NUCLEAR PLANT UPDATED FINAL SAFETY ANALYSIS REPORT</b></p>	<p>Revised: 29.0 Section:14.3.4.1 Page: 13 of 21</p>
--	--	--

7. The air return fan is effective 300 seconds after accident initiation.
8. No maldistribution of steam flow to the ice bed is assumed.
9. No ice condenser bypass is assumed. (This assumption depletes the ice in the shortest time and is thus conservative.)
10. The initial conditions in the containment are temperatures of 56°F in the upper, 60°F in the lower, 60°F in the dead ended and 27°F in the ice bed volumes. All volumes are at a pressure of 0.3 psig and 15 percent relative humidity, with the exception of the ice bed, which is at 100 percent relative humidity.
11. During the injection phase when the containment spray pumps are taking suction from the RWST, spray pump flow of 1960 gpm is used for the upper compartment and 706 gpm for the lower compartment. During the recirculation phase when the containment spray pumps are taking suction from the recirculation sump, containment spray flow to the upper compartment is 1960 gpm, containment spray flow to the lower compartment is 706 gpm.
12. Operators establish RHR spray no later than 70 minutes following the start of the accident, if the following conditions exist; 1) The Containment Spray System is in operation; 2) fewer than two (2) Containment Spray System (CTS) pumps are operating, and 3) the RHR system has been transferred to cold leg recirculation. The analysis uses the RHR spray flowrate of 1956.4 gpm..
13. Containment structural heat sink data are found in Table 14.3.4-4, and are assumed with conservatively low heat transfer coefficients, as listed in Table 14.3.4-5.
14. The operation of one containment spray heat exchanger ( $UA = 2.3 \times 10^6$  Btu/hr-°F) for containment cooling and the operation of one residual heat removal heat exchanger ( $UA = 2.2 \times 10^6$  Btu/hr-°F) for core cooling. The component cooling heat exchanger was modeled at  $3.433 \times 10^6$  Btu/hr-°F.
15. The air return fan returns air at a rate of 39,000 cfm from the upper to lower compartment.
16. A containment sump volume of 72,000 ft<sup>3</sup> is used.
17. The refueling water storage tank is at a temperature of 105°F.

## UFSAR Revision 30.0

 An AEP Company	<b>INDIANA MICHIGAN POWER</b> <b>D. C. COOK NUCLEAR PLANT</b> <b>UPDATED FINAL SAFETY ANALYSIS REPORT</b>	Revised: 29.0 Section:14.3.4.1 Page: 14 of 21
---	---	---

18. A core power of 3482 MWt (100.34% of 3470 MWt) is used in the calculation (see section 14.3.4.1.1, item 3 of the accident input assumptions and conditions).
19. Credit is taken for cooling of the ECCS water from the RHR heat exchanger during the recirculation mode, starting with the time water is first drawn from the recirculation sump.
20. Essential service water flow to the containment spray heat exchanger was modeled as 2400 gpm. The essential service water flow to the component cooling heat exchanger was modeled as 5000 gpm.
21. The component cooling flow to the RHR heat exchanger was modeled as 5000 gpm.
22. The spurious operation of the upper containment ventilation heaters is included in the model as a 288 kW additional heat input.

With these assumptions, the heat removal capability of the containment is sufficient to absorb the energy releases and still keep the maximum calculated pressure well below design.

The following plots are provided:

- Figure 14.3.4-6, Containment pressure transient.
- Figure 14.3.4-7, Upper compartment temperature transients.
- Figure 14.3.4-8, Lower compartment temperature transients.
- Figure 14.3.4-9, Containment sump temperature transient.
- Figure 14.3.4-10, Ice melt transient.


In addition, Tables 14.3.4-6A and 14.3.4-6B give energy accountings at various points in the transient.

The analysis results show that the maximum calculated containment pressure is 10.51 psig, for the double-ended cold leg minimum safeguards case. This pressure peak occurs at approximately 11,170 seconds, with ice bed meltout at approximately 7,855 seconds.

Non-condensable hydrogen gas is generated during the limiting design basis LOCA event (i.e. the double ended rupture of a cross-over leg), by several sources: hydrogen that is dissolved in the RCS, hydrogen generated by fuel clad oxidation, radiolysis in the core or by core material that has relocated to the containment sump, and hydrogen generated by corrosion of metal surfaces inside containment. The total hydrogen produced was calculated as a function of time,



## UFSAR Revision 30.0

 An AEP Company	<p style="text-align: center;"><b>INDIANA MICHIGAN POWER</b> <b>D. C. COOK NUCLEAR PLANT</b> <b>UPDATED FINAL SAFETY ANALYSIS REPORT</b></p>	<p>Revised: 29.0 Section: 14.3.4.1 Page: 15 of 21</p>
---	--	---

and the result used to calculate a partial pressure, which is then added to the peak containment pressure. The peak pressure was calculated to increase by 0.1 psig due to non-condensable hydrogen.

Following a LOCA event, the control room operators use the control air system to perform certain recovery and monitoring operations. Given the potential for in-leakage from this system into the containment, the partial pressure from this air must be considered in the peak pressure transient calculation. However, the timing of these remote manual recovery and monitoring operations is not explicitly modeled, so a time-dependent partial pressure transient has not been calculated. Instead, a portion of the containment pressure margin has been allotted to address this air. The control air system leakage will be limited by operator action, such that the effect on containment pressure will be less than 0.1 psi.

The ECCS pumps take suction from the RWST during the injection phase following a LOCA. As RWST volume is injected, the control room operator will transfer the ECCS pump suctions to the recirculation sump. During transfer to recirculation, the component cooling water flow to the RHR heat exchanger is increased. The evaluated impact of up to a 15-minute delay in the increase in CCW flow, during the transfer to recirculation, has an effect on the calculated containment peak pressure of less than 0.04 psi.

A failure of a flexible hose that connects the backup air supply bottles to the pressurizer power operated relief valves (PORVs) will discharge the contents of the air bottles to the containment. The partial pressure from this air must also be considered in the peak pressure transient calculation. The additional effect on containment pressure is calculated as 0.03 psi.

Chapter 5.5.3 describes the upper compartment ventilation units. Following a LOCA event, the spurious operation of the electric heaters in these units has been considered in the containment integrity analysis.


Therefore, when considering the calculated peak containment pressure for the design basis LOCA mass and energy release, including the contribution due to non-condensable hydrogen, control air system leakage, CCW flow during transfer to recirculation, and PORV backup air bottles, the total calculated peak containment pressure is 10.78 psig, which compares favorably to the containment design pressure of 12 psig.

### **14.3.4.1.3.1.4 Structural Heat Removal**

Provision is made in the containment pressure analysis for heat storage in interior and exterior walls. Each wall is divided into a number of nodes. For each node, a conservation of energy



## UFSAR Revision 30.0

 An AEP Company	<p style="text-align: center;"><b>INDIANA MICHIGAN POWER</b> <b>D. C. COOK NUCLEAR PLANT</b> <b>UPDATED FINAL SAFETY ANALYSIS REPORT</b></p>	<p>Revised: 29.0 Section: 14.3.4.1 Page: 16 of 21</p>
---	--	---

equation expressed in finite difference form accounts for transient conduction into and out of the node and temperature rise of the node. Table 14.3.4-4 is a summary of the containment structural heat sinks used in the analysis. The material property data used are found in Table 14.3.4-5.

The heat transfer coefficient to the containment structures is based primarily on the work of Tagami. An explanation of the manner of application is given in Reference (4).

When applying the Tagami correlation, a conservative limit was placed on the lower compartment stagnant heat transfer coefficients. They were limited to 72 Btu/hr-ft<sup>2</sup>. This corresponds to a steam-air ratio of 1.4 according to the Tagami correlation. The imposition of this limitation is to restrict the use of the Tagami correlation within the test range of steam-air ratios where the correlation was derived.

#### **14.3.4.1.3.1.5 Relevant Acceptance Criteria**


The LOCA mass and energy analysis has been performed in accordance with the criteria shown in the Standard Review Plan (SRP) section 6.2.1.3. In this analysis, the relevant requirements of General Design Criteria (GDC) 50 and 10 CFR Part 50 Appendix K have been included by confirmation that the calculated pressure is less than the design pressure, and because all available sources of energy have been included, which is more restrictive than the old GDC criteria, Appendix H of the original FSAR, to which the Donald C. Cook Plants are licensed. These sources include reactor power, decay heat, core stored energy, energy stored in the reactor vessel and internals, metal-water reaction energy, and stored energy in the secondary system.

Although the Donald C. Cook Nuclear Plant is not a Standard Review Plan plant, the containment integrity peak pressure analysis has been performed in accordance with the criteria shown in the SRP Section 6.2.1.1.b, for ice condenser containments. Conformance to GDC's 16, 38, and 50 is demonstrated by showing that the containment design pressure is not exceeded at any time in the transient. This analysis also demonstrates that the containment heat removal systems function to rapidly reduce the containment pressure and temperature in the event of a LOCA.

#### **14.3.4.1.3.1.6 Conclusions**

Based upon the information presented, taking into account modifications made to the containment and ECCS systems and related changes to the accident analysis input assumptions, it has been concluded that operation with the revised plant conditions and increased operating margins for the Donald C. Cook Nuclear Plant is acceptable. Operation with the RHR crosstie valve open was modeled.

## UFSAR Revision 30.0

 An AEP Company	<p style="text-align: center;"><b>INDIANA MICHIGAN POWER</b> <b>D. C. COOK NUCLEAR PLANT</b> <b>UPDATED FINAL SAFETY ANALYSIS REPORT</b></p>	<p>Revised: 29.0 Section: 14.3.4.1 Page: 17 of 21</p>
---	--	---


The peak containment pressure of 10.78 psig is below the design pressure 12.0 psig. Thus, the most limiting case has been considered, and has been demonstrated to yield acceptable results.

### **14.3.4.1.3.2 Steam Line Break**

Following a steam line break in the lower compartment of an ice condenser plant, two distinct analyses must be performed. The first analysis, the short term pressure analysis, has been performed with the TMD Code. The second analysis, the long term analysis, does not require the large number of nodes which the TMD analysis requires. The computer code which performs this analysis is the LOTIC (Reference 1) Code.

The LOTIC Code includes the capability to calculate the superheat conditions, and has the ability to begin calculations from time zero (References 6, 7, and 8). The major thermodynamic assumption which is used in the steam break analysis is complete re-evaporation of the condensate under superheated conditions for large breaks. For the most limiting small breaks, no re-evaporation is assumed; however, convective heat transfer as detailed in (Reference 7) is used. The version of the LOTIC Code which incorporates the above is the LOTIC3 Code (Reference 9). This code was used to perform the steam line break analyses and is the version which has been accepted for this use (References 10, and 11).

## UFSAR Revision 30.0


 An AEP Company	<p style="text-align: center;"><b>INDIANA MICHIGAN POWER</b> <b>D. C. COOK NUCLEAR PLANT</b> <b>UPDATED FINAL SAFETY ANALYSIS REPORT</b></p>	<p>Revised: 29.0 Section: 14.3.4.1 Page: 18 of 21</p>
---	--	---

### **14.3.4.1.3.2.1 Peak Containment Temperature Transients**

The following are the major input assumptions used in the LOTIC3 steam break analysis:

1. Minimum safeguards are employed; e.g., one of two spray pumps and one of two air return fans.
2. The air return fan is effective 132 seconds after the high-1 containment pressure bistable signal is actuated.
3. A uniform distribution of steam flow into the ice bed is assumed.
4. The total initial ice mass is  $2.2 \times 10^6$  lbs.
5. The initial conditions in the containment are a temperature of 120°F in the lower and dead-ended volumes, a temperature of 57°F in the upper volume, and a temperature of 27°F in the ice condenser. All volumes are at a pressure of 0.3 psig and a relative humidity of 15%, with the exception of the ice bed, which is at 100% relative humidity.
6. A spray pump flow of 1967 gpm is used in the upper compartment and 706 gpm in the lower compartment. The spray initiation time assumed was 115 sec. after reaching the high-high setpoint.
7. The refueling water storage tank temperature is assumed to be 105°F.
8. ESW is not assumed for the MSLB transient.
9. Containment structural heat sinks as presented in Table 14.3.4-4 were used.
10. The air return fan empties air at a rate of 39,000 cfm from the upper to the lower compartments.
11. The material property data given in Table 14.3.4-5 were used.
12. The mass and energy releases given in Tables 14.3.4-7 and 14.3.4-8 were used. Since these rates are considerably less than the RCS double-ended breaks, and their total integrated energy is not sufficient to cause ice bed meltout, the containment pressure transients generated for the previously presented double-ended pump suction RCS break is considerably more severe.
13. The heat transfer coefficients to the containment structures are based on the work of Tagami. An explanation of their manner of application is given in References (4), (6) and (7).

## UFSAR Revision 30.0

 An AEP Company	<p style="text-align: center;"><b>INDIANA MICHIGAN POWER</b> <b>D. C. COOK NUCLEAR PLANT</b> <b>UPDATED FINAL SAFETY ANALYSIS REPORT</b></p>	<p>Revised: 29.0 Section: 14.3.4.1 Page: 19 of 21</p>
---	--	---

14. The spurious operation of the upper containment ventilation heaters is included in the model as a 288 kW additional heat input.

### **14.3.4.1.3.2.2 Results**

The results of the analysis are presented in Table 14.3.4-9. The worst case of the double ended steam line breaks was a 1.4 ft<sup>2</sup> break, occurring at 102% power with main steam line isolation valve failure (MSIV). This temperature transient is shown in Figures 14.3.4-11-A and 14.3.4-11-B.

The results from the steam line split ruptures (or small breaks) are presented in Table 14.3.4-10. The worst case for these cases is a 0.860 ft<sup>2</sup> split break, occurring at 102% of a core power of 3588 MWt, with an Auxiliary Feedwater Runout Protection (AFWRP) failure. A temperature transient of this case is presented in Figures 14.3.4-12-A and 14.3.4-12-B.

Parametric studies have been performed as part of previous analyses, varying the ice mass between 2.0 and 2.45 million pounds. These previous ice mass parameter studies have shown that the maximum calculated containment temperature is not sensitive (less than 1°F change) to ice mass over this range.

### **14.3.4.1.3.2.3 Sensitivity of the Results**

The previous section pertains to the steam line break analysis and its subsequent response in identifying the limiting small break. The following evaluation describes additional sensitivity studies of a generic nature, performed for smaller breaks up to 0.942 ft<sup>2</sup> at 30% power.


The LOTIC-3 computer code was employed in the generic analysis (Reference 9). The LOTIC-3 computer code was found to be acceptable for the analysis of steam line breaks with the following restrictions (Reference 11):

- a. Mass and energy release rates are calculated with an approved model.
- b. Complete spectrum of breaks are analyzed.
- c. Convective heat flux calculations are performed for all break sizes.

A detailed comparison of the Cook Nuclear Plant characteristics with those of the generic plant can be found in Reference 13.

Figure 14.3.4-13 illustrates a comparison of small break cases, specifically 0.942 ft<sup>2</sup>, from Cook Nuclear Plant historical analyses with a similar break from the generic plant small break submittals. The figure shows that the elevated containment temperatures for Cook Nuclear Plant last for a shorter duration than predicted in the transient for the generic plant.

## UFSAR Revision 30.0

 An AEP Company	<p style="text-align: center;"><b>INDIANA MICHIGAN POWER</b> <b>D. C. COOK NUCLEAR PLANT</b> <b>UPDATED FINAL SAFETY ANALYSIS REPORT</b></p>	<p>Revised: 29.0 Section: 14.3.4.1 Page: 20 of 21</p>
---	--	---

Further, the containment pressure High-2 setpoint, which provides the actuation signal for the containment spray and containment air recirculation fan systems, was assumed to be 3.5 psig in the generic analysis. The Safety Analysis Limit (SAL) for the Cook Nuclear Plant High-1 and High 2 containment pressure setpoints are modeled to be 1.75 and 3.5 psig, respectively. In the Cook Nuclear Plant, the fans are started on High-1 and spray is started on High-2 containment pressure signals. The actuation setpoint would have been reached sooner in the Cook Nuclear Plant compared to the generic plant; therefore the containment transient would have been mitigated more rapidly.


As a result, a generic LOTIC3 spectrum of small breaks analysis is provided here for the Cook Nuclear Plant instead of plant specific analysis. The generic analysis provides the containment responses for a spectrum of small breaks at the 30% power level with assumed failure of the auxiliary feedwater runout protection system. The analyses studied a spectrum of breaks ranging in size from 0.1 ft<sup>2</sup> up to the break identified as the most severe small split break, 0.942 ft<sup>2</sup>. The lower bound break size was established in discussions held between the NRC staff and Westinghouse Electric Corporation.

This spectrum included breaks of 0.6, 0.35 and 0.10 ft<sup>2</sup>. Figures 14.3.4-14 and 14.3.4-15 provide the upper compartment temperature and lower compartment pressure transients. As Figure 14.3.4-16 shows, similar lower compartment temperature transients were calculated for the spectrum of breaks analyzed. However, the 0.6 ft<sup>2</sup> break resulted in a slightly higher maximum lower compartment temperature (see Table 14.3.4-11). When this transient was compared to the transient identified as the most severe small break at 30% power in the previous analysis, it was found to result in very similar peaks, with the difference being incidental to the results (See Figure 14.3.4-17).

In the generic analysis, spray and fan initiation are automatic after reaching the containment High-2 setpoint. Associated times are included in Table 14.3.4-11. As described above, these times are conservative in regard to the Cook Nuclear Plant, where the containment air recirculation fans are actuated by the High-1 containment pressure bistable signal. Tables 14.3.4-12 and 14.3.4-13 provide the mass and energy release rates for the transients analyzed. These results demonstrate the conservatism of the results previously discussed and also the somewhat insensitive nature of the ice condenser plant containment response to break size.


Table 14.3.4-14 further demonstrates the conservatism of the generic analysis discussed above. The actual plant specific analysis results for the smaller breaks would be similar to the Cook Nuclear Plant results in Figure 14.3.4-13. The temperature would peak, then sharply fall off

**UFSAR Revision 30.0**


 An <b>AEP</b> Company	<p><b>INDIANA MICHIGAN POWER</b> <b>D. C. COOK NUCLEAR PLANT</b> <b>UPDATED FINAL SAFETY ANALYSIS REPORT</b></p>	<p>Revised: 29.0 Section:14.3.4.1 Page: 21 of 21</p>
--	--	--

when the sprays come on, and finally settle to a much lower temperature level for the remainder of the transient.

# UFSAR Revision 30.0

 An AEP Company	INDIANA MICHIGAN POWER D. C. COOK NUCLEAR PLANT UPDATED FINAL SAFETY ANALYSIS REPORT	Revised: 27.0 Section:14.3.4.2 Page: i of i
---	--	---

<b>14.3 REACTOR COOLANT SYSTEM PIPE RUPTURE (LOSS OF COOLANT ACCIDENT)</b>	<b>1</b>
<b>14.3.4 Containment Integrity Analysis</b>	<b>1</b>
14.3.4.2 Containment Subcompartments	1
14.3.4.2.1 Design Basis	1
14.3.4.2.2 Design Features	1
14.3.4.2.3 Design Evaluation	2
14.3.4.2.3.1 <i>Application to the Station Design</i>	3
14.3.4.2.4 Steam Generator Enclosure Evaluation	4
14.3.4.2.5 Pressurizer Enclosure Evaluation	7
14.3.4.2.6 Fan Accumulator Room Evaluation	8
14.3.4.2.7 Loop Subcompartments Evaluation	10
14.3.4.2.7.1 <i>Base Model Analysis</i>	10
14.3.4.2.7.2 <i>Current Analysis</i>	11
<i>Peak Differential Pressure</i>	14
<i>Peak Differential Pressure Between the Steam Generator Enclosure and the Ice Condenser</i>	15
14.3.4.2.8 Reactor Cavity Evaluation	16
14.3.4.2.8.1 <i>Upper Reactor Cavity</i>	19
14.3.4.2.8.2 <i>Lower Reactor Cavity</i>	20
14.3.4.2.8.3 <i>Reactor Vessel Annulus and Reactor Pipe Annulus</i>	21
14.3.4.2.8.4 <i>Reactor Vessel Nozzle Inspection Hatch Cover</i>	22
14.3.4.2.9 Short Term Containment Analysis Conclusions	22

 An AEP Company	<p>INDIANA MICHIGAN POWER D. C. COOK NUCLEAR PLANT UPDATED FINAL SAFETY ANALYSIS REPORT</p>	<p>Revised: 27.0 Section: 14.3.4.2 Page: 1 of 22</p>
---	---	--

## **14.3 REACTOR COOLANT SYSTEM PIPE RUPTURE (LOSS OF COOLANT ACCIDENT)**

### **14.3.4 Containment Integrity Analysis**

#### **14.3.4.2 Containment Subcompartments**

The containment building sub compartments are the fully or partially enclosed volumes within the containment, which contain high-energy lines. These sub compartments are designed to limit the adverse effects of a postulated high-energy pipe rupture within them.

The short term mass and energy sub compartment analysis represents the initial seconds of the blowdown phase of the postulated rupture. The short-term analyses results are used in the design of the sub compartment walls in the ice condenser containment.

##### **14.3.4.2.1 Design Basis**

Consideration is given in the design of the containment internal structures to localized pressure pulses that could occur following a postulated pipe break. If a pipe break accident were to occur due to a pipe rupture in these relatively small volumes, the pressure would build up at a rate faster than the overall containment, thus imposing a differential pressure across the walls of the structures.

These sub compartments include the steam generator enclosure, fan accumulator room, pressurizer enclosure, loop sub compartment and upper and lower reactor cavity. Each compartment is designed for the largest blowdown flow resulting from the severance of the largest connecting pipe within the enclosure or the blowdown flow into the enclosure from a break in an adjacent region.


The following sections summarize the design basis calculations.

##### **14.3.4.2.2 Design Features**

The basic performance of the Ice Condenser Reactor Containment System has been demonstrated for a wide range of conditions by the Waltz Mill Ice Condenser Test Program (Reference 2). These results have clearly shown the capability and reliability of the ice condenser concept to limit the containment pressure rise subsequent to a hypothetical loss-of-coolant accident.

To supplement this experimental proof of performance, a mathematical model has been developed to simulate the ice condenser pressure transients. This model, encoded as computer



 <b>INDIANA MICHIGAN POWER</b> <b>D. C. COOK NUCLEAR PLANT</b> <b>UPDATED FINAL SAFETY ANALYSIS REPORT</b>	Revised: 27.0 Section:14.3.4.2 Page: 2 of 22
---	--

program TMD (Transient Mass Distribution), provides a means for computing pressures, temperatures, heat transfer rates, and mass flow rates as a function of time and location throughout the containment. This model is used to compute pressure differences on various structures within the containment as well as the distribution of steam flow as the air is displaced from the lower compartment. Although the TMD Code can calculate the entire blowdown transient, the peak pressure differences on various structures occur within the first few seconds of the transient.

#### **14.3.4.2.3 Design Evaluation**

The mathematical modeling in TMD is similar to that of the SATAN blowdown code in that the analytical solution is developed by considering the conservation equations of mass, momentum, and energy and the equation of state, together with the control volume technique for simulating spatial variation. The governing equations for TMD are given in Reference (14).


The moisture entrainment modifications to the TMD Code are discussed in detail in Reference (14). These modifications comprise incorporating the additional entrainment effects into the momentum and energy equations.

As part of the review of the TMD Code, additional effects are considered. Changes to the analytical model required for these studies are described in Reference (14).

These studies consist of:

- a. Spatial acceleration effects in ice bed.
- b. Liquid entrainment in ice beds.
- c. Upper limit on sonic velocity.
- d. Variable ice bed loss coefficient.
- e. Variable door response.
- f. Wave propagation effects.

## UFSAR Revision 30.0

 An AEP Company	<p style="text-align: center;"><b>INDIANA MICHIGAN POWER</b> <b>D. C. COOK NUCLEAR PLANT</b> <b>UPDATED FINAL SAFETY ANALYSIS REPORT</b></p>	<p>Revised: 27.0 Section: 14.3.4.2 Page: 3 of 22</p>
---	--	--

### **14.3.4.2.3.1**      **Application to the Station Design**


The containment subcompartments include the steam generator enclosure, the pressurizer enclosure, the fan accumulator room, the loop subcompartment and the upper and lower reactor cavity. Each of these containment subcompartments have been divided into nodes as shown on the following figures which represent the TMD nodalization model for each subcompartment.

- Figure 14.3.4-25      Steam Generator Enclosure
- Figure 14.3.4-27      Pressurizer Enclosure
- Figure 14.3.4-30      Fan Accumulator Room
- Figure 14.3.4-31      Loop Subcompartment
- Figure 14.3.4-34      Reactor Cavity

The TMD base model includes Nodes 1-45 as illustrated on Figures 14.3.4-18 through 14.3.4-21. The base model for the loop subcompartment, the steam generator enclosure and the pressurizer enclosure are identical. The fan accumulator room model is similar to the loop subcompartment model with one exception. In the loop subcompartment model, Node 27 represents one fan accumulator room. In the fan accumulator room model, the fan accumulator room is divided into five nodes based on the geometry of the subcompartment and internal equipment. These details are illustrated in Figures 14.3.4-28 and 14.3.4-29. The reactor cavity TMD model is significantly different than the 45 node TMD base model. The reactor cavity TMD model divides the reactor cavity area into 62 nodes, based on the geometry of the reactor cavity area. This basic geometry is shown on Figure 14.3.4-33. Figure 14.3.4-34 illustrates the complete nodalization network.

The division of the lower compartment into six volumes occurs at the points of greatest flow resistance, i.e., the four steam generators, pressurizer, and refueling cavity. Each of these lower compartment sections delivers flow through ice condenser lower inlet doors into a section behind the doors and below the ice bed. Each vertical section of the ice bed is, in turn, divided into nodes. The upper plenum between the top of the ice bed and the top deck doors is represented by another node. Thus, a total of thirty nodes (Nodes 7 through 24 and 34 through 45) are used to simulate the ice condenser. The nodes at the top of the ice bed between the ice bed and top deck doors deliver to Node 25, the upper compartment. Note that cross flow in the ice bed is not accounted for in the analysis; this yields the most conservative results for the particular calculations described herein. The upper reactor cavity (Node 33) is connected to the lower compartment volumes and provides cross flow for pressure equalization of the lower

## UFSAR Revision 30.0

 An AEP Company	<p style="text-align: center;"><b>INDIANA MICHIGAN POWER</b> <b>D. C. COOK NUCLEAR PLANT</b> <b>UPDATED FINAL SAFETY ANALYSIS REPORT</b></p>	<p>Revised: 27.0 Section: 14.3.4.2 Page: 4 of 22</p>
---	--	--


compartments. The less active compartments, called dead ended compartments (Nodes 26, 28, 29, 30 and 32), and the fan accumulator compartments (Nodes 27 and 31) outside the crane wall are pressurized by ventilation openings through the crane wall into the fan compartments.

For each node in the TMD network the volume (refer to Tables 14.3.4-21 through 14.3.4-25), initial pressure, and initial temperature conditions are specified. The ice condenser elements have additional inputs of mass of ice, heat transfer area, and condensate layer length. The required flow characteristics for each flow path between nodes are: loss coefficient ( $K$ ), friction factor ( $f$ ), inertia length ( $L_I$ ), hydraulic diameter ( $D_H$ ), minimum flow path area ( $A_T$ ), equivalent length ( $L_E$ ) and area ratios ( $A_T/A$ ). In the TMD analysis, the loss coefficient ( $K$ ) is used to calculate the pressure losses due to flow across equipment, projections, or sudden expansions and contractions. The  $fL_E/D_H$  term is used to calculate the frictional pressure loss.  $A_T$  is the minimum flow area for the path. The  $L_I/A_T$  term is used to account for inertia effects of the fluid in the momentum equation. The area ratios ( $A_T/A$ ) are used to account for compressibility effects of the fluid. In addition, the ice condenser loss coefficients have been based on the 1/4 scale tests representative of the current ice condenser geometry. The loss coefficient is based on removal of door port flow restrictors. To better represent short term transient effects, the opening characteristics of the lower, intermediate, and top deck ice condenser doors have also been modeled in the TMD Code. The TMD analysis evaluates a range of containment parameters for subcompartment peak pressure and differential pressures. These parameters include containment pressure, containment temperature, containment humidity, and ice condenser temperature. The bounding conditions are listed in each subcompartment evaluation that are described in the following sections.

### **14.3.4.2.4 Steam Generator Enclosure Evaluation**

Two breaks were analyzed for the steam generator enclosure, a main steam line break and a feedwater line break. The largest and most severe break possible in the steam generator enclosure is a double-ended break of the steam line. Based upon the high-energy line break analyses, this break can only occur in the enclosure at the terminal end at the nozzle (at the top of the enclosure). For the feedwater line break event, the break is postulated to occur at the side of the steam generator at the feedwater line inlet nozzle. The limiting mass and energy releases from these breaks are from the hot shutdown condition (no load). Refer to Section 14.3.4.4.1 for the initial conditions and assumptions used to determine the short-term mass and energy releases for the steam line and feedwater line breaks. The mass and energy release rates for the steam generator enclosure analysis are presented in Table 14.3.4-15 for both the main steam line break and the feedwater line break.

## UFSAR Revision 30.0

 An AEP Company	<p style="text-align: center;"><b>INDIANA MICHIGAN POWER</b> <b>D. C. COOK NUCLEAR PLANT</b> <b>UPDATED FINAL SAFETY ANALYSIS REPORT</b></p>	<p>Revised: 27.0 Section: 14.3.4.2 Page: 5 of 22</p>
---	--	--

The range of initial containment conditions considered for the analyses are as follows:

- Temperature range of 60-185°F (Reference 45)
- Pressure range of 13.2-15.0 psia
- Humidity range of 15-100 percent
- Ice Condenser Temperature range of 10-30°F


The limiting values for containment temperature and pressure are given in Tables 14.3.4-33 and 14.3.4-34. For all cases, the limiting condition for humidity is at 15%. For the steam line break, the limiting ice condenser temperature is 30°F and for the feedwater line break the limiting values are presented in Table 14.3.4-34. In addition, the jet momentum from the steam blowdown from the main steam or feedwater line break within the steam generator enclosure would be large enough to blow the HVAC ductwork out the enclosures.

The steam generator enclosure TMD nodalization network is similar to the models for the pressurizer enclosure and the loop subcompartment for the first 45 nodes. Nodes 46-63 represent the steam generator enclosures. The nodalization network for the steam generator enclosures are illustrated in Figures 14.3.4-18 through 14.3.4-21 and Figures 14.3.4-24 and 14.3.4-25. Figure 14.3.4-18 illustrates the TMD model plan view at the equipment room elevation. Figure 14.3.4-19 provides the TMD model containment section view. Figure 14.3.4-20 is the plan view at the ice condenser compartments. Figure 14.3.4-21 contains the layout of the containment shell for the TMD model. Figures 14.3.4-22 and 14.3.4-23 show the details of the steam generator subcompartment used in the analysis. Figures 14.3.4-24 and 14.3.4-25 show the 18 node TMD steam generator enclosure model (9 nodes per enclosure) which was used in the analytical model.

This TMD model is designed to represent a steam generator pair as denoted in Figure 14.3.4-25 as Enclosure A and Enclosure B. The steam line break was postulated to occur in the steam generator enclosure in either Node 46 or 55. The feedwater line break was postulated to occur in the steam generator enclosure in either Node 54 or 63.

The TMD input flow path characteristics are based upon incompressible flow modeling. The TMD program adjusts the incompressible flow equations with the area ratios ( $A_T/A$ ) to account for compressible effects in the high subsonic flow regime. The TMD flow path input data for the steam generator enclosure is contained in Tables 14.3.4-26 and 14.3.4-27.

## UFSAR Revision 30.0


 An AEP Company	<p style="text-align: center;"><b>INDIANA MICHIGAN POWER</b> <b>D. C. COOK NUCLEAR PLANT</b> <b>UPDATED FINAL SAFETY ANALYSIS REPORT</b></p>	<p>Revised: 27.0 Section: 14.3.4.2 Page: 6 of 22</p>
---	--	--

The steam generator enclosure free volumes and vent areas, which represent Enclosure A, and Enclosure B are given in Table 14.3.4-32. As shown in Table 14.3.4-32, the free volume and vent area for the steam generator pair is not identical. The vent area represents the minimum flow path area leaving the steam generator enclosure. The vent area for the steam generator enclosure (Enclosure A) is determined by summing the minimum flow path areas from Nodes 46-47, 48, 49, 50, 55, 47-56, 48-57, 47-51, 48-52, 49-53 and 50-54. The vent area for Enclosure B is determined in a similar fashion.

The maximum calculated differential pressure between the steam generator enclosure and the upper compartment due to a postulated steam line break is 42.77 psid (Reference 45). The maximum calculated differential pressure between the steam generator enclosure and the upper compartment due to a postulated feedwater line break is 16.29 psid. A complete summary of the peak differential pressures across the structures and the steam generator vessel are shown in Table 14.3.4-33 for the steam line break and Table 14.3.4-34 for the feedwater line break. Figures 14.3.4-35 through 14.3.4-52 present the differential pressure time histories for the steam line break. The Steam Line Break (SLB) Figures are for information only, and have not been updated to reflect results of Reference 45, and should not be used as input in other analyses. Figures 14.3.4-53 through 14.3.4-70 present the differential time histories for the feedwater line break.

It should be noted that the analyses discussed above are only for short term pressure peaks and are not applicable to long term type analyses. The dynamic analysis of the affected structures and of the steam generator vessel supports has shown that the effects of the short duration peak pressures will not result in consequences that will adversely affect the public health and safety.

## UFSAR Revision 30.0

 An AEP Company	<p style="text-align: center;"><b>INDIANA MICHIGAN POWER</b> <b>D. C. COOK NUCLEAR PLANT</b> <b>UPDATED FINAL SAFETY ANALYSIS REPORT</b></p>	<p>Revised: 27.0 Section: 14.3.4.2 Page: 7 of 22</p>
---	--	--

### **14.3.4.2.5 Pressurizer Enclosure Evaluation**

The largest break possible in the pressurizer enclosure, a double-ended break of the spray line from the reactor coolant system, is postulated to occur at the top of the enclosure. The spray line break mass and energy releases are presented in Table 14.3.4-16. The RCS data utilized for the analysis is as follows:

- |                                      |               |
|--------------------------------------|---------------|
| • NSSS Power                         | 3600 MWt      |
| • RCS Pressure (psia)                | 2250          |
| • Core Average Temperature (°F)      | 549.9 - 584.9 |
| • Vessel Outlet Temperature (°F)     | 582.2 - 615.2 |
| • Vessel/Core Inlet Temperature (°F) | 511.7 - 547.6 |

Measurement uncertainties of +67 psi for system pressure and +/-5.1°F for temperature are applied to the RCS data. The spray line mass and energy releases were determined utilizing the following bounding RCS initial conditions:


- Vessel/Core Inlet Temperature of 506.6°F
- RCS Pressure of 2317 psia

The range of initial containment conditions bounded by the TMD analysis for the pressurizer enclosure includes the following:

- Temperature range of 60-171°F
- Pressure range of 13.2-15.0 psia
- Humidity range of 15-100 percent
- Ice Condenser Temperature range of 10-30°F

The low pressure (13.2 psia), low temperature (60°F), low humidity (15%) case was determined to be bounding for evaluation of the pressurizer enclosure and containment response. Sensitivity studies were performed to evaluate the effect of varying the ice condenser temperature on the peak differential pressure. The analysis for the pressurizer enclosure was performed using an ice condenser temperature of 30°F. Using an ice condenser temperature of 10°F will increase the resulting peak differential pressure acting across the wall between the inside of the enclosure and the upper compartment. This increase is bounded by the margin currently applied to the pressurizer enclosure analysis.

## UFSAR Revision 30.0

 An AEP Company	<p style="text-align: center;"><b>INDIANA MICHIGAN POWER</b> <b>D. C. COOK NUCLEAR PLANT</b> <b>UPDATED FINAL SAFETY ANALYSIS REPORT</b></p>	<p>Revised: 27.0 Section: 14.3.4.2 Page: 8 of 22</p>
---	--	--

The loop subcompartment model (without the nodalization for the steam generator enclosures) was used as a base model for the pressurizer enclosure. The loop subcompartment model was modified to include Nodes 46-49 which represent the pressurizer enclosure in the model.

The pressurizer enclosure TMD nodalization network is similar to the models for the loop subcompartment and the steam generator enclosure for the first 45 nodes. Nodes 46-49 represents the pressurizer enclosure in the model. The nodalization network for the pressurizer enclosure is illustrated in Figures 14.3.4-18 through 14.3.4-21 and Figure 14.3.4-27. Figure 14.3.4-18 illustrates the TMD model plan view at the equipment room elevation. Figure 14.3.4-19 provides the TMD model containment section view. Figure 14.3.4-20 is the plan view at the ice condenser compartments. Figure 14.3.4-21 contains the layout of the containment shell for the TMD model. Figure 14.3.4-26 illustrates the nodalization specific to the pressurizer enclosure and Figure 14.3.4-27 illustrates the nodalization network and flow paths. The spray line break was postulated to occur at the top of the pressurizer enclosure in Node 46.

The TMD input flow path characteristics are based upon incompressible flow modeling. The TMD program adjusts the incompressible flow equations with the area ratios ( $A_T/A$ ) to account for compressible effects in the high subsonic flow regime. The TMD flow path input data for the pressurizer enclosure is contained in Table 14.3.4-28. Refer to Section 14.3.4.2.3.1 for definition of table terms.

The net free volume and the vent area for the pressurizer enclosure is presented in Table 14.3.4-32. The vent area represents the minimum flow path area leaving the pressurizer enclosure. The vent area for the pressurizer enclosure is determined by summing the minimum flow path areas from Nodes 47-4, 48-4 and 49-4.


Figures 14.3.4-71 through 14.3.4-75 illustrate the pressure time histories for the upper compartment and the pressurizer enclosure. The maximum calculated differential pressure is 8.82 psid. The maximum calculated differential pressure across the vessel is 0.45 psid. An additional 10% margin is included in the results to bound the results and provide conservatism.

### **14.3.4.2.6 Fan Accumulator Room Evaluation**

The fan accumulator room enclosure is designed for a double-ended break in the 30 inch steam line (inside area of 4.27 ft<sup>2</sup>) downstream of the steam line flow restrictor. This is the inline flow venturi downstream of the steam generator nozzle. The break occurs in the longest line with an orifice of 1.4 ft<sup>2</sup> in the cross connection with the steam dump header. This orifice in the turbine building restricts backflow so that the entrained flow from the other three steam generators will



## UFSAR Revision 30.0

 An AEP Company	<b>INDIANA MICHIGAN POWER</b> <b>D. C. COOK NUCLEAR PLANT</b> <b>UPDATED FINAL SAFETY ANALYSIS REPORT</b>	Revised: 27.0 Section: 14.3.4.2 Page: 9 of 22
---	---	---

not reach the break before the main steam isolation valves close at ten seconds, reducing the pressure peak. The mass and energy release rates for this case are presented in Table 14.3.4-17.

The mass and energy releases consist of both the initial steam blowdown from the steam generator side of the break (forward flow) with choking conditions reached in the inline flow venturi and the reverse flow (steam flow coming out of the turbine end of the break). The blowdown consists of steam at 1192 BTU/lb, which corresponds to the saturation enthalpy at 1020 psia. The TMD computer code assuming unaugmented critical flow was used to calculate the pressurization response inside the fan accumulator room to the postulated break in the main steam line. The range of initial containment conditions considered for the analysis are as follows:

- Temperature range of 60-120°F
- Pressure range of 13.2-15.0 psia
- Humidity range of 15-100 percent
- Ice Condenser Temperature range of 10-30°F


The low pressure (13.2 psia), low temperature (60°F), low humidity (15%), low ice condenser temperature (10°F) case was determined to be bounding for determination of the peak differential pressure. High pressure (15.0 psia), low temperature (60°F), low humidity (15%), high ice condenser temperature (30°F) case was determined to be bounding for the determination of the peak pressure in the fan accumulator room.

The nodalization network for the fan accumulator room is illustrated in Figures 14.3.4-19, 14.3.4-20 and 14.3.4-28 through 14.3.4-30. Figure 14.3.4-28 illustrates the TMD model plan view at the equipment room elevation. Figure 14.3.4-19 provides the TMD model containment section view. Figure 14.3.4-20 is the plan view at the ice condenser compartments. Figure 14.3.4-29 contains the layout of the containment shell for the TMD model. Figures 14.3.4-22 illustrate the noding, flow paths and TMD network for the fan accumulator room subcompartment. Nodes 27, 31 and 54-57, as shown on Figure 14.3.4-28, represent the fan accumulator rooms in the TMD model. The steam line break was postulated to occur in the fan room in Node 55.

The TMD input flow path characteristics are based upon incompressible flow modeling. The TMD program adjusts the incompressible flow equations with the area ratios ( $A_T/A$ ) to account



## UFSAR Revision 30.0

 An AEP Company	<b>INDIANA MICHIGAN POWER</b> <b>D. C. COOK NUCLEAR PLANT</b> <b>UPDATED FINAL SAFETY ANALYSIS REPORT</b>	Revised: 27.0 Section:14.3.4.2 Page: 10 of 22
---	---	---

for compressible effects in the high subsonic flow regime. The TMD flow path input data for the fan accumulator room is contained in Table 14.3.4-29.

The fan accumulator room free volume and vent area are presented in Table 14.3.4-32. The vent area is determined by summing the flow areas leaving the fan accumulator room subcompartment (Nodes 27-3, 28, 29, 54-3, 28, 55-2, 26, 28, 56-1, 26 and 57-1, 26).

Figures 14.3.4-76 through 14.3.4-97 illustrate the pressure time histories for the peak differential pressure across the key internal structures and walls of the fan accumulator room. Figures 14.3.4-98 through 14.3.4-102 illustrate the pressure time histories for the peak pressure in the fan accumulator room. The calculated peak pressure in the fan accumulator room is 15.40 psig. The peak calculated differential pressure between the fan accumulator room and the ice condenser lower plenum is 15.69 psid, between the adjoining instrument room is 15.20 psid and between the upper compartment is 13.00 psid.

### **14.3.4.2.7 Loop Subcompartments Evaluation**


#### **14.3.4.2.7.1 Base Model Analysis**

As part of the  $T_{hot}$  Reduction Program in the late 1980's, the mass and energy releases for the DEHL and DECL breaks were recalculated. Results showed that the peak rates increased by approximately 10% and 20% for the DECL and DEHL cases respectively when compared to the original analysis. The results of this analysis are shown in the following table:

	<b>Peak Differential Pressure</b>			
Item	DP [1-25] DP [6-25]	DP [2-25] DP [5-25]	DP (7,8,9 TO 25)	Shell Peak Pressure (40, 45)
1988 Base <sup>1</sup>	16.8 psid	12.2 psid	10.7 psid	13.1 psig
1988 Total <sup>2</sup>	18.7 psid	13.0 psid.	11.2 psid	14.0 psig

---

<sup>1</sup> 1988 Base refers to the TMD analysis conducted in 1988 that formed the basis for the  $T_{hot}$  Reduction Program results in 1988. This item is called "base" because these are the raw results from the TMD computer runs. This information does not include effects of 15% flow blockage, variation in initial subcompartment pressure and temperature, and uncertainty.

 An AEP Company	<p style="text-align: center;"><b>INDIANA MICHIGAN POWER</b> <b>D. C. COOK NUCLEAR PLANT</b> <b>UPDATED FINAL SAFETY ANALYSIS REPORT</b></p>	<p>Revised: 27.0 Section: 14.3.4.2 Page: 11 of 22</p>
---	--	---

Figures 14.3.4-103 through 14.3.4-110 present the pressure time histories for the lower compartment elements (1-6), the upper compartment (25) and element 40 on the shell for the DEHL break in compartment 1 case. Figures 14.3.4-111 and 14.3.4-112 present the pressure time histories for element 2 and element 25 for the DEHL in compartment 2 case. Figure 14.3.4-113 present the pressure time history for element 40 on the shell for the DECL case.

These results were used as a starting point for the current analysis. The current analysis for the loop sub compartment utilizes adders and scaling factors to account for changes in initial RCS conditions and uncertainties and as-built data for the compartment.

#### **14.3.4.2.7.2 Current Analysis**


The current methodology is an evaluation that includes a representative TMD run that is used to determine the impact of geometric changes associated with as-built plant subcompartment information on past loop sub compartment analysis results. The results from the TMD run was used to scale prior results to include as-built effects.

The loop sub compartment, including the lower crane wall, upper crane wall, containment shell and operating deck are designed to withstand the pressures which are due to a postulated double-ended primary loop break in the loop sub compartments. The TMD computer code assuming unaugmented critical flow was used to calculate the pressurization response inside the loop sub compartments. Both the DEHL and DECL breaks were evaluated for development of differential pressures. The double-ended cold leg break (DECL) results from previous analysis is augmented by the results of the DEHL break to account for changes in TMD input due to as-built plant data.

---

<sup>2</sup> 1988 Total refers to the total pressure results that were generated for the T<sub>hot</sub> Reduction Program in 1988. This item includes the raw results from the TMD computer runs (1988 Base), and the effects of 15% flow blockage, variation in initial subcompartment pressure and temperature, and uncertainty.

## UFSAR Revision 30.0

 <b>INDIANA MICHIGAN POWER</b> D. C. COOK NUCLEAR PLANT <b>UPDATED FINAL SAFETY ANALYSIS REPORT</b>	Revised: 27.0 Section:14.3.4.2 Page: 12 of 22
--	---

Mass and energy releases were developed for a double-ended hot leg break (DEHL) and are presented in Table 14.3.4-18. SATAN-V models, consistent with the methodology of reference (21), were developed utilizing the appropriate RCS data, such as enthalpies, pressures and flows. The RCS data utilized for the analysis is as follows:

- NSSS Power 3600 MWt
- RCS Pressure (psia) 2250
- Core Average Temperature (°F) 549.9 - 584.9
- Vessel Outlet Temperature (°F) 582.2 - 615.2
- Vessel/Core Inlet Temperature (°F) 511.7 - 547.6


Measurement uncertainties of +67 psi for system pressure and +/-5.1°F for temperature are applied to the RCS data. For the short term mass and energy releases, low RCS temperatures and high pressure are bounding. The bounding RCS initial conditions are as noted below.

- Vessel/Core Inlet Temperature of 506.6°F
- RCS Pressure of 2317 psia

The initial containment conditions bounded by the TMD analysis includes the following:

- Temperature range of 60-120°F
- Pressure range of 13.2-15.0 psia
- Humidity range of 15-100 percent
- Ice Condenser Temperature rang of 10-30°F

## UFSAR Revision 30.0

 An <b>AEP</b> Company	<b>INDIANA MICHIGAN POWER</b> <b>D. C. COOK NUCLEAR PLANT</b> <b>UPDATED FINAL SAFETY ANALYSIS REPORT</b>	Revised: 27.0 Section: 14.3.4.2 Page: 13 of 22
--	---	--

The bounding initial conditions utilized in the analysis for the loop subcompartment are as follows:


- Initial pressure of 15.0 psia
- Lower compartment temperature of 110°F
- Ice condenser temperature of 30°F
- Upper compartment temperature of 75°F
- Fan accumulator/pipe trench temperature of 98°F
- Upper reactor cavity temperature of 110°F
- Steam generator enclosure temperature of 110°F
- Humidity of 15%

Sensitivity studies were performed to evaluate the effect of varying the ice condenser temperature on the peak differential pressure. The analysis for the loop subcompartment was performed using an ice condenser temperature of 30°F. Using an ice condenser temperature of 10°F will increase the resulting peak differential pressures. These increases are bounded by the margins currently applied to the loop subcompartment analysis. Additionally, included in the evaluation of the loop subcompartment is consideration of 15% ice condenser flow blockage and the effects of both DEHL and DECL break locations.

The loop subcompartment TMD nodalization network is similar to the models for the pressurizer enclosure and the steam generator enclosure for the first 45 nodes. Nodes 46-53, which are specific for the loop subcompartment model, represent the steam generator enclosures. The nodalization network for the loop subcompartment is illustrated in Figures 14.3.4-18 through 14.3.4-21 and Figure 14.3.4-31. Figure 14.3.4-18 illustrates the TMD model plan view at the equipment room elevation. Figure 14.3.4-19 provides the TMD model containment section view. Figure 14.3.4-20 is the plan view at the ice condenser compartments. Figure 14.3.4-21 contains the layout of the containment shell for the TMD model. Figure 14.3.4-31 illustrates the specific nodalization network for the loop subcompartment. Contained within this figure are the flow paths from the loop subcompartment.

The TMD input flow path characteristics are based upon incompressible flow modeling. The TMD program adjusts the incompressible flow equations with the area ratios ( $A_T/A$ ) to account for compressible effects in the high subsonic flow regime. The TMD flow path input data for the

## UFSAR Revision 30.0

 An AEP Company	<b>INDIANA MICHIGAN POWER</b> <b>D. C. COOK NUCLEAR PLANT</b> <b>UPDATED FINAL SAFETY ANALYSIS REPORT</b>	Revised: 27.0 Section: 14.3.4.2 Page: 14 of 22
---	---	--

loop subcompartment is contained in Table 14.3.4-30. Refer to Section 14.3.4.2.3.1 for definition of table terms.

The DEHL in Node 1 was determined to be the limiting break for determination of peak differential pressure across the operating deck, across the lower and upper crane wall, the ice condenser ice basket uplift force and lattice frame forces and the intermediate and top deck drag forces. The DECL break in Node 1 was determined to be limiting for the differential pressure across the containment shell. Pressure time history plots are included as Figures 14.3.4-114 through 14.3.4-122 for the loop subcompartment analysis.


The following tables provide the peak differential across the operating deck, upper and lower crane wall, containment shell and the peak differential pressure between the steam generator enclosure and the ice condenser.

<b><u>Peak Differential Pressure</u></b>				
Item	DP [1-25] DP [6-25]	DP [2-25] DP [5-25]	DP (7,8,9 TO 25)	Shell Peak Pressure (40, 45)
Original base <sup>3</sup>	14.1 psid	10.6 psid	8.2 psid	10.8 psig
2001 Base <sup>4</sup>	18.2 psid	12.2 psid	10.7 psid	13.1 psig
2001 Total <sup>5</sup>	20.2 psid	14.0 psid	11.8 psid	14.8 psig

3 Original Base refers to the TMD analysis conducted in 1974. This item is called “base” because these are the raw results from the TMD computer runs. This information does not include effects of 15% flow blockage, variation in initial subcompartment pressure and temperature, and uncertainty.

4 2001 Base refers to the TMD analysis & evaluation conducted in 2001 that formed the basis for the results. This item is called “base” because these are the raw results from the base TMD run. This information does not include effects of 15% flow blockage, variation in initial subcompartment pressure and temperature, and uncertainty.

## UFSAR Revision 30.0

 An AEP Company	<b>INDIANA MICHIGAN POWER</b> <b>D. C. COOK NUCLEAR PLANT</b> <b>UPDATED FINAL SAFETY ANALYSIS REPORT</b>	Revised: 27.0 Section:14.3.4.2 Page: 15 of 22
---	---	---

<b><u>Peak Differential Pressure Between the Steam Generator Enclosure and the Ice Condenser</u></b>				
Item	DP [46-41]	Time	DP [50-10,11,12]	Time
2001 Base <sup>4</sup>	9.42 psid	0.0621 s	10.03 psid	0.3624 s
2001Total <sup>5</sup>	11.36 psid	0.0621 s	11.97 psid	0.3624 s


In addition to the results provided above, the vertical distribution of peak differential pressure for the ice condenser end wall for the lower plenum is 14.8 psid and 11.8 / 9.2 / 7.4 psid for the bottom/middle/top 16 feet of the ice bed region, respectively. The azimuthal distribution of peak differential pressure for the ice condenser is presented in Table 14.3.4-35. The loop subcompartment analysis also generates the peak blowdown differential pressure across the ice condenser lower plenum floor and horizontal seal acting downward. The peak differential pressure was calculated to be 10.4 psid. Pressure time history plots which can be used for the ice condenser lower plenum and for the fan accumulator room are contained in Figures 14.3.4-121 and 14.3.4-122, respectively.

Early sensitivity studies, illustrated in Table 14.3.4-36 (see Section 14.3.4.5.3.4, "Early Sensitivity Studies"), demonstrated the effects of changes in certain variables on the operating deck differential pressure and the shell pressure. The purpose of that study was to illustrate the sensitivity of the TMD code results to different input and assumption conditions and to illustrate the inherent analysis conservatism. The purpose of the tables was not to supply an extrapolation tool for all subcompartments since the work was done for a specific subcompartment and trends may be different for other compartments. For example, the effect of initial compartment pressure on the peak differential pressure can be either a benefit or a penalty depending upon the flow regime before and during the peak. Additionally, if the peak occurs later in time the trend

---

<sup>5</sup> 2001 Total refers to the total pressure results that were generated for the analysis and evaluation program in conducted 2001. This item includes the raw results from the TMD computer runs (2001 Base), and the effects of 15% flow blockage, variation in initial subcompartment pressure and temperature, and uncertainty.

## UFSAR Revision 30.0

 An AEP Company	<b>INDIANA MICHIGAN POWER</b> <b>D. C. COOK NUCLEAR PLANT</b> <b>UPDATED FINAL SAFETY ANALYSIS REPORT</b>	Revised: 27.0 Section:14.3.4.2 Page: 16 of 22
---	---	---

will be geometry dependent. That is, the pertinent downstream element would pressurize differently based upon specific key variables, such as flow areas and resistance into and out of the element. A combination of both sonic and subsonic flow regime periods could occur over the total transient. Since the new analysis is sufficiently different when compared to the original sensitivity basis, Table 14.3.4-36 should only be used for guidance.

### **14.3.4.2.8 Reactor Cavity Evaluation**

The reactor cavity is designed for a single ended break of an RCS loop at its connection to the reactor vessel nozzle. The break is considered to be a longitudinal split in the loop piping at the primary shield wall of an area equivalent to the cross sectional area of a reactor coolant pipe, i.e. 4.12 ft<sup>2</sup>. A circumferential failure of the pipe at this location would result in a much smaller flow discharge area because the vessel, pipe and sleeve arrangement is such that no significant relative movement can take place.


The purpose of this analysis is to calculate the initial pressure response in the reactor cavity to a loss of coolant accident. The reactor cavity pressure analysis was performed for the upper and lower reactor cavities, the reactor vessel annulus and the reactor pipe annulus. The mass and energy releases for the analysis is presented in Table 14.3.4-19 for the single-ended cold leg break (SECL) and Table 14.3.4-20 for the single-ended hot leg break (SEHL). The RCS data utilized for the analysis is as follows:

- |                                      |               |
|--------------------------------------|---------------|
| • NSSS Power                         | 3600 MWt      |
| • RCS Pressure (psia)                | 2250          |
| • Core Average Temperature (°F)      | 549.9 - 584.9 |
| • Vessel Outlet Temperature (°F)     | 582.2 - 615.2 |
| • Vessel/Core Inlet Temperature (°F) | 511.7 - 547.6 |

Measurement uncertainties of +67 psi for system pressure and +/-5.1°F for temperature are applied to the RCS data. The mass and energy releases were determined utilizing the following bounding RCS initial conditions.

- Vessel/Core Inlet Temperature of 506.6°F
- RCS Pressure of 2317 psia

## UFSAR Revision 30.0

 <b>INDIANA MICHIGAN POWER</b> <small>An AEP Company</small>	<b>INDIANA MICHIGAN POWER D. C. COOK NUCLEAR PLANT UPDATED FINAL SAFETY ANALYSIS REPORT</b>	Revised: 27.0 Section:14.3.4.2 Page: 17 of 22
--	---	---

In this evaluation, the effect of the following initial containment conditions was also assessed:

- Temperature range of 60-160°F in the loop subcompartments.
- Temperature range of 60-120°F in the upper and lower reactor cavities.
- Pressure range of 13.2-15.0 psia.
- Humidity range of 15-100 percent.

The effects of the ice condenser are conservatively neglected in this analysis. Various assumptions concerning reactor cavity insulation and HVAC ductwork are included in the analysis for the reactor cavity. Due to the blowdown forces associated with the break, the insulation on the broken loop pipe was assumed to be displaced outward through the penetration in the primary shield wall. The insulation on the reactor vessel wall will either be crushed or displaced from the reactor vessel region. The HVAC ductwork in the upper reactor cavity is assumed to collapse and the HVAC ductwork in the windows at the top of the biological shield will be crushed and displaced into the loop compartment. In addition, three inspection hatch covers furthest from the break location are assumed to be held closed. This is represented by the flow paths from Nodes 41, 42 and 43 to Node 38.


As described previously, the reactor cavity TMD model is significantly different than the TMD model for the other containment subcompartments. The reactor cavity TMD model nodalization is illustrated in Figures 14.3.4-32, 14.3.4-33 and 14.3.4-34. Figure 14.3.4-32 shows the reactor cavity TMD model containment section view. Figure 14.3.4-33 illustrates the reactor cavity TMD model layout of reactor vessel annulus elements and Figure 14.3.4-34 illustrates the reactor cavity TMD model nodalization network. The break is postulated to occur in Node 1.

The TMD input flow path characteristics are based upon incompressible flow modeling. The TMD program adjusts the incompressible flow equations with the area ratios ( $A_T/A$ ) to account for compressible effects in the high subsonic flow regime. The TMD flow path input data for the reactor cavity is contained in Table 14.3.4-31.

The Steam Generator Tube Plugging Program, SGTP, parameters affect the Reactor Cavity Pressure Analysis through the mass and energy releases provided as input into the analysis. There is no direct impact of SGTP level on short-term mass and energy release rate calculations. The major impact results from changes to RCS temperature. For short-term effects, higher release rates typically result from cooler RCS conditions. The mass and energy releases used as input for the Reactor Cavity Pressure Analysis reflected limiting conditions and therefore, the NSSS performance parameters for the SGTP Program did not impact the results.



## UFSAR Revision 30.0

 <b>INDIANA MICHIGAN POWER</b> <b>D. C. COOK NUCLEAR PLANT</b> <b>UPDATED FINAL SAFETY ANALYSIS REPORT</b>	Revised: 27.0 Section:14.3.4.2 Page: 18 of 22
---	---


Based upon a review of Reference 34, it was concluded that the analysis assumptions used to perform the Reactor Cavity Pressure Analysis remain bounding. The assumptions and design inputs that are changed in Reference 34 relate to systems and components that do not affect the Reactor Cavity Pressure Analysis.

The net free volume and vent area from the upper and lower reactor cavities is documented in Table 14.3.4-32. The vent area represents the available flow path area leaving the reactor cavities and entering the loop subcompartment. The upper cavity vent area is determined by summing the available flow path areas from Nodes 38-51 and 38-52. The lower cavity vent area is determined by summing the available flow path areas from Nodes 46-51, 47-51, 48-51, 50-51, 41-52, 42-52, 43-52, 49-52, and the limiting area from Nodes 2-60-58-51. As shown in Table 14.3.4-32, vent areas from the upper and lower reactor cavities were 165 and 172 square feet, respectively.

Figures 14.3.4-123 through 14.3.4-129 present pressure time histories for the break compartment (TMD node 1), the lower reactor cavity (TMD node 2), the reactor vessel annulus near the break (TMD node 3), the upper reactor cavity (TMD node 38), the broken loop pipe sleeve (TMD node 46), the loop subcompartments (TMD node 51) and the broken loop inspection port (TMD node 53).

Figures 14.3.4-130 through 14.3.4-132 present the differential pressure time histories for the lower reactor cavity wall, the upper reactor cavity wall, and the missile shield.

## UFSAR Revision 30.0

 An AEP Company	<b>INDIANA MICHIGAN POWER</b> <b>D. C. COOK NUCLEAR PLANT</b> <b>UPDATED FINAL SAFETY ANALYSIS REPORT</b>	Revised: 27.0 Section: 14.3.4.2 Page: 19 of 22
---	---	--


### **14.3.4.2.8.1 Upper Reactor Cavity**

The limiting break for the upper reactor cavity is a single-ended break of the primary cold leg. As shown in Table 14.3.4-19, mass and energy releases were developed for this break using SATAN-V models. High initial temperature (120°F), low initial pressure (13.2 psia) and low humidity (15%) are limiting for this analysis for both peak pressure and peak differential pressure. Upper reactor cavity pressurization effects were calculated with the TMD code assuming unaugmented critical flow.

The following results are summarized:

	<b>Peak Upper Cavity Pressure</b>	<b>Peak Missile Shield Differential Pressure</b>	<b>Peak Cavity Wh 1 Differential Pressure</b>
Calculation current	48.5 psig	50.84 psid	50.0 psid
Original calculation	47.0 psig	44.1 psid	44.1 psid

## UFSAR Revision 30.0

 An AEP Company	<b>INDIANA MICHIGAN POWER</b> <b>D. C. COOK NUCLEAR PLANT</b> <b>UPDATED FINAL SAFETY ANALYSIS REPORT</b>	Revised: 27.0 Section:14.3.4.2 Page: 20 of 22
---	---	---


### **14.3.4.2.8.2 Lower Reactor Cavity**

As in the upper reactor cavity analysis, the limiting break for the lower reactor cavity is a single-ended break of the primary cold leg. Low initial temperature (60°F), low initial pressure (13.2 psia) and low humidity (15%) are limiting for this analysis for peak differential pressure. Low initial temperature (60°F), high initial pressure (15.0 psia) and low humidity (15%) are limiting for this analysis for peak pressure.

The results are summarized below:

	<b>Peak Lower Cavity Pressure</b>	<b>Peak Differential Pressure Between Lower Cavity And Lp Subcompartments</b>
Current calculation	17.12 psig	18.22 psid
Original calculation	13.8 psig	12.3 psid

## UFSAR Revision 30.0

 An AEP Company	<b>INDIANA MICHIGAN POWER</b> <b>D. C. COOK NUCLEAR PLANT</b> <b>UPDATED FINAL SAFETY ANALYSIS REPORT</b>	Revised: 27.0 Section: 14.3.4.2 Page: 21 of 22
---	---	--

### **14.3.4.2.8.3 Reactor Vessel Annulus and Reactor Pipe Annulus**

The reactor vessel annulus and pipe annuli peak pressures were evaluated using a homogeneous, unaugmented critical flow model. The peak break flow rates for the single-ended cold leg (SECL) and single-ended hot leg (SEHL) breaks were considered. The limiting break was found to be the SEHL break because, even though the peak break flow rate was higher for the SECL, the enthalpy was higher for the SEHL. High initial temperature (120°F), low initial pressure (13.2 psia) and low humidity (15%) are limiting for this analysis for peak pressure. The results are summarized below:

	<b>Peak Pipe Annulus Pressure (SEHL)</b>	<b>Peak Reactor Vessel Annulus Pressure (SEHL)</b>
Revised calculation <sup>6</sup>	630 psig	160 psig
TMD Analysis Peak Values	665 psig <sup>7</sup>	675 psig <sup>8</sup>
Original calculation <sup>9</sup>	735 psig	95 psig

The revised calculation results are based upon a manual calculation method consistent with the original licensing methodology. This evaluation was then compared to the TMD analysis results. For the peak pipe annulus pressure, the original manual calculation bounds both the revised calculation and the TMD analysis results. For the peak reactor vessel annulus pressure, the TMD analysis results are considerably higher than the results from the manual calculation. However, this TMD pressure is highly localized near the break. The peak reactor vessel annulus pressure on the opposite side of the vessel is less than 50 psig.

---


<sup>6</sup> These values represent the average hand calculated values for the two annuli utilizing the M&E release data and volume/flow path data.

<sup>7</sup> This is the broken loop pipe annulus (Node 46).

<sup>8</sup> This is the vessel annulus area directly below the break location (Node 3).

<sup>9</sup> Original calculation refers to the values determined during initial licensing (1973).

## UFSAR Revision 30.0

 An AEP Company	<p style="text-align: center;"><b>INDIANA MICHIGAN POWER</b> <b>D. C. COOK NUCLEAR PLANT</b> <b>UPDATED FINAL SAFETY ANALYSIS REPORT</b></p>	<p>Revised: 27.0 Section: 14.3.4.2 Page: 22 of 22</p>
---	--	---


### **14.3.4.2.8.4 Reactor Vessel Nozzle Inspection Hatch Cover**

The above analyses were performed with the replacement inspection hatch covers. Theoretically, the inspection hatch covers could either remain closed or be fully opened. In the subcompartment analyses the most limiting action is assumed. To maximize the resulting pressure in the subcompartment, three inspection hatch covers were assumed to remain closed in the analysis. The selected covers were the three furthest from the break location represented by the flow paths from Nodes 41, 42 and 43 to Node 38. The individual flow paths for each reactor vessel nozzle inspection hatch covers vary. To determine the resulting flow areas, refer to Table 14.3.4-31. In the event of a primary leg break, the hinged door is designed to open. Based on the pressure time histories, it can be determined that all hatch covers would open. This would result in a decreased peak upper cavity pressure.


### **14.3.4.2.9 Short Term Containment Analysis Conclusions**

The results of the short-term containment analyses and evaluations for the Cook Nuclear Power Plants demonstrate that, for the steam generator enclosure, the pressurizer enclosure, the fan accumulator room, the loop subcompartment and the reactor cavity area, the resulting peak pressures/differential pressures remain below the allowable design peak pressures/differential pressures. Refer to Table 5.2-8 for a listing of the equivalent design pressure capabilities. The structural adequacy was confirmed through evaluations using Section 5.2.2.3 of the UFSAR as acceptance criteria.

# UFSAR Revision 30.0

 An AEP Company	INDIANA MICHIGAN POWER D. C. COOK NUCLEAR PLANT UPDATED FINAL SAFETY ANALYSIS REPORT	Revised: 29.0 Section:14.3.4.3 Page: i of i
---	--	---

<b>14.3 REACTOR COOLANT SYSTEM PIPE RUPTURE (LOSS OF COOLANT ACCIDENT) .....</b>	<b>1</b>
<b>14.3.4 Containment Integrity Analysis .....</b>	<b>1</b>
14.3.4.3 Mass And Energy Release Analysis For Postulated Loss-Of-Coolant Accidents .....	1
14.3.4.3.1 Mass and Energy Release Data .....	2
14.3.4.3.1.1 Short Term Mass and Energy Release Data .....	2
14.3.4.3.1.1.1 Early Design Analyses (Historical) .....	2
14.3.4.3.1.1.2 Current Design Basis Analyses .....	5
14.3.4.3.1.2 Long Term Mass and Energy Release Data .....	5
14.3.4.3.1.2.1 Application of Single Failure Analysis .....	5
14.3.4.3.1.2.2 Mass and Energy Release Data .....	6
14.3.4.3.1.2.3 Deleted .....	8
14.3.4.3.1.2.4 Deleted .....	8
14.3.4.3.1.2.5 Sources of Mass and Energy .....	8
14.3.4.3.1.2.6 Significant Modeling Assumptions .....	9

 An AEP Company	INDIANA MICHIGAN POWER D. C. COOK NUCLEAR PLANT UPDATED FINAL SAFETY ANALYSIS REPORT	Revised: 29.0 Section: 14.3.4.3 Page: 1 of 9
---	--	--

## **14.3 REACTOR COOLANT SYSTEM PIPE RUPTURE (LOSS OF COOLANT ACCIDENT)**

### **14.3.4 Containment Integrity Analysis**

#### **14.3.4.3 Mass And Energy Release Analysis For Postulated Loss-Of-Coolant Accidents**


This analysis presents the mass and energy releases to the containment subsequent to a hypothetical loss-of-coolant accident (LOCA).

The containment system receives mass and energy releases following a postulated rupture in the RCS. These releases continue over a time period, which, for the LOCA mass and energy analysis, is typically divided into four phases:

1. Blowdown: The period of time from accident initiation (when the reactor is at steady state operation) to the time that the lower plenum begins to re-pressurize after initial coolant evacuation.
2. Refill: The period of time when the reactor vessel lower plenum is being filled by accumulator and ECCS water. The WCOBRA/TRAC code mechanistically calculates this phase.
3. Reflood: The period of time that begins when the water from the reactor vessel lower plenum enters the core and ends when the core is completely quenched.
4. Post-Reflood: The period of time following the reflood phase. It is during this portion of the transient that (for the DECL and DEPS breaks) a two phase mixture exiting the core enters the steam generators, resulting in reverse heat transfer from the secondary side to the primary side. Heat transfer from the steam generator secondary metal to the fluid, and then from the fluid to the tubes, is accounted for in a mechanistic fashion.

The WCAP-17721-P-A [23] methodology uses a single code for all phases of the LOCA transient through the time of peak containment pressure.

## UFSAR Revision 30.0

 An AEP Company	<b>INDIANA MICHIGAN POWER</b> <b>D. C. COOK NUCLEAR PLANT</b> <b>UPDATED FINAL SAFETY ANALYSIS REPORT</b>	Revised: 29.0 Section: 14.3.4.3 Page: 2 of 9
---	---	--

Three distinct locations in the reactor coolant system loop can be postulated for pipe rupture.

1. Hot leg (between vessel and steam generator)
2. Cold leg (between pump and vessel)
3. Pump suction (between steam generator and pump)

Using the WCAP-17721-P-A WCOBRA/TRAC methodology [23], full double-ended ruptures were analyzed in the cold leg and the pump suction leg, each with 1 and 2 trains of safety injection, to cover the spectrum of possible limiting break locations for D. C. Cook Unit 1 in the context of the new methodology.

Full double-ended double ruptures of the cold leg and pump suction leg behave similarly, or more specifically, both behave dissimilarly from a double-ended rupture of the hot leg. This is because the hot leg break provides a direct vent path to containment for the core exit flow during the post-blowdown phases. This has the effect of allowing the two phase mixture to bypass the steam generators, yielding significantly reduced integrated energy release in the long term. While the blowdown has the potential to be more severe for the hot leg break, ice condenser plants are inherently limited by the long term mass and energy releases after the ice bed is depleted. Therefore, the hot leg break has been excluded from the spectrum of runs. The double-ended pump suction and double-ended cold leg breaks both provide a mechanism to transport a two phase mixture to both the intact and broken steam generators, and so both have been analyzed with WCOBRA/TRAC.

### **14.3.4.3.1 Mass and Energy Release Data**


#### **14.3.4.3.1.1 Short Term Mass and Energy Release Data**

##### **14.3.4.3.1.1.1 Early Design Analyses (Historical)**

The mass and energy release rate transients for all the design cases are given in Figures 14.3.4-133 through 14.3.4-140. All cases are generated with the SATAN-V break model consisting of Moody-Modified Zaloudek critical flow correlations applied at the break element. Since no mechanistic constraints have been established for full guillotine rupture, an instantaneous pipe severance and disconnection is assumed for all transients. Assumptions specific to the early design transients are as follows:



## UFSAR Revision 30.0

 An <b>AEP</b> Company	<b>INDIANA MICHIGAN POWER</b> <b>D. C. COOK NUCLEAR PLANT</b> <b>UPDATED FINAL SAFETY ANALYSIS REPORT</b>	Revised: 29.0 Section: 14.3.4.3 Page: 3 of 9
--	---	--

For the hot leg mass and energy release rate transient to loop subcompartments:

Figures 14.3.4-133, -134


1. A double ended guillotine type break.
2. A break located just outside the biological shield.
3. A break located in the worst loop.
4. A six node upper plenum model.
5. A 16 node broken hot leg pipe model.
6. A discharge coefficient ( $C_D$ ) equal to 1.
7. A 100% power condition with  $T_{hot} = 606.4^{\circ}\text{F}$  and  $T_{cold} = 540.4^{\circ}\text{F}$ .

For the cold leg mass and energy release rate transient to loop subcompartments:

Figures 14.3.4-135, -136

1. A double ended guillotine type break.
2. A break located just outside the biological shield.
3. A break located in the worst loop.
4. A seven node downcomer model.
5. A 16 node broken hot leg pipe model.
6. A discharge coefficient ( $C_D$ ) equal to 1.
7. A full power condition with  $T_{hot} = 606.4^{\circ}\text{F}$  and  $T_{cold} = 540.4^{\circ}\text{F}$ .

## UFSAR Revision 30.0

 An <b>AEP</b> Company	<b>INDIANA MICHIGAN POWER</b> <b>D. C. COOK NUCLEAR PLANT</b> <b>UPDATED FINAL SAFETY ANALYSIS REPORT</b>	Revised: 29.0 Section: 14.3.4.3 Page: 4 of 9
--	---	--

For hot leg mass and energy release rate transients to subcompartments:

Figures 14.3.4-137, -138


1. A single ended split type break.
2. A break just outside the hot leg nozzle.
3. A break in the pressurizer loop.
4. A six node upper plenum model.
5. A 16 node broken hot leg pipe model.
6. A discharge coefficient ( $C_D$ ) equal to 1.
7. Full power condition  $T_{\text{hot}} = 606.4^\circ\text{F}$  and  $T_{\text{cold}} = 540.4^\circ\text{F}$ .

For the cold leg mass and energy release rate transient to subcompartments:

Figures 14.3.4-139, -140

1. A single ended split type break.
2. A break just outside the cold leg nozzle.
3. A break in the pressurizer loop.
4. A seven node downcomer model.
5. A 16 node broken hot leg pipe model.
6. A discharge coefficient ( $C_D$ ) equal to 1.
7. A full power condition  $T_{\text{hot}} = 606.4^\circ\text{F}$  and  $T_{\text{cold}} = 540.4^\circ\text{F}$ .

## UFSAR Revision 30.0

 An AEP Company	<b>INDIANA MICHIGAN POWER</b> <b>D. C. COOK NUCLEAR PLANT</b> <b>UPDATED FINAL SAFETY ANALYSIS REPORT</b>	Revised: 29.0 Section: 14.3.4.3 Page: 5 of 9
---	---	--

For the mass and energy release rate transient to the pressurizer enclosure, a 6 inch spray line pipe break was considered (Figures 14.3.4-141, -142):

1. A guillotine type break modeled as a 0.147 ft<sup>2</sup> split in the cold leg at the pump discharge (area of the six inch pressurizer spray feed line) and a 0.087 ft<sup>2</sup> split in the top of the pressurizer (area of 4 inch spray nozzle).
2. Valves in spray lines are assumed to be open.
3. No pipe resistance for the feed line considered.
4. A full power condition  $T_{\text{hot}} = 606.4^{\circ}\text{F}$  and  $T_{\text{cold}} = 540.4^{\circ}\text{F}$ .
5. A discharge coefficient ( $C_D$ ) equal to 1.

The mass and energy release rate transients for all the generated cases are supported by an extensive investigation of short term phenomena. Section 14.3.4.5 includes detailed discussion of the phenomena and the results.

### **14.3.4.3.1.1.2 Current Design Basis Analyses**

Analyses were conducted to support changes in Reactor Power and revised RCS parameters, such as enthalpy, on the mass and energy releases. Details of the subcompartment evaluation are presented in Section 14.3.4.2.5 for the Pressurizer Enclosure Evaluation, Section 14.3.4.2.7 for the Loop Subcompartments Evaluation and, Section 14.3.4.2.8, for the Reactor Cavity Evaluation.


### **14.3.4.3.1.2 Long Term Mass and Energy Release Data**

#### **14.3.4.3.1.2.1 Application of Single Failure Analysis**

An analysis of the effects of the single failure criteria has been performed on the mass and energy release rates for the double ended cold leg (DECL) break. An inherent assumption in the generation of the mass and energy release is that offsite power is lost. This results in the actuation of the emergency diesel generators, required to power the safety injection system. This is not an issue for the blowdown period, which is limited by the compression peak pressure.

The limiting minimum safety injection case has been analyzed for the effects of a single failure. In the case of minimum safeguards, the single failure postulated to occur is the loss of an emergency diesel generator. This results in the loss of one pumped safety injection train, thereby minimizing the safety injection flow. The analysis further considers the RHR and SI pump head curves to be degraded by 15% and the charging pump head curve to be degraded by 10%. This results in the greatest SI flow reduction for the minimum safeguards case.

# UFSAR Revision 30.0

 An AEP Company	<b>INDIANA MICHIGAN POWER</b> <b>D. C. COOK NUCLEAR PLANT</b> <b>UPDATED FINAL SAFETY ANALYSIS REPORT</b>	Revised: 29.0 Section: 14.3.4.3 Page: 6 of 9
---	---	--

## **14.3.4.3.1.2.2 Mass and Energy Release Data**


WCOBRA/TRAC consists of two primary source codes, COBRA-TF and TRAC-PD2. COBRA-TF is a three dimensional thermal hydraulic code that is used to model the vessel in detail, and TRAC-PD2 is a one dimensional code that is used to model loop piping, pumps, steam generators, and various boundary conditions. The WCOBRA/TRAC computer code is currently used as the PWR ECCS evaluation model by Westinghouse; it is fully capable of calculating the thermal/hydraulic RCS response to a large pipe rupture. The use of WCOBRA/TRAC for this application has been qualified by comparison with scalable test data covering the expected range of conditions and important phenomena. Modifications to WCOBRA/TRAC were required to model the specifics of importance to the LOCA M&E analysis, and these updates are discussed below.

The WCOBRA/TRAC steam generator, modeled in accordance with the ECCS evaluation model, was shown to over predict the reverse heat transfer from the steam generators. Updates were made to more accurately calculate the steam generator cool down. These updates were validated by comparison to FLECHT-SEASET steam generator separate effects tests. The result is a computer code capable of modeling phenomena associated with the large break LOCA conditions that provides significant margin relative to the current WCAP-10325-P-A [22] methodology because the stored RCS and SG energy is released at a mechanistically calculated rate instead of forced out over a conservatively short duration.

Beginning with the peak clad temperature (PCT) D. C. Cook Unit 2 model, specific updates were made to the model to bias it for containment integrity purposes. These key updates included:

1. Updated the PCT nodding structure to include safety injection and accumulator injection in all loops
2. Maximized the RWST temperature (105°F, technical specification maximum)
3. Applied accumulator upper limit pressure (672.7 psia), lower limit liquid volume (921 ft<sup>3</sup>), and maximum temperature (120°F)
4. RCS volume was biased high
5. SG tube plugging level was minimized
6. Increased the RCS temperatures to the high end of the operating range band and included uncertainty for a target T<sub>avg</sub> of 583.2°F
7. Increased the RCS initial pressure to 2317 psia (including uncertainties)

## UFSAR Revision 30.0

 An AEP Company	<b>INDIANA MICHIGAN POWER</b> <b>D. C. COOK NUCLEAR PLANT</b> <b>UPDATED FINAL SAFETY ANALYSIS REPORT</b>	Revised: 29.0 Section: 14.3.4.3 Page: 7 of 9
---	---	--


8. Increased the pressurizer liquid level, targeting maximum water volume of 1215 ft<sup>3</sup>
9. Increased core power to account for uncertainty at full power, targeting 3482 MWt
10. Applied ANS 1979 + 2 $\sigma$  decay heat
11. Turned off fuel rod swelling model
12. Used Baker-Just correlation for metal/water reaction
13. Updated the steam generator nodding structure per WCOBRA/TRAC M&E methodology
14. Biased the steam generator secondary side volumes high

The resulting model was used to calculate the mass and energy releases for the limiting break scenario, a double-ended cold leg break with minimum safeguards. The WCOBRA/TRAC tool calculates all phases of the peak pressure LOCA transient, including blowdown, refill, reflood, and post reflood long term. The resulting blowdown and post blowdown mass and energy releases are found in Table 14.3.4-41 and Table 14.3.4-42, respectively. Evaluations have shown that these releases are applicable to D.C. Cook Unit 2 in both vessel barrel/baffle down flow and upflow configurations.

The mass and energy release from decay heat is based on the 1979 ANSI/ANS Standard, shown in Reference 24 and the following input:

1. The highest decay heat release rates come from the fission of U-238 nuclei. Thus, to maximize the decay heat rate a maximum value (8%) has been assumed for the U-238 fission fraction.
2. The second highest decay heat release rate comes from the fission of U-235 nuclei. Therefore, the remaining fission fraction (92%) has been assumed for U-235.
3. The factor which accounts for neutron capture in fission products has been taken directly from Table 10 of the standard.
4. The number of atoms of Pu-239 produced per second has been assumed to be 70% of the fission rate.

## UFSAR Revision 30.0

 An AEP Company	<p style="text-align: center;"><b>INDIANA MICHIGAN POWER</b> <b>D. C. COOK NUCLEAR PLANT</b> <b>UPDATED FINAL SAFETY ANALYSIS REPORT</b></p>	<p>Revised: 29.0 Section: 14.3.4.3 Page: 8 of 9</p>
---	--	---

5. The total recoverable energy associated with one fission has been assumed to be 200 MeV/fission.
6. The fuel has been assumed to be at full power for  $10^8$  seconds.
7.  $2\sigma$  uncertainty has been applied to the fission product decay. This accounts for a 98% confidence level.

### **14.3.4.3.1.2.3 Deleted**

### **14.3.4.3.1.2.4 Deleted**

### **14.3.4.3.1.2.5 Sources of Mass and Energy**


The sources of mass and energy considered in the LOCA mass and energy release analysis are listed below for the double-ended cold leg break with minimum safety injection.

The mass sources are the reactor coolant system, accumulators, and pumped safety injection. The energy sources include:

1. Reactor coolant system water
2. Accumulator water
3. Pumped injection water
4. Decay Heat
5. Core stored energy
6. Reactor coolant system metal (including the steam generator tube metal)
7. Steam generator metal (including shell, wrapper and internals)
8. Steam generator secondary fluid energy (liquid and steam)

All sources of mass and energy listed above are considered in the WCOBRA/TRAC portion of the analysis. The water in the RCS, accumulators, safety injection boundary conditions, and SG secondary is explicitly modeled. Core decay heat (including feedback effects during blowdown) is included in the WCOBRA/TRAC fuel rod model. The fuel rod model also includes an energy term to represent core stored energy. The reactor coolant system (RCS) and steam generator (SG) metal, and the associated heat transfer from these sources, is modeled in the WCOBRA/TRAC analysis.

## UFSAR Revision 30.0

 An AEP Company	<b>INDIANA MICHIGAN POWER</b> <b>D. C. COOK NUCLEAR PLANT</b> <b>UPDATED FINAL SAFETY ANALYSIS REPORT</b>	Revised: 29.0 Section: 14.3.4.3 Page: 9 of 9
---	---	--

In the mass and energy release data presented, no zirconium-water reaction heat was considered because the clad temperature did not rise high enough for the rate of the zirconium-water reaction heat to be of any significance.

The consideration of the various energy sources in the mass and energy release analysis provides assurance that all available sources of energy have been included in the analysis. Although Cook Nuclear Plant Unit 2 is not a Standard Review Plan Plant, the review guidelines presented in Standard Review Plan Section 6.2.1.3 have been satisfied.


The methods and assumptions used to release the various energy sources are given in Reference 23, which has been approved as a valid evaluation model by the Nuclear Regulatory Commission.

### **14.3.4.3.1.2.6 Significant Modeling Assumptions**

The following assumptions were employed to ensure that the mass and energy releases are conservatively calculated, thereby maximizing energy release to containment:


1. Maximum expected operating temperatures of the reactor coolant system (100% full power conditions).
2. An allowance in temperature for instrument error and dead band (+5.1°F).
3. RCS volume is biased conservatively high.
4. Core rate thermal power of 3482 MWt (100.34% of 3470 MWt).
5. Steam generator secondary side mass was biased conservatively high.
6. Initial fuel temperatures, and thus the core stored energy, were based on late in life conditions that included the effects of fuel pellet thermal conductivity degradation.
7. A maximum containment backpressure equal to design pressure.
8. An allowance for RCS initial pressure uncertainty (+67 psi)
9. Steam generator tube plugging leveling (0% uniform)
  - a. Maximizes reactor coolant volume and fluid release
  - b. Maximizes heat transfer area across the SG tubes
  - c. Reduces coolant loop resistance, which reduces delta-p upstream of the break, and increases break flow

# UFSAR Revision 30.0

 <small>An AEP Company</small>	<b>INDIANA MICHIGAN POWER</b> <b>D. C. COOK NUCLEAR PLANT</b> <b>UPDATED FINAL SAFETY ANALYSIS REPORT</b>	Revised: 27.0 Section:14.3.4.4 Page: i of i
--	---	---

<b>14.3 REACTOR COOLANT SYSTEM PIPE RUPTURE (LOSS OF COOLANT ACCIDENT) .....</b>	<b>1</b>
<b>14.3.4 Containment Integrity Analysis .....</b>	<b>1</b>
14.3.4.4 Mass and Energy Release Analysis for Postulated Secondary System Pipe Ruptures Inside Containment .....	1
14.3.4.4.1 Short Term Mass and Energy Releases.....	1
14.3.4.4.1.1 <i>Steam Generator Doghouse</i> .....	2
14.3.4.4.1.2 <i>Fan Accumulator Room</i> .....	3
14.3.4.4.2 Long Term Mass and Energy Release Data.....	3
14.3.4.4.2.1 <i>Pipe Break Blowdowns Spectra and Assumptions</i> .....	3
14.3.4.4.2.2 <i>Break Flow Calculations</i> .....	6
14.3.4.4.2.3 <i>Single Failure Effects</i> .....	6



 An AEP Company	<p>INDIANA MICHIGAN POWER D. C. COOK NUCLEAR PLANT UPDATED FINAL SAFETY ANALYSIS REPORT</p>	<p>Revised: 27.0 Section: 14.3.4.4 Page: 1 of 7</p>
---	---	---

## **14.3 REACTOR COOLANT SYSTEM PIPE RUPTURE (LOSS OF COOLANT ACCIDENT)**

### **14.3.4 Containment Integrity Analysis**

#### **14.3.4.4 Mass and Energy Release Analysis for Postulated Secondary System Pipe Ruptures Inside Containment**


A series of steamline breaks were analyzed to determine the most severe break condition for the containment temperature and pressure response. The assumptions on the initial conditions are taken to maximize the mass and energy released. The range of possible operating conditions for the Donald C. Cook Nuclear Plants are presented in Table 14.1-1 for Unit 1 and Table 14.1.0-1 for Unit 2. The subsections that follow discuss; the short-term mass and energy releases, which addresses steamline break effects in the steam generator enclosure and the fan accumulator room, and a feedwater line break in the steam generator enclosure, followed by the long-term mass and energy releases.

##### **14.3.4.4.1 Short Term Mass and Energy Releases**

The short term mass and energy releases are broken down into steamline break locations in the fan accumulator room and steam line and feedwater line breaks in the steam generator doghouses. The details of each of these break locations are discussed below. The limiting plant condition in terms of both steam generator mass inventory and initial secondary system pressure are obtained when the plant is at hot shutdown. Since the no-load conditions are identical for both Unit 1 and Unit 2, one group of short term mass and energy release analyses will be applicable for both units.

Initial blowdown from the steam generator will be dry steam as a result of the approximately 5000 lbm. of steam in the upper head. This accentuates the initial peak compartment pressure. For the doghouse break, the flow rate was based on the Moody correlation for an initial reservoir pressure of 1106 psia, and included the steam generator exit nozzle loss. This was the value originally used for Unit 2 at the time of initial licensing. This is conservative to the licensing basis no-load pressure of 1020 psia. Depressurization of the steam generator causes an initial decrease in steam flow.

## UFSAR Revision 30.0

 An AEP Company	<p style="text-align: center;"><b>INDIANA MICHIGAN POWER</b> <b>D. C. COOK NUCLEAR PLANT</b> <b>UPDATED FINAL SAFETY ANALYSIS REPORT</b></p>	<p>Revised: 27.0 Section: 14.3.4.4 Page: 2 of 7</p>
---	--	---

The following assumptions were made for calculating steam generator blowdown with entrainment. Note that these assumptions are in the conservative direction for maximum water entrainment.


1. No credit was taken for the separation capability of the steam generator internals (swirl vanes and dryers).
2. Flow between regions of the steam generator was assumed as homogeneous with no slip or separation. Regions of the steam generator are the downcomer, bundle, swirl vane cylinders, and dryers.
3. Flow resistance between the steam generator regions was considered.
4. No credit was taken for flow resistance in the piping between the steam generator and the break.
5. Break flow was determined by the Moody (Reference 25 of Section 14.3.4.7) correlation with the discharge coefficient conservatively assumed as unity.

The mass and energy releases were also calculated for a postulated break in the main feedwater piping. For the feedwater line break event, the no-load steam generator pressure is 1020 psia and the full-power feedwater temperature is 449°F. Both the steam generator and the main feedwater system are assumed at saturation conditions for purposes of determining the liquid enthalpy values. The initial mass in the steam generator is 180,400 lb<sub>m</sub>.

### **14.3.4.4.1 Steam Generator Doghouse**

The mass and energy release to the steam generator doghouse from a steamline break and a feedwater line break has been analyzed. One case considers a steam line break between the steam generator shell and the steam line flow restrictor (break at the steam generator nozzle). The postulated break area is 4.60 ft<sup>2</sup> in the forward flow direction (normal direction of the steam flow) based on the inside diameter of the pipe. The break area defined in the reverse flow direction (opposite direction of the normal steam flow) is 4.909 ft<sup>2</sup> based on the inside diameter of the pipe. After the initial blowdown of the steam pipe, the reverse direction flowrate is limited by the area (1.4 ft<sup>2</sup>) defined by the inline flow restrictor (venturi) on the faulted steam line. The inline flow restrictor is located in the turbine bypass header in the turbine building. The second case models a feedwater line break at the nozzle to the steam generator, downstream of the feedwater line check valve. The feedwater line break area is 1.117 ft<sup>2</sup>, which corresponds to a nominal pipe diameter of 16" with an inside diameter of 14.314".

## UFSAR Revision 30.0

 An AEP Company	<p style="text-align: center;"><b>INDIANA MICHIGAN POWER</b> <b>D. C. COOK NUCLEAR PLANT</b> <b>UPDATED FINAL SAFETY ANALYSIS REPORT</b></p>	<p>Revised: 27.0 Section: 14.3.4.4 Page: 3 of 7</p>
---	--	---

The calculated mass and energy release rates into the steam generator doghouse, for both break locations, are presented as Table 14.3.4-15.

### **14.3.4.4.1.2 Fan Accumulator Room**

Blowdown of the steam piping was calculated with the SATAN-4 computer code. The SATAN-4 code does not consider momentum flux. Neglect of this effect is conservative for high velocity steam blowdown since it overpredicts the steam pressure near the break. Since steam pressure and steam density are overpredicted, frictional losses are underpredicted.

Piping blowdown consists of steam at 1192 Btu/lbm (saturation enthalpy at 1020 psia).

Steam piping blowdown consists of reverse flow (steam flow coming out the turbine end of the break), and -- for the break in the fan room -- the initial steam blowdown from the steam generator end until choking conditions are reached in the flow restrictor.

The SATAN model consists of 69 elements simulating the four steam generators and steam lines and the steam dump header. For the fan room analysis, flow restrictors with a throat area of 1.4 ft<sup>2</sup> were assumed in the steam line cross ties near the turbine.

Reverse flow was assumed to be terminated after 10 seconds as a result of steam line isolation. No credit was taken for partial isolation valve closure prior to 10 seconds.

The calculated mass and energy release rates for the fan accumulator room steam line break analyses are presented in Table 14.3.4-17.

### **14.3.4.4.2 Long Term Mass and Energy Release Data**


The mass / energy release calculations were conservatively performed assuming a bounding uprated power level. The upper bound parameters used for the analysis are presented in Table 14.3.4-47.

#### **14.3.4.4.2.1 Pipe Break Blowdowns Spectra and Assumptions**

The following assumptions were used in the analysis:


- a. Double ended pipe breaks were assumed to occur at the nozzle of one steam generator and also downstream of the flow restrictor. Split pipe ruptures were assumed to occur at the nozzle of one steam generator.
- b. The blowdown was assumed to be dry saturated steam.
- c. The steamline break protection system design was assumed to actuate on low steam line pressure.

## UFSAR Revision 30.0

 An AEP Company	<p style="text-align: center;"><b>INDIANA MICHIGAN POWER</b> <b>D. C. COOK NUCLEAR PLANT</b> <b>UPDATED FINAL SAFETY ANALYSIS REPORT</b></p>	<p>Revised: 27.0 Section: 14.3.4.4 Page: 4 of 7</p>
---	--	---

- d. Steamline isolation was assumed complete 11.0 seconds after the setpoint is reached for either low steam pressure or hi-hi containment pressure. The isolation time allows 8 seconds for valve closure plus 3 seconds for electronic delays and signal processing. The total delay time for steamline isolation of 11 seconds was assumed to support the relaxation of the main steam isolation valve (MSIV) closure time.
- e. 4.6 and 1.4 square foot double ended pipe breaks were evaluated at 102, 70, 30 and zero percent power levels of 3588 MWt core thermal power.
- f. Four (4) combinations of steamline ruptures were evaluated assuming split pipe ruptures: 0.86 square foot equivalent diameter at 102 percent power, 0.908 square foot equivalent diameter at 70 percent power, 0.942 square foot equivalent diameter at 30 percent power, and 0.40 square foot equivalent diameter at hot shutdown.
- g. Failure of a main steam isolation valve, failure of feedwater isolation or main feed pump trip, and failure of auxiliary feedwater runout control were considered. Two cases for each break size and power level scenario were evaluated with one case modeling the MSIV failure and the other case modeling the AFW runout control failure. Each case assumed conservative main feedwater addition to bound the feedwater isolation or main feed pump trip failure.
- h. The end-of-life shutdown margin was assumed to be 1.3%  $\Delta k/k$  at no load, equilibrium xenon conditions, and the most reactive RCCA stuck in its fully withdrawn position.
- i. A moderator density coefficient of 0.54  $\Delta k/gm/cc$  was assumed.
- j. Minimum capability for injection of boric acid (2400 ppm) solution was assumed corresponding to the most restrictive single failure in the safety injection system. The emergency core cooling system (ECCS) consists of the following systems:
  - 1. the passive accumulators,
  - 2. the low head safety injection (residual heat removal) system,
  - 3. the intermediate head safety injection system, and
  - 4. the high head safety injection (charging) system.

## UFSAR Revision 30.0

 An <b>AEP</b> Company	<b>INDIANA MICHIGAN POWER</b> <b>D. C. COOK NUCLEAR PLANT</b> <b>UPDATED FINAL SAFETY ANALYSIS REPORT</b>	Revised: 27.0 Section: 14.3.4.4 Page: 5 of 7
--	---	--


Only the high head safety injection (charging) system and the passive accumulators were modeled for the steam line break accident analysis.

The modeling of the safety injection system in LOFTRAN is described in Reference 26. Figure 3.3-52 of WCAP-11902 presents the safety injection flow rates as a function of RCS pressure assumed in the analysis. The flow corresponded to one charging pump delivering its full flow to the cold legs. The safety injection flows assumed in this analysis take into account the degradation of the ECCS charging pump performance. No credit was taken for the low concentration borated water that must be swept from the lines downstream of the boron injection tank isolation valves prior to the delivery of boric acid to the reactor coolant loops. For this analysis, a boron concentration of 0 ppm for the boron injection tank was assumed.

After the generation of the safety injection signal (appropriate delays for instrumentation, logic and signal transport included), the appropriate valves begin to operate and the safety injection charging pump starts. In 27 seconds, the valves were assumed to be in their final position and the pump was assumed to be at full speed and to draw suction from the RWST. The volume containing the low concentration borated water is swept into the core before the 2400 ppm borated water reaches the core. This delay, described above, was inherently included in the modeling.

- k. For the at-power cases, reactor trip was available by safety injection signal, overpower protection signal (high neutron flux reactor trip or OPΔT reactor trip), and low pressurizer pressure reactor trip signal.
- l. Offsite power was assumed available. Continued operation of the reactor coolant pumps maximizes the energy transferred from the reactor coolant system to the steam generators.
- m. No steam generator tube plugging was assumed to maximize the heat transfer characteristics.

## UFSAR Revision 30.0

 An AEP Company	<p style="text-align: center;"><b>INDIANA MICHIGAN POWER</b> <b>D. C. COOK NUCLEAR PLANT</b> <b>UPDATED FINAL SAFETY ANALYSIS REPORT</b></p>	<p>Revised: 27.0 Section: 14.3.4.4 Page: 6 of 7</p>
---	--	---

### **14.3.4.4.2.2 Break Flow Calculations**

a. Steam Generator Blowdown

The LOFTRAN computer code (Reference 26) was used to calculate the break flows and enthalpies of the release through the steam line break. Blowdown mass/energy releases determined using LOFTRAN include the effects of core power generation, main and auxiliary feedwater additions, engineered safeguards systems, reactor coolant thick metal heat storage, and reverse steam generator heat transfer.


b. Steam Plant Piping Blowdown

The calculated mass and energy releases include the contribution from the secondary steam piping. For all ruptures, the steam piping volume blowdown begins at the time of the break and continues until the entire piping inventory is released. The flow rate is determined using the Moody correlation and the pipe cross sectional area.

### **14.3.4.4.2.3 Single Failure Effects**

- a. Failure of a main steam isolation valve (MSIV) increases the volume of steam piping that is not isolated from the break. When all valves operate, the piping volume capable of blowing down is located between the steam generator and the first isolation valve. If this valve fails, the volume between the break and the isolation valves in the other steam lines, including safety and relief valve headers and other connecting lines, will feed the break. For all cases, the steam line volumes associated with Unit 1 were conservatively assumed since the volume available for blowdown is greater than Unit 2.
- b. Failure of a diesel generator would result in the loss of one containment safeguards train, resulting in minimum heat removal capability.
- c. Failure of the main feedwater regulating valve (MFRV) to close results in additional inventory in the feedwater line that would not be isolated from the steam generator. The mass in this volume can flash to steam and exit through the break. All steamline break cases conservatively assumed failure of the MFRV to close, which resulted in the additional inventory available for release through the steamline break as well as a longer duration for the higher than normal main


## UFSAR Revision 30.0

 <b>INDIANA MICHIGAN POWER</b> <small>An AEP Company</small>	<b>INDIANA MICHIGAN POWER D. C. COOK NUCLEAR PLANT UPDATED FINAL SAFETY ANALYSIS REPORT</b>	Revised: 27.0 Section:14.3.4.4 Page: 7 of 7
--	---	---

feedwater flows before the backup main feedwater motor-operated isolation valve (MFIV) closes.

- d. Failure of the auxiliary feedwater runout control equipment could result in higher auxiliary feedwater flows entering the steam generator prior to realignment of the auxiliary feedwater system. For cases where the runout control operates properly, a constant auxiliary feedwater flow of 775 gpm to the faulted steam generator was assumed. This value was increased to 1381 gpm to simulate a failure of the runout control.


The long-term steamline break analysis calculated mass and energy rates for both the double-ended rupture and the split-breaks are presented in Tables 14.3.4-7 and 14.3.4-8, respectively.

 <p><b>INDIANA MICHIGAN POWER</b> <small>An AEP Company</small></p>	<p><b>INDIANA MICHIGAN POWER</b> <b>D. C. COOK NUCLEAR PLANT</b> <b>UPDATED FINAL SAFETY ANALYSIS REPORT</b></p>	<p>Revised: 29.0 Section: 14.3.4: .5; .6; &amp; .7 Page: i of ii</p>
--	--	--


<b>14.3 REACTOR COOLANT SYSTEM PIPE RUPTURE (LOSS OF COOLANT ACCIDENT) .....</b>	<b>1</b>
<b>14.3.4 Containment Integrity Analysis.....</b>	<b>1</b>
14.3.4.5 Containment Integrity Analysis - Background Information .....	1
14.3.4.5.1 LOCA Mass and Energy Release Data .....	1
14.3.4.5.1.1 Model Description .....	1
14.3.4.5.1.2 Comparison To Other Critical Flow Models .....	2
14.3.4.5.1.3 Comparison To Experimental Data .....	3
14.3.4.5.1.4 Application to Transient Conditions .....	4
14.3.4.5.1.5 Parametric Studies .....	5
14.3.4.5.1.6 Break Size, Type and Location .....	5
14.3.4.5.1.7 Hot Leg Nodal Configuration.....	6
14.3.4.5.1.8 Cold Leg Studies .....	6
14.3.4.5.1.9 Nodal Configuration .....	6
14.3.4.5.1.10 Pump Modeling.....	7
14.3.4.5.1.11 Summary .....	7
14.3.4.5.2 Experimental Verification.....	8
14.3.4.5.2.1 Early Tests.....	8
14.3.4.5.2.2 1973 Waltz Mill Tests.....	9
14.3.4.5.2.2.1 Test Purpose .....	9
14.3.4.5.2.2.2 Test Facility.....	9
14.3.4.5.2.2.3 Test Procedure .....	10
14.3.4.5.2.2.4 Results.....	11
14.3.4.5.3 Short Term Containment Response .....	11
14.3.4.5.3.1 Results Based On 1973 Waltz Mill Tests.....	11
14.3.4.5.3.2 Subcritical Flow Model Studies .....	12
14.3.4.5.3.3 Derivation of the Compressibility Multiplier .....	13
14.3.4.5.3.4 Choked Flow Characteristics .....	14
14.3.4.5.3.5 Early Sensitivity Studies.....	15



# UFSAR Revision 30.0

 An AEP Company	<b>INDIANA MICHIGAN POWER</b> <b>D. C. COOK NUCLEAR PLANT</b> <b>UPDATED FINAL SAFETY ANALYSIS REPORT</b>	Revised: 29.0 Section: 14.3.4: .5; .6; & .7 Page: ii of ii
---	---	---

14.3.4.5.4	Ice Condenser Performance Criteria .....	17
14.3.4.5.4.1	<i>Inlet Door Performance</i> .....	19
14.3.4.5.4.1.1	<i>Introduction</i> .....	19
14.3.4.5.4.1.2	<i>Design Criteria</i> .....	21
14.3.4.5.4.1.3	<i>Performance Capability</i> .....	22
14.3.4.5.4.2	<i>Top and Intermediate Deck Door Performance</i> .....	24
14.3.4.5.4.2.1	<i>Design Criteria</i> .....	24
14.3.4.5.4.2.2	<i>Performance Capability</i> .....	25
14.3.4.5.4.3	<i>Vent Design And Performance</i> .....	26
14.3.4.5.4.3.1	<i>Introduction</i> .....	26
14.3.4.5.4.3.2	<i>Large Break Performance Requirements</i> .....	26
14.3.4.5.4.3.3	<i>Small Break Performance Requirements</i> .....	27
14.3.4.5.4.4	<i>Drain Design And Performance</i> .....	27
14.3.4.5.4.4.1	<i>Introduction</i> .....	27
14.3.4.5.4.4.2	<i>Large Break Performance Requirements</i> .....	27
14.3.4.5.4.4.3	<i>Small Break Performance Requirements</i> .....	28
14.3.4.5.4.4.4	<i>Normal Operational Performance</i> .....	29
14.3.4.6	Changes from Base Containment Analyses: Note Concerning Tables and Figures .....	29
14.3.4.7	References for Section 14.3.4 .....	29

	<b>INDIANA MICHIGAN POWER</b> <b>D. C. COOK NUCLEAR PLANT</b> <b>UPDATED FINAL SAFETY ANALYSIS REPORT</b>	Revised: 29.0 Section: 14.3.4: .5; .6; .7 Page: 1 of 33
---	---	--

## **14.3 REACTOR COOLANT SYSTEM PIPE RUPTURE (LOSS OF COOLANT ACCIDENT)**

### **14.3.4 Containment Integrity Analysis**

#### **14.3.4.5 Containment Integrity Analysis - Background Information**

##### **14.3.4.5.1 LOCA Mass and Energy Release Data**

###### **14.3.4.5.1.1 Model Description**


Mass and energy release rate transients generated for the TMD pressure calculation are supported by an extensive investigation of short term blowdown phenomena. The SATAN-V code was used to predict early blowdown transients. The study concerned a verification of the conservatism of the SATAN-V calculated transients. This verification was accomplished through two approaches: a review of the validity of the SATAN-V break model, and a parametric study of significant physical assumptions.

The SATAN-V code uses a control volume approach to model the behavior of the Reactor Coolant System resulting from a large break in a main coolant pipe. Release rate transients are determined by the SATAN-V break model which includes a critical flow calculation and an implicit representation of pressure wave propagation.

The SATAN-V critical flow calculation uses appropriately defined critical flow correlations applied for fluid conditions at the break element. For the early portion of blowdown, subcooled, saturated, and two-phase critical flow regimes are encountered. SATAN-V uses the Moody (Reference 25) correlation for saturated and two-phase fluid conditions and a slight modification of the Zaloudek (Reference 27) correlation for the subcooled blowdown regime.

Since most short term blowdown transients are characterized by a peak mass and energy release rate that occurs during a subcooled condition, the Zaloudek application is particularly significant. The Zaloudek correlation is modified to merge to Moody predicted mass velocities at saturation in the break element. This correlation appears in the critical flow routine of SATAN-V in the form:

# UFSAR Revision 30.0

 <p>INDIANA MICHIGAN POWER <small>An AEP Company</small></p>	<p>INDIANA MICHIGAN POWER D. C. COOK NUCLEAR PLANT UPDATED FINAL SAFETY ANALYSIS REPORT</p>	<p>Revised: 29.0 Section: 14.3.4: .5; .6; .7 Page: 2 of 33</p>
---	---	--

$$G_{crit} = CK1 \sqrt{(5.553 * 10^5)(P - C_1 P_{sat})}$$

where:

- $G_{crit}$  = critical flow in lb. mass/sec-ft<sup>2</sup>  
 $P$  = reservoir pressure (psia)  
 $P_{sat}$  = reservoir saturation pressure (psia)  
 $C_1$  = constant where .5 <  $C_1$  < 1

$$CK1 = \sqrt{\frac{.1037}{1 - C_1}} = \text{constant adjusted such that when } P = P_{sat}, G_{crit} \text{ from Zaloudek matches the}$$

SATAN-V Moody critical flow calculated at zero quality. For the present analysis,  $C_1$  equals 0.9 and  $CK1$  equals 1.018. The modification also more conservatively accounts for the phenomena of increasing mass velocity with increasing degrees of subcooling. The slope of the subcooled  $G$  vs.  $P$  curve is steeper for the modified correlation. The low quality portion of the SATAN-V critical flow model is presented in Figure 14.3.4-143. The Moody saturation line corresponds to the condition upstream in the break element where quality equals zero and pressure equals saturation pressure. Thus when pressure equals saturation pressure in the break element the Zaloudek and Moody critical flow values are equal. When pressure exceeds saturation pressure in the break element, the modified Zaloudek is used for the critical flow calculation. The steep slope of the Zaloudek  $G$  vs.  $P$  line indicates the over-accounting for the subcooling effect.


## **14.3.4.5.1.2 Comparison To Other Critical Flow Models**

The Henry-Fauske critical flow correlation was considered for comparison (References 16, 28, and 29). This correlation models flow nonequilibrium via an approach which includes an empirical parameter. This parameter describes the deviation from equilibrium mass transfer and depends on flow geometry.

The value is selected for a particular configuration based on the range of throat equilibrium qualities. The value for constant area ducts is used in the present analysis. This choice is based on the worst possible double-ended break geometry described below.

For cold leg and hot leg breaks, the majority of the flow, about 65%, comes from the vessel side of the break. For this side, the geometry may be described as an entrance nozzle and a straight pipe of approximately 12 feet in length with a diameter of 29 inches. This length of pipe represents the distance from the reactor vessel to the periphery of the biological shield. No double-ended

## UFSAR Revision 30.0

 An AEP Company	<p style="text-align: center;"><b>INDIANA MICHIGAN POWER</b> <b>D. C. COOK NUCLEAR PLANT</b> <b>UPDATED FINAL SAFETY ANALYSIS REPORT</b></p>	Revised: 29.0 Section: 14.3.4: .5; .6; .7 Page: 3 of 33
---	--	--

break can occur within the biological shield because of the restricted movement within the pipe annulus. Hence the constant area value is appropriate.

Like the SATAN-V model, the Henry-Fauske correlation yields a  $G_{crit}$  in terms of upstream conditions and like the SATAN-V model it also exhibits a steeper slope of the  $G$  vs.  $P$  line for subcooled conditions. As can be seen in Figure 14.3.4-143, the Henry-Fauske saturated liquid line is below the Moody saturated line (SATAN-V model) for pressures greater than about 1000 psia.


For short term blowdown calculations, the significant pressure region is from 1000 psia to 1800 psia, with increased emphasis on subcooled conditions for the 1000 psia end. Subcooled mass velocity versus pressure is given for the two fluid temperatures corresponding to  $P_{sat} = 1000$  and  $P_{sat} = 1800$ . It is clear from the figure that the slope of the Zaloudek  $G$  vs.  $P$  line is steeper in both cases. This increased sensitivity coupled with the higher value for Moody at saturation causes the SATAN-V model to predict higher mass velocities. Hence the SATAN-V model is a more conservative treatment of critical flow than the Henry-Fauske model.

In the original FLASH model,(Reference 30) the Moody correlation was extended to subcooled conditions. This treatment is employed in many blowdown codes and thus it is appropriate to compare the SATAN-V model to these values. This is illustrated in Figure 14.3.4-144. Again, the Zaloudek treatment yields higher mass velocities and the SATAN-V model is more conservative.

### **14.3.4.5.1.3 Comparison To Experimental Data**

The margin included in the modified Zaloudek prediction of subcooled critical flow rates is demonstrated by a review of experimental subcooled critical flow data. Figures 14.3.4-145 and -146 present a plot of measured vs. predicted critical flow values for Zaloudek's own data.(References 27 and 31) The figures indicate that when the modified correlation is applied to Zaloudek's data, the predicted critical flow values are significantly higher than measured flow rates.

The margin associated with the SATAN-V critical flow calculation may also be demonstrated by a review of the low quality data presented by Henry in ANL-7740 (Reference 29). Exit plane quality, in terms of the Moody model, is determined as a function of upstream conditions by assuming an isentropic expansion to exit plane (i.e., critical) pressure. The lowest exit plane qualities where the Moody model is applied in the SATAN-V code occur for expansion from saturated liquid conditions; a plot of these are shown in Figure 14.3.4-147. For exit plane qualities above the line, the Moody model is used in the SATAN-V code. Below the line, the Modified Zaloudek model is used.

 <b>INDIANA MICHIGAN POWER</b> <b>D. C. COOK NUCLEAR PLANT</b> <b>UPDATED FINAL SAFETY ANALYSIS REPORT</b>	Revised: 29.0 Section: 14.3.4: .5; .6; .7 Page: 4 of 33
---	--

Henry's comparison between data and model shows that for the range of exit plane quality greater than 0.02, the Moody model overpredicts the data, hence is conservative.

For the region below 0.02, it is appropriate to compare Henry's results with the Modified Zaluodek model, as used in the SATAN-V code. This is done in Figure 14.3.4-148 for all of Henry's data points. As can be seen, the Zaluodek model overpredicts the flow. A discharge coefficient of 0.6 would be more reasonable than the 1.0 value used in SATAN-V.

#### **14.3.4.5.1.4 Application to Transient Conditions**

The Zaluodek correlation was developed for stagnation (reservoir) pressure and quasi-steady-state critical flow conditions. It is extended to application in the SATAN-V break element and transient flow conditions. This extension is justified because of the following considerations.


The pressure in the break element differs from the value in a nearby large volume because of three effects:

1. Pressure drop due to friction
2. Pressure drop due to spatial acceleration (momentum flux)
3. Pressure drop due to the transient

The friction term in the reactor application is quantifiable; this term is less important than the other two. The sensitivity of the break flow rate to fluid friction was evaluated via a parametric study. For the purposes of this study, an analysis was made wherein the frictional resistance between the vessel and the break was reduced from the design values by a factor of one hundred. Over the period from 0.0 to 60 milliseconds (which includes the peak break flow), the integrated mass flow differed by less than 18 lbm from the design friction case; the total release over this period was about 5000 lbm.

Spatial acceleration is the major source of pressure drop upstream of the break between the reservoir and the pipe, causing steep pressure gradients in the approach region to critical flow. This term is not calculated explicitly in the SATAN-V code. Spatial acceleration is accounted for by the use of critical flow correlations (Zaluodek or Moody) which contain this effect. No credit is taken for pressure drop due to spatial acceleration for elements other than the break element. Hence the pressure calculated by SATAN-V may be interpreted as a stagnation pressure which is the appropriate pressure for the Zaluodek and Moody models.

Prior to the occurrence of the peak release rate, the break element and upstream reservoir pressures differ as a result of the transient described by pressure wave propagation. The applicability of the

 An AEP Company	<p style="text-align: center;"><b>INDIANA MICHIGAN POWER</b> <b>D. C. COOK NUCLEAR PLANT</b> <b>UPDATED FINAL SAFETY ANALYSIS REPORT</b></p>	<p>Revised: 29.0 Section: 14.3.4: .5; .6; .7 Page: 5 of 33</p>
---	--	--

SATAN-V break model to this situation is verified by the code's ability to match recorded semi-scale transients. SATAN simulations of LOFT transients support the SATAN-V transient calculation. Figure 14.3.4-149 presents a comparison of LOFT pressure transients recorded near the break to the SATAN-V model of the LOFT break element transient. The graphs demonstrate the ability of the SATAN-V code to track pressure waves in the broken pipe.

Moreover, the critical flow correlation is implemented in the present analysis by combining the correlation with the appropriate momentum equation. This provides a model for predicting break flow acceleration vis-a-vis a quasi-steady simulation. This is found to have little effect on containment pressure but is a more physical representation.

Thus the SATAN-V break model is supported by subcooled critical flow data, by comparison to other correlations, and by ability to simulate short term transients.

#### **14.3.4.5.1.5 Parametric Studies**


With confirmation of the conservatism of the SATAN-V break model, a series of parametric studies were undertaken to identify the blowdown transient corresponding to the most severe TMD results. A series of basic sensitivities were first studied to set the scope of the more detailed investigations. The assumptions of break size, break type and break location were considered. The results of this analysis were evaluated using the TMD code.

#### **14.3.4.5.1.6 Break Size, Type and Location**

A break of an area corresponding to twice the coolant pipe area was the most severe for mass and energy release. For this size break both double-ended guillotine and double-ended split type breaks were considered. These break types differ in that the split allows full communication between approach regions at each side of the break while the guillotine models a complete severance of two ends of a broken coolant pipe.

SATAN-V transients were generated for both type double-ended breaks with the guillotine break resulting in higher mass and energy release rates. The split type break is less severe because flow is reduced from the loop side of the break. This is because communication makes the break element pressure higher than would occur for the loop end in a guillotine rupture. The higher break element pressure yields a smaller pressure gradient for driving loop side flow. The vessel end is relatively unaffected by break type because a choked condition remains at the nozzle. In particular, the split type break results in a 10,000 lbm/sec reduction in peak mass flow rate.

The influence of break location on TMD peak pressure was considered by generating blowdown transients for possible worst break locations. The results indicated that a double-ended break in

 An AEP Company	<p style="text-align: center;"><b>INDIANA MICHIGAN POWER</b> <b>D. C. COOK NUCLEAR PLANT</b> <b>UPDATED FINAL SAFETY ANALYSIS REPORT</b></p>	<p>Revised: 29.0 Section: 14.3.4: .5; .6; .7 Page: 6 of 33</p>
---	--	--

the pump suction leg was clearly less severe for short term blowdown release rates and that no such clear decision could be made between hot and cold leg breaks.

More detailed parametric studies were continued for the cold leg and the hot leg double-ended guillotine breaks. The two locations produce intrinsically different TMD pressure responses and therefore must be dealt with in separate parametric surveys.

#### **14.3.4.5.1.7 Hot Leg Nodal Configuration**

A study of the SATAN-V nodal configuration has been applied to the hot leg double-ended guillotine break. It was found that for this break the nodal configuration of the broken hot leg and the upper plenum are significant to short term transients. Spatial convergence was achieved for the upper plenum after the addition of four nodes to the standard SATAN-V two node upper plenum model. These nodes are hemispherical shells arranged concentrically from the broken hot leg nozzle and approximate the propagation of the pressure wave in the upper plenum. They are significant in that they specify the inertial response of the upper plenum. Spatial convergence was demonstrated because doubling the number of nodes yielded less than a one percent change in break flow at all times.

Sensitivity to nodal configuration in the broken hot leg pipe was also investigated. Models with from 4 to 16 nodes were used to generate transients. Increasing the number of nodes was found to give a better simulation of pressure wave propagation in the pipe.

#### **14.3.4.5.1.8 Cold Leg Studies**

The cold leg break transient was also reviewed in terms of significant parameters.

The Reactor Coolant System behavior is different for cold leg breaks and the peak containment pressure occurs later for cold leg breaks.


#### **14.3.4.5.1.9 Nodal Configuration**

For the cold leg break the nodal configuration of the broken cold leg and the downcomer is significant to the transient. Spatial convergence was achieved with the addition of three additional nodes to the standard SATAN-V model. These are annular rings arranged concentrically from the broken cold leg nozzle and model propagation of the pressure wave in the downcomer.

As in the hot leg sensitivity, from 4 to 16 pipe node models were tried for the cold leg transient. Again, more nodes gave a better simulation of pressure wave propagation in the broken pipe.



## UFSAR Revision 30.0

 An AEP Company	<p style="text-align: center;"><b>INDIANA MICHIGAN POWER</b> <b>D. C. COOK NUCLEAR PLANT</b> <b>UPDATED FINAL SAFETY ANALYSIS REPORT</b></p>	<p>Revised: 29.0 Section: 14.3.4: .5; .6; .7 Page: 7 of 33</p>
---	--	--

### **14.3.4.5.1.10 Pump Modeling**

For the time period of interest, the variation in pump inlet density is small and the variation in pump speed is small. This model was found to have no effect.

### **14.3.4.5.1.11 Summary**

From the hot leg and cold leg studies, the design basis mass and energy release rates have been finalized. The mass and energy release rate transients for all the design cases are given in Figures 14.3.4-133 to -142. All cases are generated from the SATAN-V break model consisting of Moody-Modified Zaloudek critical flow correlations applied at the break element. Since no mechanistic constraints have been established for full guillotine pipe rupture, an instantaneous pipe severance and disconnection is assumed for all transients. Assumptions specific to the presented transients are discussed in section 14.3.4.3.1.1.

Figures 14.3.4-137, -138 -139, and -140 present mass and energy release rate transients for hot leg and cold leg split type breaks of a single ended pipe area. For breaks of this size, the split type break is used as a design basis and this choice is justified by a generic study of the effect of break type on short term release rates. A discussion of this study and of break type influence was given as a response to question 6.71 to the Catawba PSAR (USNRC Docket No's. 50-413 and 50-414). It is sufficient for this discussion to note that for single ended breaks, a split type break results in higher release rates.


Differences in blowdown mass and energy release rates between hot leg and cold leg single ended split breaks result from the influence of the hot water in the upper plenum and hot legs. For a cold leg single ended split, the flashing fluid in the upper plenum and hot legs sustains flow to the break from both the vessel and from the loop through the broken loop pump. This flashing, then, acts to maintain a subcooled blowdown for the cold leg break.

For the hot leg single ended split no such pressurization effect occurs at the break. Flashing fluid in the hot leg and upper plenum, rather, results in an extensive two-phase blowdown condition. The broken leg pump continues to remain effective during the hot leg split transient and thus draws flow away from the break.

The hot leg and cold leg double ended release rate transients presented in the figures discussed above are the result of a guillotine type break. This basis is again justified as a result of the generic break type study referenced above. The study indicated that for breaks of twice the coolant pipe area, a guillotine type break resulted in the highest release rates.



## UFSAR Revision 30.0

 An AEP Company	<p style="text-align: center;"><b>INDIANA MICHIGAN POWER</b> <b>D. C. COOK NUCLEAR PLANT</b> <b>UPDATED FINAL SAFETY ANALYSIS REPORT</b></p>	Revised: 29.0 Section: 14.3.4: .5; .6; .7 Page: 8 of 33
---	--	--

An explanation of the differences in the release rate transients presented for hot leg and cold leg double-ended breaks is complicated by the fact that these are guillotine type breaks. Since the guillotine break models a complete separation of the broken pipe, conditions at each end of the break must be considered individually. The total release rate is then the sum of contributions from each end.

Flashing of the fluid in the hot legs again accounts for the higher mass flow rates observed for the cold leg double-ended break in comparison to the hot leg double-ended transient. However, two other influences are significant for breaks of this type and area.

For the cold leg guillotine, the increased break area requires higher flows if a subcooled blowdown condition is to be maintained at the break. A subcooled blowdown occurs at the vessel end of the broken pipe but because of the broken loop pump resistance to increased flow, a two-phase blowdown occurs at the loop end of the break.

Since for both hot leg and cold leg breaks the loop side of the break experiences a two-phase blowdown, the loop layout geometry determines the difference in their release rates. Higher release rates are observed for the loop side of hot leg break because it is fed from the reservoir of water in the inlet plenum of the steam generator. No such supply of water exists at the loop side of the cold leg break. In fact, flow to the cold leg loop side is restricted by the resistance of the broken loop pump.

The differences in release rates for the double-ended break are thus the result of two effects. A higher vessel side mass flow rate for the cold leg break results from a subcooled blowdown maintained by the pressurizing effect of flashing hot leg fluid.


A lower loop side mass flow is observed for the cold leg break because of the differences accountable to loop layout geometry. However, since the subcooled blowdown effect dominates the total release rate, the cold leg double-ended guillotine still results in highest total mass discharge rates.

### **14.3.4.5.2 Experimental Verification**

#### **14.3.4.5.2.1 Early Tests**

The performance of the TMD Code was verified against the 1/24 scale air tests and the 1968 Waltz Mill tests. For the 1/24 scale model the TMD Code was used to calculate flow rates to compare against experimental results. The effect of increased nodalization was also evaluated. The Waltz Mill test comparisons involved a reexamination of test data. In conducting the reanalyses, representation of the 1968 Waltz Mill test was reviewed with regard to parameters such as loss

## UFSAR Revision 30.0

	<b>INDIANA MICHIGAN POWER</b> <b>D. C. COOK NUCLEAR PLANT</b> <b>UPDATED FINAL SAFETY ANALYSIS REPORT</b>	Revised: 29.0 Section: 14.3.4: .5; .6; .7 Page: 9 of 33
---	---	--

coefficients and blowdown time history. The details of this information are given in Reference 14.

### **14.3.4.5.2.2 1973 Waltz Mill Tests**

#### **14.3.4.5.2.2.1 Test Purpose**

The Waltz Mill Ice Condenser Blowdown Test Facility was reactivated in 1973 (Reference 2) to verify the ice condenser performance with the following redesigned plant hardware scaled to the test configuration:

1. Perforated metal ice baskets and new design couplings.
2. Lattice frames sized to provide the correct loss coefficient relative to plant design.
3. Lower support beamed structure and turning vanes sized to provide the correct turning loss relative to the plant design.
4. No ice baskets in the lower ice condenser plenum opposite the inlet doors.


The primary objective of these tests was to determine the transient heat transfer and fluid flow performance of the ice condenser design and to confirm that conclusions derived from previous Waltz Mill tests had not been significantly changed by the redesign of plant hardware. Consequently, the design of the test hardware was configured to provide heat transfer and fluid flow characteristics which were equivalent to those in the plant design. It should be noted that test hardware was not representative of structural characteristics for the plant design since structural response to blowdown was not one of the test objectives. In addition, responses of lower, intermediate, and upper deck doors to blowdown were not included in the test objectives.

#### **14.3.4.5.2.2.2 Test Facility**

The Waltz Mill Ice Condenser Blowdown Facility consists of a boiler, receiver vessel, and instrumentation room, and also ice storage and ice machine rooms which are used in conjunction with the ice technology facility. Figure 14.3.4-150 shows the general arrangement of the facility. The boiler and receiver vessels are connected by a 12" schedule 160 pipe in which is located a rupture disc assembly.

The boiler is 3 feet in diameter and 20 feet long, mounted on a structural frame. It can be heated electrically to pressurize a maximum of 117 cubic feet of water to an allowable maximum of 1586 psig pressure at 600°F. Strip heaters mounted on the outside of the boiler shell provide the heat. The flow rate from the boiler is controlled by an orifice located in the piping between the boiler and receiver vessel.

## UFSAR Revision 30.0

 An AEP Company	<p style="text-align: center;"><b>INDIANA MICHIGAN POWER</b> <b>D. C. COOK NUCLEAR PLANT</b> <b>UPDATED FINAL SAFETY ANALYSIS REPORT</b></p>	<p>Revised: 29.0 Section: 14.3.4: .5; .6; .7 Page: 10 of 33</p>
---	--	---

The 12" piping between the boiler and receiver vessel is heated by strip heaters attached to the outside surface of the pipe. Figure 14.3.4-151 shows the piping is arranged into three sections as far as flow and heater capability are concerned. This permits operating the piping and sections of the piping at various subcooled temperatures relative to the boiler.

Figure 14.3.4-152 shows the internal arrangement of the receiver vessel. The ice chest section contains eight ice baskets, 12" diameter by 36 feet high, arranged in a 2 x 4 array. Lattice frames are located at six foot levels of the ice baskets. The baskets set on a lower support structure with flow blockage areas proportional to the plant. Turning vanes are located below the ice baskets and direct the flow entering the lower inlet up through the ice baskets. The vessel is divided into lower and upper compartments. The flow enters the lower compartment from the 12" pipe diffusers, is directed into the ice chest, past the ice baskets and then vents into the upper compartment. The ice chest is wood. All metal surfaces are insulated to limit the heat transfer to these surfaces.

Figure 14.3.4-153 shows the location and typical arrangement for the temperature and pressure measurements that will be made inside the receiver vessel ice chest. The outputs from the transducers are connected to a data acquisition system with scanning rates of 2000 samples per second or 200 samples per second.


### **14.3.4.5.2.2.3 Test Procedure**

The ice baskets are filled in the penthouse at the top of the receiver vessel by a blower system before being lowered into the ice chest. Prior to installing ice baskets, the receiver vessel and building is cooled down by an air recirculation and refrigeration system. A lattice frame is installed after each six foot array of ice baskets and a hold down bar attached through the ice chest walls to prevent basket uplift. After all baskets are installed, the receiver vessel top manhole is closed and the boiler then brought to test conditions.

The boiler is evacuated and filled with demineralized water and the heatup started by energizing the strip heaters. As the water heats in the boiler and expands, it is vented through a letdown heat exchanger. The initial fill of the boiler is measured as well as the water relieved so that the total amount of water in the boiler and piping is always known. Water is circulated between the boiler and downstream piping during heatup by the recirculation system to the various sections of the 12" piping (Figure 14.3.4-151). Subcooled conditions can, thus, be obtained for the water preceding the saturated water in the boiler itself. By using the heaters, recirculating systems, and letdown system, test energy conditions are obtained.

The flow from the boiler and subcooled piping to the receiver vessel is controlled by an orifice plate located in front of the rupture disc assembly. By varying the size of orifice, the blowdown

## UFSAR Revision 30.0

 An AEP Company	<b>INDIANA MICHIGAN POWER</b> <b>D. C. COOK NUCLEAR PLANT</b> <b>UPDATED FINAL SAFETY ANALYSIS REPORT</b>	Revised: 29.0 Section: 14.3.4: .5; .6; .7 Page: 11 of 33
---	---	---

rate can be changed in accordance with the test plans. It is calculated that the maximum orifice required is 5.5".

After the boiler has reached test pressure and temperature, the blowdown is initiated by the rupture disc assembly. This is a double disc assembly with the pressure between the discs normally at about half the boiler operating pressure. The rupture disc burst pressure rating is 60 - 75% of the boiler operating pressure. The pressure between the discs is provided by a high pressure gas cylinder of nitrogen. At blowdown, the gas pressure is quickly released from the cavity between the discs by venting it into the downstream side of the rupture disc, causing the discs to rupture and the water upstream of the discs to be released into the receiver vessel.

At the time the pressure is started to vent from between the rupture discs, the data acquisition systems is actuated so that data is recorded throughout the blowdown transient. Data recording continues for ten seconds at high speed and then is reduced to a 1/10 speed for five minutes.

A preliminary set of test conditions is presented in Table 14.3.4-37.

#### **14.3.4.5.2.2.4 Results**

Confirmation of the predicted ice condenser pressure performance was determined by comparing test results with TMD code predictions for the appropriate test conditions and configuration. Initially, the TMD code predictions were based on assumptions that provided best agreement with previous Waltz Mill test results (e.g., 30% entrainment).


The TMD Code has, as a result of the 1973 test series, been modified to match ice bed heat transfer performance.

#### **14.3.4.5.3 Short Term Containment Response**

##### **14.3.4.5.3.1 Results Based On 1973 Waltz Mill Tests**

A number of analyses have been performed to determine the various pressure transients resulting from hot and cold leg reactor coolant pipe breaks in any one of the six lower compartment elements. The analyses were performed using the following assumptions and correlations:

1. Flow was limited by the unaugmented critical flow correlation.
2. The TMD variable volume door model, which accounts for changes in the volumes of TMD elements as the door opens, was implemented.
3. The heat transfer calculation used was based on performance during the 1973-74 Waltz Mill test series. A higher value of the ELJAC parameter has been used and

	<b>INDIANA MICHIGAN POWER</b> <b>D. C. COOK NUCLEAR PLANT</b> <b>UPDATED FINAL SAFETY ANALYSIS REPORT</b>	Revised: 29.0 Section: 14.3.4: .5; .6; .7 Page: 12 of 33
---	---	---

an upper bound on calculated heat transfer coefficients has been imposed (see Reference 3).

### **14.3.4.5.3.2 Subcritical Flow Model Studies**

For high Mach number subsonic flow, the TMD momentum equation incorporates a compressibility multiplier to account for compressibility effects resulting from area changes, and uses an average density along constant area flow paths.

With these modifications, both inertial and density effects are modeled by the TMD computer code.


A description of the compressibility multiplier, its derivation and application, is presented in this section. A brief description of the method by which the polytropic exponent (a necessary parameter in the compressibility multiplier approach) is calculated is also provided.

These effects have been examined for the D. C. Cook plant short term transient analysis by comparing previous analyses where these methods were not used to analyses using these methods.

For the plant the worst case RCS pipe break is a DEHL rupture in the lower compartment element 6. Results are presented also, for comparison purposes, for a DECL rupture in element 6.

The results of the short term pressure analysis are summarized in Table 14.3.4-38. The values given in parentheses are those pressures calculated on the same basis but without using a compressibility multiplier. As can be seen from the table, the effects of the modifications to the TMD code are minimal.

Consideration was given to determining the effect of a varying polytropic exponent of the flow mixture across the throat section of a flow path. This was done by lowering the steam-water polytropic exponent calculated by the code by 5, 10 and 20%. The lowered polytropic exponent variance computer runs were made for a DEHL break in lower compartment element #6. The results are presented in Table 14.3.4-39 and it is apparent that the polytropic exponent variance has virtually no effect on the results.

 <p><b>INDIANA MICHIGAN POWER</b> <small>An AEP Company</small></p>	<p align="center"><b>INDIANA MICHIGAN POWER D. C. COOK NUCLEAR PLANT UPDATED FINAL SAFETY ANALYSIS REPORT</b></p>	<p>Revised: 29.0 Section: 14.3.4: .5; .6; .7 Page: 13 of 33</p>
--	---	---

**14.3.4.5.3.3 Derivation of the Compressibility Multiplier**

The system under study is shown in Figure 14.3.4-154. The flow assumptions are:

1. Steady flow
2. Zero gravity effects
3. Isentropic conditions
4. Fluid is an ideal gas
5. Channel wall is non-conducting (no heat transfer)

The resulting compressibility multiplier is:

$$y = \left[ r^{2/\gamma} \left( \frac{\gamma}{\gamma-1} \right) \left( \frac{(1-r) \left( \frac{\gamma-1}{\gamma} \right)}{1-r} \right) \right]^{1/2} \left[ \frac{1-B^4}{1-B^4 r^{2/\gamma}} \right]^{1/2}$$

The choked mass flow rate is:

$$\dot{m} = ay \left[ \frac{2g\rho_1(P_1 - P_2)}{1-B^4} \right]^{1/2}$$

where

$$B = (a/A)^{1/2}$$


We next apply the compressibility multiplier to the friction term of the TMD momentum equation written as:

$$\Delta P = \left( \frac{K + f_1 / D}{2\rho g} \right) \left( \frac{\dot{m}^2}{a^2} \right) \quad (3)$$

Incorporating the compressibility multiplier into the TMD momentum equation, eqn. (3) takes on the form:

$$\Delta P = \frac{(K + f_1 / d) \dot{m}^2}{2\rho g y^2 a^2} \quad (4)$$

## UFSAR Revision 30.0

 An AEP Company	<p style="text-align: center;"><b>INDIANA MICHIGAN POWER</b> <b>D. C. COOK NUCLEAR PLANT</b> <b>UPDATED FINAL SAFETY ANALYSIS REPORT</b></p>	<p>Revised: 29.0 Section: 14.3.4: .5; .6; .7 Page: 14 of 33</p>
---	--	---

Coupling eqn. (4) with the inertia term presently used in TMD, the momentum equation for general flow systems (non-steady state) appears as:

$$\Delta P = \frac{L}{A} \frac{dm}{dt} + \frac{(K + f_1 D) \dot{m}^2}{2 \rho g y^2 a^2} \quad (5)$$

It should be noted that the TMD (Reference 14) computer code also employs a critical flow correlation as a check on sonic flow conditions. This critical flow correlation has not been modified as a result of this present work.

The compressibility multiplier as it is used in eqn. (4) (and in TMD) is calculated by the code; the only information needed as input is the B factor.

The polytropic exponent is also calculated within the code, dependent upon the flow mixture conditions.


### **14.3.4.5.3.4 Choked Flow Characteristics**

The data in Figure 14.3.4-155 illustrate the behavior of mass flow rate as a function of upstream and downstream pressures, including the effects of flow choking. The upper plot shows mass flow rate as a function of upstream pressure for various assumed values of downstream pressure. For zero back pressure ( $P_d = 0$ ), the entire curve represents choked flow conditions with the flow rate approximately proportional to upstream pressure,  $P_u$ . For higher back pressure, the flow rates are lower until the upstream pressure is high enough to provide choked flow. After the increase in upstream pressure is sufficient to provide flow choking, further increases in upstream pressure cause increases in mass flow rate along the curve for  $P_d = 0$ . The key point in this illustration is that flow rate continues to increase with increasing upstream pressure, even after flow choking conditions have been reached. Thus choking does not represent a threshold beyond which dramatically sharper increases in compartment pressures would be expected because of limitations on flow relief to adjacent compartments.

The phenomenon of flow choking is more frequently explained by assuming a fixed upstream pressure and examining the dependence of flow rate with respect to decreasing downstream pressure. This approach is illustrated for an assumed upstream pressure of 30 psia as shown in the upper plot with the results plotted vs. downstream pressure in the lower plot. For fixed upstream conditions, flow choking represents an upper limit flow rate beyond which further decreases in back pressure will not produce any increase in mass flow rate.

The augmented choked flow relationship used in TMD is based on experimental data obtained for choked two-phase flow through long tubes, short tubes, and nozzles. The short tube data was cited



 An AEP Company	<p style="text-align: center;"><b>INDIANA MICHIGAN POWER</b> <b>D. C. COOK NUCLEAR PLANT</b> <b>UPDATED FINAL SAFETY ANALYSIS REPORT</b></p>	<p>Revised: 29.0 Section: 14.3.4: .5; .6; .7 Page: 15 of 33</p>
---	--	---

by Henry and Fauske in Reference (16). Henry and Fauske conclude that an identical discharge coefficient may be applied to two-phase critical flow through sharp-edged orifices and short tubes to represent the actual critical flow rate through each geometry. On this basis, since the augmented choked flow correlation is based on short-tube data, it is applicable to sharp-edged orifices as well. Figure 14.3.4-156, from Reference (17), presents experimental data for two phase critical flow through several different geometries. The dashed line on the graph represents the augmented homogeneous equilibrium critical flow relationship used in TMD. Below a quality of 0.2 the augmentation correlation is not applicable. 0.62 is the highest quality at which critical flow is calculated by TMD to occur in a major flow path following a DEHL break in the Cook containment. It is apparent that the augmented critical flow calculated by TMD is conservative within the quality range of interest.

Carofano and McManus (18) have published data for the two-phase flow of air-water and steam-water mixtures. Actually, water vapor was present in the gas phase of the so-called air-water test, making it in effect an air-steam-water test. The data presented in Reference (18) demonstrates that the ratio of experimental air-(steam)-water critical flow values to homogeneous equilibrium model predictions is equal to or greater than the ratio of steam-water experimental critical flow values to homogeneous equilibrium model predictions. Therefore augmentation factors derived by comparing steam-water data to the homogeneous equilibrium model may be used in air-steam-water calculations.


#### **14.3.4.5.3.5 Early Sensitivity Studies**

The TMD computer code was used to establish peak pressures and peak pressure differentials for double-ended hot and cold leg breaks, double-ended steam line breaks in the steam generator and fan room enclosures, a 6 inch spray line break for the pressurizer enclosure, and a single-ended pipe break in the reactor cavity of the D. C. Cook Plant. These cases were analyzed with and without augmentation of the calculated homogeneous equilibrium critical mass flow rates, to study the sensitivity of compartment pressures to augmentation. The double-ended hot leg break was assumed to occur in node 6, and the double-ended cold leg break was assumed to occur in node 1 of the TMD model network given in Figure 14.3.4-20. These were the worst locations for a hot leg and a cold leg break, respectively.

The pressure response to a hot leg break is only slightly affected by augmentation; the cold leg break pressure response exhibits significant sensitivity to augmentation. Since the hot leg break parameters are limiting for the D. C. Cook Plant, omitting augmentation increases the design basis peak operating deck  $\Delta P$  less than 5%.



## UFSAR Revision 30.0

 An AEP Company	<p style="text-align: center;"><b>INDIANA MICHIGAN POWER</b> <b>D. C. COOK NUCLEAR PLANT</b> <b>UPDATED FINAL SAFETY ANALYSIS REPORT</b></p>	<p>Revised: 29.0 Section: 14.3.4: .5; .6; .7 Page: 16 of 33</p>
---	--	---

No change in the compartment peak pressures or pressure differentials occurred when unaugmented critical flow was used in analyzing the D. C. Cook Plant fan room and steam generator enclosure. Removing augmentation increased the peak pressure and the peak differential pressure in the pressurizer enclosure by 27% and 25%, respectively, in the upper reactor cavity by 17.5% and 19.5%, respectively, and in the lower reactor cavity by 13% and 8%, respectively.


The reason that there is no change in the peak pressures in the steam generator enclosure is that both the peak pressure and peak differential pressure are due to inertia. The fan room pressures remain constant because of high resistances in the flow paths from the fan room to the lower compartment which prevent choking.

In the reactor cavities and pressurizer enclosure, peak pressures occur in the transient coincidental with choking, and therefore a significant change in calculated pressures will occur when the critical flow model is changed (see Table 14.3.4-40).

A number of analyses have been performed using 100 percent moisture entrainment to determine the various pressure transients resulting from hot and cold leg reactor coolant pipe breaks in any one of the six lower compartment elements. The maximum peak pressure and differential pressure for all cases have been determined for each compartment element. Figure 14.3.4-157 is representative of the upper and lower compartment pressure transients that result from a hypothetical double ended rupture of a reactor coolant pipe for the worst possible location in the lower compartment of the containment, a hot leg break (DEHL) in element 6.

In addition, a series of TMD runs investigated the sensitivity of peak pressures to variations in individual input parameters for the design basis blowdown rate and 100% entrainment. This analysis used a DEHL break in element 6, and investigated effects from blowdown sensitivity to addition of the compressibility factor in the momentum equation. Table 14.3.4-36 gives these results.

The sensitivity study results demonstrate that variations in the plant geometric parameters and in ice bed loss coefficients, both of which are known with a high degree of accuracy, have little effect on the peak pressure calculated by TMD for DEHL break in element 6. However, variations in blowdown and entrainment, which are not known with great accuracy, greatly affect the pressure calculated. The highly conservative values used in the design basis analysis ensure a conservative prediction of the peak break compartment pressure.

 An AEP Company	<p style="text-align: center;"><b>INDIANA MICHIGAN POWER</b> <b>D. C. COOK NUCLEAR PLANT</b> <b>UPDATED FINAL SAFETY ANALYSIS REPORT</b></p>	<p>Revised: 29.0 Section: 14.3.4: .5; .6; .7 Page: 17 of 33</p>
---	--	---

#### **14.3.4.5.4 Ice Condenser Performance Criteria**

The performance of the ice condenser containment is demonstrated by results and analysis of ice condenser tests performed on a full-scale section test at the Westinghouse Waltz Mill Site. These tests confirmed the ability of the ice condenser to perform satisfactorily over a wide range of conditions, exceeding the range of conditions that might be experienced in an accident inside the containment.

The ice condenser containment performance has been evaluated by testing the following important parameters. A partial list of parameters tested include blowdown rate, blowdown energy, deck leakage, compression ratio, drain performance, ice condenser hydraulic diameter, dead-ended volumes and long term performance. Analytic models have been developed to correlate and supplement these test results in the evaluation of the containment design. The results indicate that the analytical models are conservative and that the performance of the ice condenser containment is predictable relative to these variables.

The layout of the reactor containment compartments and ice condenser provides for effective and efficient use of the ice condenser to suppress pressure buildup.

The lower (Reactor Coolant System) compartment is bounded by the divider barrier such that essentially all of the energy released in this compartment is directed through doors at the bottom of the ice condenser.


Seals are provided on the boundary of compartments and hatches in the operating deck to prevent steam from bypassing the ice condenser.

Layout, size, and flow communication among compartments is arranged to minimize the containment volume compression ratio.

The ice bed geometry provides sufficient ice heat transfer area and flow passages so that the magnitude of the pressure transient resulting from an accident does not exceed the containment design pressure for all reactor coolant pipe breaks sizes up to and including the hypothetical double-ended severance of the reactor coolant piping.

The initial containment peak pressure and peak asymmetrical containment pressure loads are determined by analysis. The analytical results are experimentally verified by comparison with the ice condenser tests. This analysis supplements the experimental proof of performance tests and provides pressure transients for application of the plant design.

## UFSAR Revision 30.0

 <b>INDIANA MICHIGAN POWER</b> <small>An AEP Company</small>	<b>INDIANA MICHIGAN POWER D. C. COOK NUCLEAR PLANT UPDATED FINAL SAFETY ANALYSIS REPORT</b>	Revised: 29.0 Section: 14.3.4: .5; .6; .7 Page: 18 of 33
--	---	---

The final peak pressure occurring at or near the end of blowdown is determined by a containment volume air compression calculation. A method of analysis of the final peak pressure was developed based on the results of full-scale section tests.


Steam bypass of the ice condenser during the postulated RCS blowdown is to be avoided. The divider deck and any other leakage paths between the lower and upper compartments are reasonably sealed to limit bypass steam flow. For the containment, the analysis considered bypass area as composed of two parts: a conservatively assumed leakage area around the various hatches in the deck, and a known leakage area through the deck drainage holes for spray located at the bottom of the refueling cavity.

Flow distribution to the ice condenser for any RCS pipe rupture that opens the ice condenser inlet doors, up to and including the double-ended RCS pipe rupture, is limited such that the maximum energy input into any section of the ice condenser does not exceed its design capability. The door port flow resistance and size provides this flow distribution for breaks that fully open the ice condenser inlet doors. For breaks that partially open the inlet doors, the lower inlet doors proportion flow into the ice bed limiting maldistribution.

For large pipe breaks, the containment final peak pressure is mainly determined by the displacement of air from the lower compartment into the upper compartment. Only a small amount of steam bypasses the ice condenser by passing through the operating deck and into the upper compartment. This steam bypass then adds a small amount to the final peak pressure.

For small pipe breaks, which generate less than the pressure drop required to fully open the spring-hinged, ice condenser inlet doors and result in the door performance being in the flow proportioning range, a larger than normal fraction of the break flow will pass through the deck by way of the divider deck bypass area and into the upper compartment. Unlike a postulated large break, which sweeps all of the air out of the lower compartment, the smaller breaks do not. Below some break size, only a portion of the lower compartment air will be displaced by the break flow. Also, for breaks less than approximately 10,000 gpm, the ice condenser inlet doors will open; however, only a fraction of the air may be displaced from the lower compartment by the incoming steam. For these small energy release rates, operation of the containment spray system eventually is required to limit the containment pressure rise.

Another case has been examined where it is postulated that a small break loss-of-coolant accident precedes a larger break accident which occurs before all of the coolant energy is released by the small break, (i.e., a double accident). During the small break blowdown, some quantity of steam and air will bypass the ice condenser and enter the upper compartment via leakage in the divider

 An AEP Company	<p style="text-align: center;"><b>INDIANA MICHIGAN POWER</b> <b>D. C. COOK NUCLEAR PLANT</b> <b>UPDATED FINAL SAFETY ANALYSIS REPORT</b></p>	<p>Revised: 29.0 Section: 14.3.4: .5; .6; .7 Page: 19 of 33</p>
---	--	---

deck. The important design requirement for the case of a double accident is that the amount of steam leakage into the upper compartment must be limited during the first part (small break) of the accident so that only a small increase in final peak pressure results for the second part (double-ended break) of the postulated accident. The steam which reaches the upper compartment will then add to the peak pressure for the second part of the accident. Therefore, the containment spray system is used to limit the partial pressure of steam in the upper compartment due to deck bypass. The key elements which determine the double accident performance are the ice condenser lower doors, which open at a low differential pressure to admit steam to the ice condenser and limit the bypass flow of steam and thus the partial pressure of steam in the upper compartment, and the sprays which condense this bypass flow of steam and limit the partial pressure of steam in the upper compartment to a low value, less than 2 psia. The containment spray set point actuation pressure has been set at 3 psig to limit steam partial pressure to less than 2 psia in the upper compartment for the double accident use.

After a LOCA, the ice condenser has sufficient remaining heat absorption capacity such that, together with the containment spray system, subsequent assumed heat loads are absorbed without exceeding the containment design pressure. The subsequent heat loads considered include reactor core and coolant system stored heat, residual heat, substantial margin for an undefined additional energy release, and consideration of steam generators as active heat sources.


The primary purpose of the Containment Spray System is to spray cool water into the containment atmosphere in the event of a loss-of-coolant accident, thereby ensuring that containment pressure cannot exceed the containment design pressure. Protection is afforded for all pipe break sizes up to and including the hypothetical instantaneous circumferential rupture of a reactor coolant pipe. Adequate containment heat removal capability for the Ice Condenser Containment is provided by two separate full capacity containment spray systems. The Containment Spray System is designed based on the conservative assumption that the core residual heat is continuously released to the containment as steam, eventually melting all ice in the ice condenser. The heat removal capability of each spray system is sized to keep the containment pressure below design after all the ice has melted and residual heat generated steam continues to enter the containment. The spray system is designed to keep the pressure below the design pressure with adequate margin.

#### **14.3.4.5.4.1 Inlet Door Performance**

##### **14.3.4.5.4.1.1 Introduction**

The ice condenser inlet doors form the barrier to air flow through the inlet ports of the ice condenser for normal plant operation. They also provide the continuation of thermal insulation

## UFSAR Revision 30.0

 An AEP Company	<p style="text-align: center;"><b>INDIANA MICHIGAN POWER</b> <b>D. C. COOK NUCLEAR PLANT</b> <b>UPDATED FINAL SAFETY ANALYSIS REPORT</b></p>	<p>Revised: 29.0 Section: 14.3.4: .5; .6; .7 Page: 20 of 33</p>
---	--	---

around the lower section of the crane wall to minimize heat input that would promote sublimation and mass transfer of ice in the ice condenser compartment. In the event of a loss-of-coolant incident that would cause a pressure increase in the lower compartment, the doors open, venting air and steam relatively evenly into all sections of the ice condenser.


The inlet doors are essentially pairs of insulated composite panels vertically hinged to a rectangular shaped angle section frame that has a center post. This assembly is fastened to the crane wall support columns which frame the ports through the crane wall from the containment lower compartment to the ice condenser compartment.

The door panels are made of composite steel sheets and urethane foam construction, comprising a total thickness of 7 inches to provide proper insulating characteristics. Each door is mounted to the frame with ball bearing hinges. The door panels are normally held shut against a bulb type gasket seal by the differential pressure produced by the higher density cold air of the ice condenser, sealing against loss of the ice condenser air to the lower compartment.

The door panels are provided with tension spring mechanisms that produce a small closing torque on the door panels as they open. The magnitude of the closing torque is equivalent to providing a one pound per square foot pressure drop through the inlet ports with the door panels open to a position that develops full port flow area.

The zero load position of each spring mechanism is set so that with zero differential pressure across the door panels the gasket seal holds the door slightly open. This provides assurance that all doors will be open slightly and relatively uniformly, prior to development of sufficient lower compartment pressure to cause flow into the ice condenser, therefore eliminating significant inlet maldistribution for very small incidents. For larger incidents the doors open fully and flow distribution is controlled by the inlet ports.

## UFSAR Revision 30.0

 An AEP Company	<b>INDIANA MICHIGAN POWER</b> <b>D. C. COOK NUCLEAR PLANT</b> <b>UPDATED FINAL SAFETY ANALYSIS REPORT</b>	Revised: 29.0 Section: 14.3.4: .5; .6; .7 Page: 21 of 33
---	---	---

### **14.3.4.5.4.1.2 Design Criteria**


#### Normal Operation

- a. Doors shall be instrumented to allow remote monitoring of their closed position.
- b. Doors shall be capable of being inspected to determine that they are functioning properly.
- c. The inlet doors shall limit the leakage of air out of the ice condenser to the minimum practical limit.
- d. The inlet doors shall restrict the heat input into the ice condenser to the minimum practical limit.
- e. Normal maintenance and inspection must be performed in a manner that does not hinder the ice condenser performance or availability.

#### Accident Conditions

- a. All doors shall open to allow venting of energy to the ice condenser for any leak rate which results in a divider deck differential pressure in excess of the ice condenser cold head.  
  
The force required to open the doors of the ice condenser is sufficiently low such that the energy from any leakage of steam through the divider barrier can be readily absorbed by the containment spray system without exceeding containment design pressure.
- b. Doors and door ports shall limit maldistribution to 150% maximum, peak to average mass input for the accident transient which provides adequate margin in the design ice bed loadings. This is used for any reactor coolant system energy release of sufficient magnitude to cause the doors to open. The inlet doors of the ice condenser are designed to open and distribute steam to the ice condenser in accordance with design basis above, for any postulated loss-of-coolant accident.
- c. The doors are designed to eliminate the possibility of doors remaining closed, even for small break conditions. In particular, two degrees of freedom of rotation are incorporated in the hinges and the sealing gasket is designed to pull out for a postulated condition of sticking. The gasket material is itself selected to prevent sticking.

## UFSAR Revision 30.0

 An AEP Company	<p style="text-align: center;"><b>INDIANA MICHIGAN POWER</b> <b>D. C. COOK NUCLEAR PLANT</b> <b>UPDATED FINAL SAFETY ANALYSIS REPORT</b></p>	<p>Revised: 29.0 Section: 14.3.4: .5; .6; .7 Page: 22 of 33</p>
---	--	---

- d. The basic performance requirement for lower inlet doors for design basis accident conditions is to open rapidly and fully, to ensure proper venting of released energy into the ice condenser. The opening rate of the inlet doors is important to ensure minimizing the pressure buildup in the lower compartment due to the rapid release of energy to that compartment.
- e. Ice condenser doors shall be protected from direct steam jet following a postulated steam line break.

### **14.3.4.5.4.1.3 Performance Capability**

#### Normal Operation

The normal operation mode for the ice condenser inlet doors is to serve as an insulated barrier to natural convection heat and air flow through the ice bed, providing a sufficient insulating value to limit heat input into the ice bed. In addition the design and performance of the doors must be consistent with ensuring continuous availability of the ice condenser function.

The importance of normal operation criteria is the establishment of design parameters that provide for long term ice bed life, and for constant ice condenser availability for plant protection. In this context two inlet door design parameters affect these factors. They are heat conductivity and leak tightness.

Heat input is the parameter of prime concern, as it is the major factor influencing ice bed sublimation. Leakage out of the ice bed has been reduced to an insignificant amount. The heat input is a calculated value using a two dimensional heat conductance computer program that has been verified by tests.


The inlet door leakage is predicted by tests to be significantly less than the 50 CFM total used for the ice condenser design. This predicted leakage value has negligible effect on reinforcing the convective flow developed in the ice bed, therefore not affecting sublimation rates significantly. The effect of the make-up air entering the ice condenser due to this leakage is also negligible on refrigeration load or ice condenser air handling unit coil defrost frequency.

Seismic analyses associated with response data for the Cook Nuclear Plant shows that the ice condenser inlet doors will not be opened by the maximum seismic forces. This is due to the very low frequency of the rotational or opening mode, at which the response is negligible, and the ice condenser cold head pressure holds the doors closed.

Figure 14.3.4-158 shows the door opening characteristics as a function of door differential pressure based on a linear spring constant. Notably, there is no special significance to be attached to a linear



## UFSAR Revision 30.0

 An AEP Company	<p style="text-align: center;"><b>INDIANA MICHIGAN POWER</b> <b>D. C. COOK NUCLEAR PLANT</b> <b>UPDATED FINAL SAFETY ANALYSIS REPORT</b></p>	<p>Revised: 29.0 Section: 14.3.4: .5; .6; .7 Page: 23 of 33</p>
---	--	---

spring constant, and detail design of the door and spring system indicated that non-linear spring characteristics changed the release rate at which maximum maldistribution would occur, but did not change the maximum maldistribution value. The performance characteristics to be expected from the inlet doors would be typical of those shown in Figure 14.3.4-158.

The effect of maximum variation of door proportioning characteristics indicates significantly less maldistribution than the 150% limit.

Importantly, and as discussed in other reports, the ratio of maximum to average flow of steam into the ice condenser for pipe break sizes large enough to fully open the doors is limited by the door ports themselves to a reasonably low value, about 116 percent of the average.

The equilibrium position of the inlet door panels with zero differential pressure is slightly open (about 3/8 inch), which provides a small flow area at each door for uniform inlet flow into each segment of the ice bed. The doors are designed to eliminate the possibility of doors remaining closed, even for small break conditions. In particular two degrees of freedom of rotation are incorporated in the hinges, and the sealing gasket is designed to pull out for a postulated condition of sticking. The gasket material is itself selected to prevent sticking.


Consideration is, however, given in the analysis of ice condenser performance to a hypothetical case of stuck doors at which the most severe of the above postulated malfunctions is overcome by the force on the door. Even in this hypothetical case the door panels would rupture, providing a sufficient flow path into the ice condenser to permit the ice condenser to function to limit containment pressure below design limits.

It is recognized that the springs are an important part of the lower ice condenser doors. These spring assemblies are designed such that the failure of any spring will not significantly change the operating characteristics of the ice condenser doors. This objective has been achieved in a practical manner by the use of four separate tension springs per door, which provides redundancy and assures adequate opening characteristics.

### Accident Conditions

The basic lower inlet door performance requirement for design basis accident conditions is to open rapidly and fully, to insure proper venting of released energy into the ice condenser. The opening rate of the inlet doors is important to insure minimizing the pressure buildup in the lower compartment due to the rapid release of energy to that compartment. The rate of pressure rise and the magnitude of the peak pressure in any lower compartment region is related to the confinement of that compartment, and in particular the active volume and flow restrictions out of that



 An AEP Company	<p style="text-align: center;"><b>INDIANA MICHIGAN POWER</b> <b>D. C. COOK NUCLEAR PLANT</b> <b>UPDATED FINAL SAFETY ANALYSIS REPORT</b></p>	<p>Revised: 29.0 Section: 14.3.4: .5; .6; .7 Page: 24 of 33</p>
---	--	---

compartment. The time period to reach peak lower compartment pressure due to the design basis accident is a fraction of a second. It is dependent upon flow restrictions and proximity to the break location. The opening rate of the inlet doors is wholly dependent upon the inertia of the door and the magnitude of the forcing function, which is the pressure buildup in the lower compartment due to the energy release. The ice condenser inlet door inertia is slightly less than the doors tested in the ice condenser full scale section tests. These tests demonstrate that door inertia has essentially no effect on the initial peak pressure.

The maximum inlet door structural loading is due to the design basis accident for the doors adjacent to the lower compartment in which the release occurs. Structural analysis for maximum loaded conditions shows that all door members remain well below allowable stress levels. Further verification of the structural adequacy of the door is provided by the proof load testing carried out on the full prototype doors.

The necessary performance of the ice condenser is further ensured by the door design incorporating a low pressure fail open characteristic. Even if it is postulated that the doors were held rigidly along the bottom edge, they would fail open at a differential pressure sufficiently low to allow venting from the lower compartment well within the limits of pressure capability of the structures.

#### **14.3.4.5.4.2 Top and Intermediate Deck Door Performance**

The doors enclosing the top of the ice condenser and forming the roof of the upper plenum are of a non-rigid design lighter than the intermediate deck doors. These top doors are supported by the ice condenser bridge crane support structure. The crane support structure consists of radial beams spanning the ice condenser annulus at the top of the crane wall.


The intermediate deck doors enclose the ice compartment and forming the floor of the upper plenum. These doors are supported by the lattice frame support columns.

The intermediate deck door panels are a 2 1/2 inch foam plastic core with bonded sheet metal facings. These doors are hinged horizontally and are normally closed. The top deck doors are flexible foam bonded to high strength foil steel. These doors are hinged (clamped) on the crane wall side of the top deck and are normally closed. On an increase in pressure in the ice condenser compartment, these doors will open as required, allowing air to flow into the upper containment volume.

#### **14.3.4.5.4.2.1 Design Criteria**

Normal Operations

## UFSAR Revision 30.0

 <p><b>INDIANA MICHIGAN POWER</b> <small>An AEP Company</small></p>	<p style="text-align: center;"><b>INDIANA MICHIGAN POWER D. C. COOK NUCLEAR PLANT UPDATED FINAL SAFETY ANALYSIS REPORT</b></p>	<p>Revised: 29.0 Section: 14.3.4: .5; .6; .7 Page: 25 of 33</p>
--	--	---

1. The top deck will be provided with a total vent area of approximately 20 ft<sup>2</sup>.
2. Doors will limit heat input within their immediate vicinity to the minimum practical limit.
3. Doors will be capable of being inspected during plant shutdown to determine that they are functioning properly.

### Accident Conditions

1. All doors will open fully for a low differential pressure loading.
2. All doors will be light-weight to have a minimum effect on the initial peak pressure.
3. Doors will be of simple mechanical design to minimize the possibility of malfunction.
4. Doors will not be required to remain either open or closed following an accident.


#### **14.3.4.5.4.2.2 Performance Capability**

On an increase in pressure in the ice condenser compartment, these doors will open as required to allow air to flow into the upper compartment. The primary design criterion for these doors is their insulating capability to limit heat flow. The flow area provided by the open doors is that area available in the compartment, considering area reduction by support structures. Both the inertia of the door with the desired insulation capability and the available flow area have been modeled in the ice condenser door tests.

The mean heat input to the plenum through the top deck is about 4.5 Btu/hr-ft<sup>2</sup>. This heat input is removed from the plenum ambient by the ice condenser air handling units and does not affect ice bed sublimation. The effect of this heat load on refrigeration heat load and plenum ambient conditions has been investigated and provides for operation well within the ice condenser design operating parameters.

Incorporation of the vents imposes no operational problem to the ice condenser. The lower doors will effectively seal the ice condenser compartment and limit any flow of air through the compartment to a negligible value. Therefore tight seals are not necessary at the intermediate deck doors. A balanced flapper is provided to minimize migration of moisture into the ice condenser through the vents.

The open flow area through each deck for air flow due to an incident is slightly larger than the ice condenser test ratio equivalent, providing slightly less resistance to air flow. The slightly larger

 An AEP Company	<b>INDIANA MICHIGAN POWER</b> <b>D. C. COOK NUCLEAR PLANT</b> <b>UPDATED FINAL SAFETY ANALYSIS REPORT</b>	Revised: 29.0 Section: 14.3.4: .5; .6; .7 Page: 26 of 33
---	---	---

flow area does not produce any significant change in ice condenser performance, other than to assure flow resistances slightly less restrictive than the reference design.

The top and intermediate deck and doors have been analyzed for all loading combinations. This structural analysis shows that all members remain below allowable stress levels.

#### **14.3.4.5.4.3 Vent Design And Performance**

##### **14.3.4.5.4.3.1 Introduction**


The upper and intermediate doors are not required to remain open following the reactor coolant system blowdown and also are not required to open for small breaks. For these situations, a vent was provided through both the top and intermediate deck to allow air to flow into or from the ice condenser compartment as required. This vent air first passes into the fan cooler plenum at the top of the ice condenser compartment where it mixes with the cooling air. The temperature and humidity of the vent air that passes from this plenum into the ice condenser compartment are therefore about the same as the average temperature and humidity of the air in the condenser compartment.

Accordingly, sublimation or frosting in the ice bed due to this vent flow of air will be limited to a negligible value. Specific performance requirements are given below both for large breaks and for small breaks.

##### **14.3.4.5.4.3.2 Large Break Performance Requirements**

Following the reactor coolant system blowdown, the vents were designed to allow air to return from the upper compartment into the ice condenser without imposing an excessive pressure drop across the upper and intermediate doors. The maximum pressure decay rate and therefore the maximum reverse flow rate of air results from the case where reactor residual heat is not released to the containment following the reactor coolant system blowdown. The pressure decay for this case was measured in a full-scale section test. In this test, the pressure decayed from 6.2 psig to 4.5 psig during the one minute period immediately following the reactor coolant system blowdown. From this pressure decay rate, the plant equivalent flow rate of air was calculated to be 98 lbm/sec. This flow rate developed a pressure drop across each of the upper doors of 0.28 psi, which was well within the structural capability of the upper and intermediate doors and support structures. Further, in this calculation it was conservatively assumed that no air flowed through the deck or through the containment air recirculation fan duct.

## UFSAR Revision 30.0

 An AEP Company	<p style="text-align: center;"><b>INDIANA MICHIGAN POWER</b> <b>D. C. COOK NUCLEAR PLANT</b> <b>UPDATED FINAL SAFETY ANALYSIS REPORT</b></p>	<p>Revised: 29.0 Section: 14.3.4: .5; .6; .7 Page: 27 of 33</p>
---	--	---

### **14.3.4.5.4.3 Small Break Performance Requirements**

For small breaks which generate less than the required opening pressure of the upper and intermediate doors, the vent was designed to limit the flow of steam through the deck to an acceptable level during the period of air flow through the condenser and into the upper compartment. For breaks less than approximately 5000 gpm, the full-scale section tests have shown that only a fraction of air is displaced from the lower compartment. The 20 sq. ft. vent area in both the top and intermediate deck provides a low resistance air flow path through the ice condenser to the containment upper compartment for these small break conditions.

### **14.3.4.5.4.4 Drain Design And Performance**

#### **14.3.4.5.4.4.1 Introduction**

Drains are provided at the bottom of the ice condenser compartment to allow the melt-condensate water to flow out of the compartment during a loss-of-coolant accident. These drains are provided with check valves that are counter-weighted to seal the ice condenser during normal plant operation and to prevent steam flow through the drains into the ice condenser during a loss-of-coolant accident. These check valves will remain closed against the cold air head (1 psf) of the ice condenser and open before the water level rises to the point where it can interfere with the operation of the lower inlet doors, as described in Chapter 5.3.


For a small pipe break, the water inventory in the ice condenser will be produced at a rate proportional to the rate of energy addition from the accident. The water collecting on the floor of the condenser compartment will then flow out through the drains and through the doors, which are open during the blowdown.

For a large pipe break, a short time (on the order of seconds) will be required for the water to fall from the ice condenser to the floor of the compartment. Therefore, it is possible that some water will accumulate at the bottom of the condenser compartment at the completion of the blowdown. Such water accumulation could exert a back pressure on the inlet doors, requiring an additional pressure rise in the lower compartment to open the doors and admit steam to the ice condenser. However, results of full-scale section tests indicated that, even for the design blowdown accident, a major fraction of the water drained from the ice condenser, and no increase in containment pressure was indicated even for the severe case with no drains.

#### **14.3.4.5.4.4.2 Large Break Performance Requirements**

A number of tests were performed with the reference flow proportional-type door installed at the inlet to the ice condenser, the reference-type hinged door installed at the top of the condenser.

# UFSAR Revision 30.0

 An AEP Company	<b>INDIANA MICHIGAN POWER</b> <b>D. C. COOK NUCLEAR PLANT</b> <b>UPDATED FINAL SAFETY ANALYSIS REPORT</b>	Revised: 29.0 Section: 14.3.4: .5; .6; .7 Page: 28 of 33
---	---	---

Tests were conducted with and without the reference water drain area, equivalent to 15 ft<sup>2</sup> for the plant,<sup>1</sup> at the bottom of the condenser compartment.

Tests were conducted with various assumed blowdown conditions. These tests were performed with the maximum reference blowdown rate, with an initial low blowdown rate followed by the reference rate, with a low blowdown rate alone, and with the maximum reference blowdown rate followed by the simulated core residual heat rate.

The results of all of these tests showed satisfactory condenser performance with the reference type doors, vent, and drain for a wide range of blow-down rates. Also, these tests demonstrate the insensitivity of the final peak pressure to the water drain area. In particular, the results of these full-scale section tests indicated that, even for the reference blowdown rate, and with no drain area provided, the drain water did not exert a significant back pressure on the ice condenser lower doors. This showed that a major fraction of the water had drained from the ice condenser compartment by the end of the initial blowdown. The effect of this test result is that containment final peak pressure is not affected by drain performance.

Although drains are not necessary for the large break performance, approximately 13 ft<sup>2</sup> of drain area are required for small breaks.


#### **14.3.4.5.4.4.3 Small Break Performance Requirements**

For small breaks, water will flow through the drains at the same rate that it is produced in the ice condenser. Therefore, the water on the floor of the compartment will reach a steady height which is dependent only on the energy input rate.

To determine that the 12.63 ft<sup>2</sup> drain area met these requirements, the water height was calculated for various small break sizes up to a 30,000 gpm break. Above 30,000 gpm the ice condenser doors would be open to provide additional drainage. The maximum height of water required was calculated to be 2.2 ft above the drain check valve. Since this height resulted in a water level which was more than 1 ft below the bottom elevation of the inlet doors, it was concluded that water will not accumulate in the ice condenser for this condition and that a 12.63 ft<sup>2</sup> drain will give satisfactory performance.

---

<sup>1</sup> As noted in Chapter 5.3.5.1.6., the D.C. Cook ice condenser floor drains have a flow area of approximately 18 ft<sup>2</sup>. Since the reference tests were performed at Waltz Mill both with and without the reference plant drain area of 15 ft<sup>2</sup>, the D.C. Cook ice condenser drain configuration is bounded by the reference tests.

 An AEP Company	<p style="text-align: center;"><b>INDIANA MICHIGAN POWER</b> <b>D. C. COOK NUCLEAR PLANT</b> <b>UPDATED FINAL SAFETY ANALYSIS REPORT</b></p>	Revised: 29.0 Section: 14.3.4: .5; .6; .7 Page: 29 of 33
---	--	---

#### **14.3.4.5.4.4 Normal Operational Performance**

During normal plant operation, the sole function of the valve is to remain in a closed position, minimizing air leakage across the seat. To avoid unnecessary contamination of the valve seat, a 1 ½ -inch drain line is connected to the 12 inch line immediately ahead of the valve. Any spillage or defrost water will drain off without causing the valve to be opened.

Special consideration has been given in the design to prevent freezing of the check valves and to minimize check valve leakage.

To minimize the potential for valve freezing, a low conductivity (transite) section of pipe is inserted vertically below the seal slab, while the horizontal run of pipe (steel) is embedded in a warm concrete wall before it reaches the valve. The valve itself is in the upper region of the lower compartment, where ambient temperature is generally above the freezing temperature.

The valve is held in a closed position by virtue of its design as an almost vertical flapper with a hinge at the top. The slight (10°) angle from the vertical holds the flap in place by gravity.

To reduce valve leakage to an acceptable value, a sealant was applied to the seating surface after installation of the valves. Tests show that this will reduce leakage to practically zero. Maximum allowable leakage rate would be approached as a limit only if all the sealant were to disappear completely from all the valves, which is unlikely. Sealant is replaced as necessary.


#### **14.3.4.6 Changes from Base Containment Analyses: Note Concerning Tables and Figures**

If an evaluation or partial re-analysis is needed for some change from one of the base containment analyses of record, and this results in changes to information appearing in the UFSAR, a text description of the new work is provided here in Section 14.3.4. However, unless specifically indicated otherwise, the associated tables and figures for Section 14.3.4 are taken from the base analysis of record, and not any subsequent specific evaluation or partial re-analysis.

#### **14.3.4.7 References for Section 14.3.4**

1. Grimm, N.P. and Colenbrander, H. G. C., "Long Term Ice Condenser, Containment Code - LOTIC Code," WCAP-8354-P-A, September, 2017 (Proprietary) and WCAP-8355-A, September, 2017 (Non-Proprietary).
2. "Final Report Ice Condenser Full Scale Section Test at the Waltz Mill Facility," WCAP-8282, February, 1974 (Proprietary) and WCAP-8110, Supplement 6, May, 1974 (Non-Proprietary).


## UFSAR Revision 30.0

 <b>INDIANA MICHIGAN POWER</b> An AEP Company	<b>INDIANA MICHIGAN POWER</b> <b>D. C. COOK NUCLEAR PLANT</b> <b>UPDATED FINAL SAFETY ANALYSIS REPORT</b>	Revised: 29.0 Section: 14.3.4: .5; .6; .7 Page: 30 of 33
---	---	---

3. Letter from D. B. Black to B. A. Svensson, August 3, 1988, "Operation at Essential Service Water Temperatures Above 81°F."
4. Hsieh, T. and Raymond, M., "Long Term Ice Condenser Containment Code - LOTIC Code," WCAP-8354-P-A, Supplement 1, April, 1976 (Proprietary) and WCAP-8355, Supplement 1, April, 1976 (Non-Proprietary).
5. Deleted
6. NS-CE-1250, 10/22/76, C. Eicheldinger Letter to J. F. Stolz, NRC, Supplemental Information on LOTIC3 questions.
7. NS-CE-1453, 6/14/77, C. Eicheldinger letter to J. F. Stolz, NRC, Responses to LOTIC3 questions.
8. NS-CE-1626, 12/7/77, C. Eicheldinger letter to J. F. Stolz, NRC, Responses to LOTIC3 questions.
9. Hsieh, T. and Liparulo, N. J., "Westinghouse Long Term Ice Condenser Containment Code -LOTIC3 Code", WCAP-8354-P-A, Supplement 2, February 1979.
10. J. F. Stolz, NRC, to C. Eicheldinger, 5/3/78, "Evaluation of Supplement to WCAP-8354 (LOTIC3)."
11. J. F. Stolz, NRC, to C. Eicheldinger, 5/10/78, "Staff Approval of LOTIC3 Code."
12. Letter No. AEP-80-525, March 10, 1980 (F. Noon of Westinghouse to D. V. Shaller of AEPSC).
13. Letter, G. P. Maloney (AEP) to H. R. Denton (NRC), dated April 1, 1980 (Letter No. AEP:NRC:0131).
14. Salvatori, R. (approved), "Ice Condenser Containment Pressure Transient Analysis Methods," WCAP-8077, March, 1973 (Proprietary) and WCAP-8078, March, 1973 (Non-Proprietary).
15. Salvatori, R. (approved), "Ice Condenser Full Scale Section Test at the Waltz Mill Facility," WCAP-8110, Supplement 6, May, 1974.
16. Henry, R. E., and H.K. Fauske, "Two-Phase Critical Flow of One-Component Mixtures in Nozzles, Orifices, and Short Tubes," Journal of Heat Transfer, May, 1971, pp. 179-187.




## UFSAR Revision 30.0

 <b>INDIANA MICHIGAN POWER</b> An AEP Company	<b>INDIANA MICHIGAN POWER</b> <b>D. C. COOK NUCLEAR PLANT</b> <b>UPDATED FINAL SAFETY ANALYSIS REPORT</b>	Revised: 29.0 Section: 14.3.4: .5; .6; .7 Page: 31 of 33
---	---	---

17. Smith, R.V., USA Natl. Bur. of Standards Tech. Note No. 179, 1963.
18. Carofano, G.C. and H.N. McManus, "An Analytical And Experimental Study of the Flow of Air-Water and Steam-Water Mixtures in a Converging-Diverging Nozzle," Progress in Heat & Mass Transfer, Vol. 2, pp. 395-417.
19. Letter from John Tillinghast, Indiana & Michigan Power Co., to Edson G. Case, U.S. Nuclear Regulatory Commission, dated January 23, 1978.
20. Letter from G.P. Maloney, Indiana & Michigan Power Co., to Edson G. Case, U.S. Nuclear Regulatory Commission, dated February 27, 1978.
21. WCAP-8264-P-A, Rev. 1, "Westinghouse Mass and Energy Release Data for Containment Design," August 1975.
22. "Westinghouse LOCA Mass and Energy Release Model for Containment Design - March 1979 Version," WCAP-10325-P-A, May 1983 (Proprietary), WCAP-10326-A (Non-Proprietary).
23. "Westinghouse Containment Analysis Methodology – PWR LOCA Mass and Energy Release Calculation Methodology," WCAP-17721-P-A, September 2015 (Proprietary), WCAP-17721-NP-A, September 2015 (Non-Proprietary).
24. ANSI/ANS-5.1-1979, "American National Standard for Decay Heat Power in Light Water Reactors," August 1974.
25. Moody, F.J., "Maximum flow Rate of Single Component, Two-Phase Mixture," ASME publication, Paper NO. 64-HT-35.
26. Burnett, T. W. T., et al., "LOFTRAN Code Description", WCAP-7907-A, April 1, 1984.
27. Zaloudek, F.R., "Steam-Water Critical Flow From High Pressure Systems," Interim Report, HW-68936, Hanford Works, 1964.
28. Henry, R.E., "A Study of One- and Two-Component, Two-Phase Critical Flows at Low Qualities," ANL-7430.
29. Henry, R.E., "An Experimental Study of Low-Quality, Steam-Water Critical Flow at Moderate Pressures," ANL-7740.
30. Kramer, F.W., "FLASH: A Program for Digital Simulation of the Loss-of-Coolant Accident," Westinghouse Atomic Power Division, WCAP-1678, January, 1961.




# UFSAR Revision 30.0

 <p><b>INDIANA MICHIGAN POWER</b> <small>An AEP Company</small></p>	<p align="center"><b>INDIANA MICHIGAN POWER D. C. COOK NUCLEAR PLANT UPDATED FINAL SAFETY ANALYSIS REPORT</b></p>	<p>Revised: 29.0 Section: 14.3.4: .5; .6; .7 Page: 32 of 33</p>
--	---	---

31. Zaloudek, F.R., "The Critical Flow of Hot Water Through Short Tubes," HW-77594, Hanford Works, 1963.
32. Deleted
33. Deleted
34. "Donald C. Cook Nuclear Plant Units 1 and 2, Modifications to the Containment Systems, Westinghouse Safety Evaluation, (SECL 99-076, Revision 3)", WCAP-15302, September, 1999 (Westinghouse Non-Proprietary Class 3)
35. AEP-99-329, September 29,1999; Ed Dzenis (Westinghouse Electric Company LLC) to Jim Hawley (American Electric Power), "Reconciliation of Design Information Transmittal DIT No. B-00003-06".
36. AEP-99-417, November 11,1999: E. Dzenis (Westinghouse Electric Company LLC) to G. Hill (American Electric Power), "Response to AEP Questions/Comments on Chapter 14.3.4 Mark-ups".
37. Deleted
38. AEP-00-0142, May 9, 2000, W.R. Rice (Westinghouse Electric Company LLC) to Mr. Don Hafer (American Electric Power), "D.C. Cook Units 1 and 2: Containment Integrity Analysis Evaluation for Restart".
39. MD-1-SGRP-017-N "DC Cook Unit 1 RSG Safety Evaluation – Large Break LOCA B&W Replacement Steam Generators (Framatome Calculation No. 51-1266354 rev.1).
40. NED-2001-004-REP, Rev. 0, "American Electric Power Donald C. Cook Nuclear Plant Unit 1 and Unit 2 Loop Subcompartment Analysis", May 2001
41. NED-2001-005-REP, Rev. 0, "American Electric Power Donald C. Cook Nuclear Plant Unit1 and Unit 2 Pressurizer Enclosure Subcompartment Analysis", April 2001
42. NED-2001-018-REP, Rev. 0, "American Electric Power Donald C. Cook Nuclear Plant Unit 1 and Unit 2 Fan/Accumulator Room Subcompartment Analysis", May 2001

## UFSAR Revision 30.0

 <b>INDIANA MICHIGAN POWER</b> <small>An AEP Company</small>	<b>INDIANA MICHIGAN POWER D. C. COOK NUCLEAR PLANT UPDATED FINAL SAFETY ANALYSIS REPORT</b>	Revised: 29.0 Section: 14.3.4: .5; .6; .7 Page: 33 of 33
--	---	---

43. NED-2001-012-REP, Rev. 0, "American Electric Power Donald C. Cook Nuclear Plant Unit 1 and Unit 2 Steam Generator Enclosure Subcompartment Analysis", May 2001
44. NED-2001-013-REP, Rev. 2, "American Electric Power Donald C. Cook Nuclear Plant Unit 1 and Unit 2 Reactor Cavity Subcompartment Analysis", Feb 28, 2008
45. AEP-04-52, "D. C. Cook Units 1 and 2 – TMD Steam Generator Enclosure Reanalysis", dated September 13, 2004.